AMERICAN SOCIETY FOR MICROBIOLOGY | Microbiology and Molecular Biology Reviews

Physiology, Biochemistry, and Applications of F_{420}- and F_o-Dependent Redox Reactions

Chris Greening,[a]* F. Hafna Ahmed,[b] A. Elaaf Mohamed,[b] Brendon M. Lee,[b] Gunjan Pandey,[a] Andrew C. Warden,[a] Colin Scott,[a] John G. Oakeshott,[a] Matthew C. Taylor,[a] Colin J. Jackson[b]

The Commonwealth Scientific and Industrial Research Organisation, Land & Water Flagship, Acton, Australian Capital Territory, Australia[a]; Australian National University, Research School of Chemistry, Acton, Australian Capital Territory, Australia[b]

(continued)

Published 27 April 2016

Citation Greening C, Ahmed FH, Mohamed AE, Lee BM, Pandey G, Warden AC, Scott C, Oakeshott JG, Taylor MC, Jackson CJ. 2016. Physiology, biochemistry, and applications of F_{420}- and F_o-dependent redox reactions. Microbiol Mol Biol Rev 80:451–493. doi:10.1128/MMBR.00070-15.

Address correspondence to Chris Greening, chris.greening@monash.edu, or Colin J. Jackson, colin.jackson@anu.edu.au.

*Present address: Chris Greening, Monash University, School of Biological Sciences, Clayton, Victoria, Australia.

C.G. and F.H.A. contributed equally to this work.

SUMMARY

5-Deazaflavin cofactors enhance the metabolic flexibility of microorganisms by catalyzing a wide range of challenging enzymatic redox reactions. While structurally similar to riboflavin, 5-deazaflavins have distinctive and biologically useful electrochemical and photochemical properties as a result of the substitution of N-5 of the isoalloxazine ring for a carbon. 8-Hydroxy-5-deazaflavin (F_o) appears to be used for a single function: as a light-harvesting chromophore for DNA photolyases across the three domains of life. In contrast, its oligoglutamyl derivative F_{420} is a taxonomically restricted but functionally versatile cofactor that facilitates many low-potential two-electron redox reactions. It serves as an essential catabolic cofactor in methanogenic, sulfate-reducing, and likely methanotrophic archaea. It also transforms a wide range of exogenous substrates and endogenous metabolites in aerobic actinobacteria, for example mycobacteria and streptomycetes. In this review, we discuss the physiological roles of F_{420} in microorganisms and the biochemistry of the various oxidoreductases that mediate these roles. Particular focus is placed on the central roles of F_{420} in methanogenic archaea in processes such as substrate oxidation, C_1 pathways, respiration, and oxygen detoxification. We also describe how two F_{420}-dependent oxidoreductase superfamilies mediate many environmentally and medically important reactions in bacteria, including biosynthesis of tetracycline and pyrrolobenzodiazepine antibiotics by streptomycetes, activation of the prodrugs pretomanid and delamanid by *Mycobacterium tuberculosis*, and degradation of environmental contaminants such as picrate, aflatoxin, and malachite green. The biosynthesis pathways of F_o and F_{420} are also detailed. We conclude by considering opportunities to exploit deazaflavin-dependent processes in tuberculosis treatment, methane mitigation, bioremediation, and industrial biocatalysis.

1. INTRODUCTION

Flavin- and deazaflavin-dependent enzymes mediate a wide range of redox reactions in biological systems (1, 2). Flavin adenine dinucleotide (FAD) and flavin mononucleotide (FMN) are versatile flavin cofactors that are central to metabolism across the three domains of life. Some organisms also synthesize and utilize 5-deazaflavin compounds (3, 4), in which a carbon atom substitutes for the N-5 atom of the isoalloxazine ring. Two such compounds are relevant to biological systems, namely, 7,8-didemethyl-8-hydroxy-5-deazariboflavin (F_o) and its lactyl oligoglutamate phosphodiester derivative (F_{420}) (Fig. 1) (5, 6). While structurally similar to flavins, these compounds have markedly different physicochemical properties (6–9): they serve as obligate two-electron hydride carriers, have low standard redox potentials (−340 mV), and have blue-shifted intrinsic fluorescence. As elaborated upon in section 2, the chemical properties and biological functions of F_{420} are in fact more similar to nicotinamides (i.e., NAD, NADP) than flavins, leading to its description as a "nicotinamide in a flavin's clothing" (7, 10).

F_o and F_{420} have entirely distinct physiological roles. F_o is distributed across the three domains of life (*Bacteria*, *Archaea*, and *Eukarya*), but it appears to serve only one function: as a light-harvesting antenna in some DNA photolyases that repair pyrimidine dimers following exposure to UV light. As a result, F_o can be considered a chromophore rather than a cofactor; while it can substitute for F_{420} *in vitro* (11–13), it does not appear to have any redox roles in living cells. The biosynthesis, distribution, and photochemistry of this chromophore are covered in section 2. In contrast to F_o, F_{420} has a very limited taxonomic distribution and has been chemically identified in only two phyla thus far (*Euryarchaeota* and *Actinobacteria*). However, this cofactor has diverse catalytic roles in such organisms and mediates many of the challenging redox transformations necessary for their catabolic, detoxification, and biosynthetic pathways. F_{420} appears to have been selected for such processes due to its unique electrochemical properties compared to other flavins, namely, its two-electron reactivity and low redox potential. By maintaining a pool of hydride transfer redox cofactors separate from NAD(P), cells may also be able to better control the flux of specific redox reactions. The roles and enzymology of the reactions catalyzed by F_{420} are discussed in sections 3 and 4 of this review.

Nine years after the discovery of methanogenesis (14), Cheeseman et al. formally identified F_{420} in 1972 (5) in Wolfe's laboratory. They demonstrated that the compound was responsible for the characteristic 420-nm absorbance and blue-green fluorescence of oxidized lysates of *Methanobacterium bryantii* (5). The compound, thereafter named factor 420 (abbreviated F_{420}; sometimes called coenzyme F_{420} or cofactor F_{420}), was shown to be a redox-active 5-deazaflavin derivative (6) that is present at levels up to 400 mg/kg in methanogens (15). It was demonstrated that F_{420} facilitated multiple central metabolic redox reactions in methanogens, including oxidation of energy sources (H_2 and formate) (16, 17) and reduction of cofactors (NADP and tetrahydromethanopterin) (16, 18). Later, it was realized that F_{420} is also synthesized by sulfate-reducing archaea (19), halophilic archaea (20), and likely methanotrophic archaea (21). As a result of more than 5 decades of study, scientists developed a rich understanding of the physiology and biochemistry of F_{420} in the methanogenic and sulfate-reducing archaea (22), as summarized in section 3.

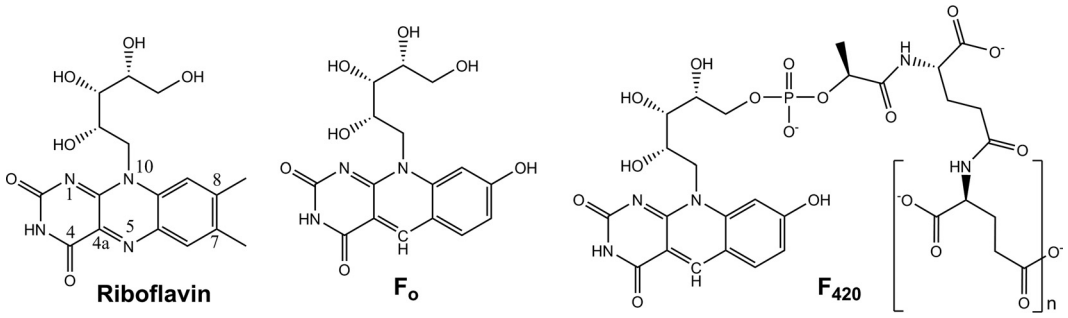

FIG 1 Structures of riboflavin, F_o, and F_{420}.

However, our understanding of the roles of F_{420} in bacteria remains in its infancy. While cofactors with properties corresponding to F_{420} were isolated in mycobacteria and streptomycetes in 1960 (23, 24), it was not until decades later that the cofactor was formally identified in these genera (25–27). As discussed throughout section 4, F_{420} is implicated in the catabolic, biosynthetic, and detoxification pathways of both saprophytic actinobacteria (28–30) and their pathogenic descendants (e.g., *Mycobacterium tuberculosis*) (31, 32). Interest in F_{420} metabolism has surged following the discovery that the recently clinically approved antimycobacterial prodrug delamanid is activated by a specific $F_{420}H_2$-dependent reductase (33–36). However, the physiological and pharmacological roles of F_{420} are still poorly understood in actinobacteria, and the majority of the predicted F_{420}-dependent enzymes in such organisms remain functionally unannotated (30, 37). There is also genomic evidence that F_{420} might be more widely distributed than previously thought, with potential roles in *Chloroflexi*, *Alphaproteobacteria*, and *Betaproteobacteria* inhabiting aerated soil ecosystems (30, 37). This review concludes by considering the diverse implications and potential environmental, medical, and industrial applications of deazaflavin compounds (section 5).

2. 5-DEAZAFLAVIN COMPOUNDS

2.1. Properties

The structure of F_o (7,8-didemethyl-8-hydroxy-5-deazariboflavin; also sometimes referred to as 8-HDF, F_0, and FO) is similar to that of riboflavin (Fig. 1). However, its physical and chemical properties are modulated by three substitutions in its isoalloxazine rings (38): N-5 is substituted for a carbon, C-7 and C-8 are demethylated, and C-7 is hydroxylated (6). F_{420} is a derivative of F_o; the ribityl side chain forms a phosphoester bond, with a lactate moiety forming the phosphodiester and linking to an oligoglutamate chain (6). While the substitutions that distinguish 5-deazaflavins from flavins may seem superficial, pioneering work by Walsh has shown that they profoundly influence the physicochemical properties of these molecules (7, 8, 39, 43). Several years prior to their discovery in biology, chemically synthesized 5-deazaflavins (3, 4, 39) were used as probes to study the flavin-dependent reactions (40–43), revealing distinct electrochemical and photochemical properties from their flavin counterparts (44). Upon the discovery of 5-deazaflavins in biological systems (5, 6), it was realized that the electrochemical properties of these compounds are central to the role of F_{420} as a redox cofactor (6), while the photochemical properties are exploited by F_o as an antenna chromophore for DNA photolyases (45). Three features define the roles of 5-deazaflavins in biology.

(i) Two-electron carrier. Whereas flavins can serve as one or two electron carriers, 5-deazaflavins are obligate two-electron (hydride) carriers (44, 46). This is because flavins are stable as semiquinones (both neutral and anionic), whereas 5-deazaflavins are not. The nitrogen atom in position 5 is required for an unpaired electron to efficiently delocalize through the isoalloxazine ring; indeed, radicals of pyrazine groups (of flavins) are much lower energy than those of pyridine groups (of 5-deazaflavins) (7, 43). Reflecting this reactivity, F_{420}-dependent enzymes mediate diverse hydride transfer reactions that transform C=C and C≡C bonds (28, 29, 47, 48), alcohol and imine groups (49, 50), and certain inorganic compounds (51, 52). Furthermore, due to the substitution, 5-deazaflavins do not readily undergo single-electron reactions. Thus, unlike flavins, reduced 5-deazaflavins are relatively stable against air oxidation with a half-life on the order of hours instead of seconds for flavins (39, 44). This autooxidation in air has also been reported to be influenced by other factors such as stimulation from ambient light (8, 44) and, in the case of F_{420} and F_o, the addition of the 8-hydroxy group that results in the formation of a delocalized paraquinoid anion upon deprotonation of the oxidized species at pH above 6 (8). The low electrophilic reactivity of this anion results in a slower disproportionation/self-exchange reaction between F_{420} and $F_{420}H_2$ (8). Similarly, 5-deazaflavins also exhibit reduced reactivity with reducing agents that act primarily as single-electron donors (e.g., dithionite) (6, 8, 39).

(ii) Strong reductant. As a result of the substitution of N-5 to C-5, 5-deazariboflavin has a much lower standard redox potential (−310 mV) than riboflavin (−210 mV), FAD (−220 mV), or FMN (−190 mV) (7, 53). Due to the electron-withdrawing groups added to the isoalloxazine ring, F_o and F_{420} are even stronger reductants (−340 mV) than 5-deazariboflavin and thus some of the lowest-potential redox cofactors in biology (8, 9). This redox potential may be modulated under physiological conditions; for example, it will be −380 mV at standard temperature in hydrogenotrophic methanogens that maintain a 10:1 ratio of oxidized to reduced F_{420} (9). This redox potential places F_{420} at the center of the redox biology of methanogens (Table 1); the compound is capable of being reduced by exogenous fuels (H_2 and formate) and reoxidized by key cofactors (NADP and tetrahydromethanopterin derivatives) in an energetically efficient manner (7, 8, 53). Bacteria likewise appear to tightly couple substrate oxidation (glucose-6-phosphate and NADPH) to F_{420} reduction, presumably to en-

TABLE 1 List of standard redox potentials for key F_{420}-linked redox reactions[a]

Substrate[b]	Reaction	E_0' (mV)	Reference
Ferredoxin	$Fd + 2\ e^- \rightarrow Fd^{2-}$	−500 to −400	487
CO_2/formate	$CO_2 + 2\ e^- + H^+ \rightarrow HCO_2^-$	−420	487
H^+/H_2	$2\ H^+ + 2\ e^- \rightarrow H_2$	−410	487
Methenyl/methylene H_4MPT	$CH{\equiv}H_4MPT + 2\ e^- + H^+ \rightarrow CH_2{=}H_4MPT$	−390	301
F_{420}	$F_{420} + 2\ e^- + 2\ H^+ \rightarrow F_{420}H_2$	−340	8
6PGL/G6P	6-Phosphogluconolactone + $2\ e^- + 2\ H^+ \rightarrow$ Glucose-6-phosphate	−330	488
Methylene/methyl H_4MPT	$CH_2{=}H_4MPT + 2\ e^- + H^+ \rightarrow CH_3\text{-}H_4MPT$	−320	301
$NAD(P)^+$	$NAD(P)^+ + 2\ e^- + H^+ \rightarrow F_{420}H_2$	−320	487
Acetone/propan-2-ol	Acetone + $2\ e^- + 2\ H^+ \rightarrow$ Propan-2-ol	−290	53
FAD	$FAD + 2\ e^- + 2\ H^+ \rightarrow FADH_2$	−220	53
Riboflavin	$Riboflavin_{ox} + 2\ e^- + 2\ H^+ \rightarrow Riboflavin_{red}$	−210	53
FMN	$FMN + 2\ e^- + 2\ H^+ \rightarrow FMNH_2$	−190	53
Methanophenazine	$Mphen_{ox} + 2\ e^- + 2\ H^+ \rightarrow Mphen_{red}$	−170	489
Heterodisulfide	CoM-S-S-CoB + $2\ e^- + 2\ H^+ \rightarrow$ CoM-SH + CoB-SH	−140	487
Sulfite/sulfide	$SO_3^- + 6\ H^+ + 6\ e^- \rightarrow S^- + 3\ H_2O$	−120	490
Menaquinone	Menaquinone + $2\ e^- + 2\ H^+ \rightarrow$ Menaquinol	−70	53
O_2/H_2O	$O_2 + 4\ H^+ + 4\ e^- \rightarrow 2\ H_2O$	+820	53

[a] This list of standard redox potentials (E_0') demonstrates that the electrochemical properties of F_{420} enable the cofactor to mediate a wide range of oxidation and reduction reactions in biological systems, especially methanogenic archaea. In whole cells, physiological redox potentials can differ considerably due to the mass action ratios of substrates/products and differences in physical conditions (487). Potentials were determined under standard conditions (25°C, 1 atm, pH 7.0) against the standard hydrogen electrode.
[b] 6PGL, 6-phosphogluconolactone; $Mphen_{ox}$ and $Mphen_{red}$, oxidized and reduced methanophenazine, respectively.

hance catalytic efficiency (Table 1). Partly due to its low redox potential, the $F_{420}H_2$ produced is capable of reducing a wide range of organic compounds otherwise recalcitrant to activation as discussed in section 4 (28, 54, 55). Recent work also indicates that F_{420} may be utilized in aerobic bacteria in hypoxic and anoxic environments, potentially substituting for high-potential nicotinamide cofactors (NAD and NADP) (−320 mV) (30, 32, 56).

(iii) Intrinsic fluorophore. Like flavins, 5-deazaflavins are intrinsically fluorescent compounds. The delocalized charge on the isoalloxazine ring undergoes $\pi \rightarrow \pi^*$ transitions upon exposure to UV-visible light. In its oxidized state, the absorbance spectrum of F_{420} peaks at 420 nm, and the emission spectrum peaks at 470 nm (6) (Fig. 2). These peaks are pH dependent with a shift in the absorbance peak to 375 nm at lower pH along with reduced intensity (6). The reduced species $F_{420}H_2$ loses the absorbance peak at 420 nm for a new peak at 320 nm with a lower molar absorption coefficient (6) (Fig. 2). Due to the substitution of C-5 to N-5, the visible absorption spectra and fluorescence emission spectra of 5-deazaflavins are blue-shifted by about 50 nm compared to flavins (6, 44). As a result, light captured by 5-deazaflavins can be efficiently transferred to flavins through Förster resonance energy transfer (FRET). As elaborated below, this is central to the mechanism of the F_o-utilizing DNA photolyases (57, 58). The autofluorescence of F_{420} has also been used for detecting methanogens (59–66) and mycobacteria (67, 68).

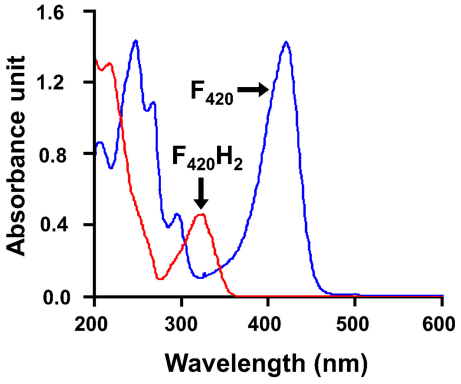

FIG 2 UV-visible absorption spectra of F_{420} (blue) and $F_{420}H_2$ (red). Adapted from reference 31.

2.2. Chromophore F_o

2.2.1. Biosynthesis

Despite its structural similarity to riboflavin, the biosynthetic pathway for F_o and other 5-deazaflavins diverges at an early step in the pathways leading to the synthesis of flavin cofactors (Fig. 3). The deazaflavin and flavin biosynthetic pathways both proceed from the pyrimidine ribityldiaminouracil (5-amino-6-ribitylamino-2,4[1*H*,3*H*]-pyrimidinedione). In the flavin pathway, this substrate is condensed with 3,4-dihydroxy-2-butanone 4-phosphate to make a lumazine derivative (6,7-dimethyl-8-ribityllumazine) (69); two of these molecules subsequently condense to regenerate 5-amino-6-ribitylamino-2,4(1*H*,3*H*)-pyrimidinedione with concomitant production of riboflavin (69). In the deazaflavin pathway, ribityldiaminouracil is instead condensed with the amino acid tyrosine (not 4-hydroxyphenylpyruvate as previously proposed [70]) leading to formation of F_o (71). The enzyme responsible for this condensation step, F_o synthase, is encoded by two polypeptides in archaea (CofG and CofH) (70) and a two-domain fusion protein (FbiC) in bacteria and eukaryotes (72). Each subunit/domain contains a radical *S*-adenosylmethionine (radical SAM) catalytic site (71, 73). A recent mechanistic study demonstrated that formation of the complex heterocycle depends on the coordinated action of the two radical SAM active sites, each of which abstract a hydrogen atom from the tyrosine (73).

2.2.2. Distribution

F_o serves as an antennal chromophore in DNA photolyases in a range of organisms across the three domains of life. Auxiliary to

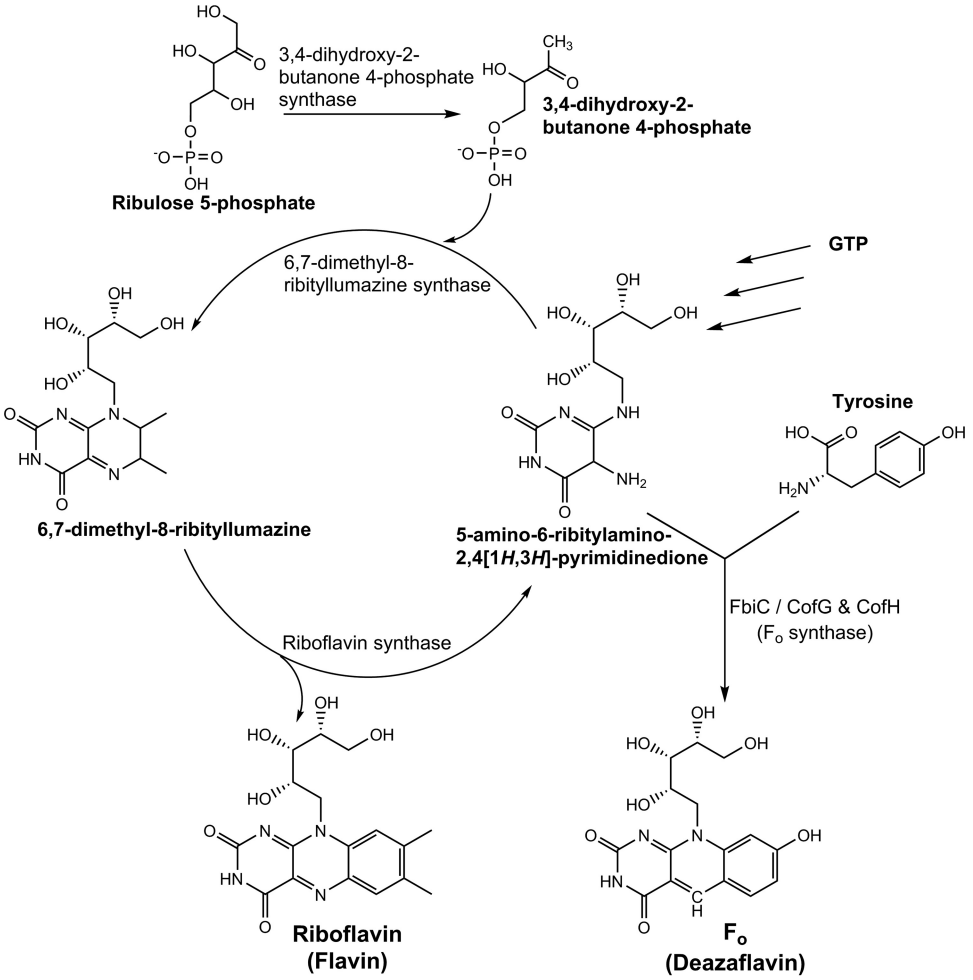

FIG 3 Summary of flavin and deazaflavin biosynthesis pathways.

the catalytic chromophore $FADH^-$, F_o captures light more effectively than $FADH^-$ owing to its longer wavelength absorption maximum and higher molar absorption coefficient (74). This is particularly important under low-light conditions, during which F_o enhances the efficiency of DNA repair by orders of magnitude (75). F_o-utilizing photolyases have been identified in multiple bacteria (e.g., *Synechococcus elongatus*, *Streptomyces griseus*) (76–80), archaea (e.g., *Methanothermobacter marburgensis*, *Methanosarcina mazei*, *Halobacterium halobium*) (81–83), and unicellular eukaryotes (e.g., *Acutodesmus obliquus*, *Chlamydomonas reinhardtii*, *Ostreococcus tauri*) (84–86). Genes encoding probable F_o synthases (CofG/CofH or FbiC) are consistently present in the genomes of such microorganisms. The question of whether F_o is utilized in higher eukaryotes is more controversial. Structural and chemical studies have demonstrated that F_o binds tightly to, and enhances the efficiency of, the two photolyases of the higher eukaryote *Drosophila melanogaster* (85, 87). Catalytically active and nucleus-targeted F_o-utilizing DNA photolyases are also known to be produced by insect baculoviruses (88–93). However, it is perplexing how such photolyases could utilize F_o *in vivo*, given that the genomes of higher eukaryotes lack F_o synthase-encoding genes (94). One explanation is that the dispensable F_o-binding domain of such enzymes is an evolutionary remnant, although it is also plausible that these organisms carry genes that encode components of a novel F_o biosynthesis pathway or acquire F_o from microbial endosymbionts and baculoviruses (85); in contrast to the highly anionic cofactors F_{420}, FMN, and FAD, F_o is uncharged and hence can readily diffuse through cell membranes (95–97). While F_o-utilizing DNA photolyases are widespread, they are hardly universal: photolyases of many species use different antennal chromophores or lack them altogether (75, 98), while eutherian lineages appear to have lost the capacity for light-driven DNA repair (99).

2.2.3. Enzymology

Enzymes of the DNA photolyase superfamily use the energy of blue light (350 to 450 nm) to facilitate the reductive cleavage of DNA pyrimidine dimers formed by far UV irradiation (200 to 300 nm). Distinct, but related, photolyases cleave cyclobutane pyrimidine dimers (CPD photolyases) and pyrimidine-pyrimidone photoproducts (6-4 photolyases) (75, 98). All DNA photolyases use the twice-reduced flavin $FADH^-$ as the catalytic chromophore. Most photolyases also use an antennal chromophore to optimize light capture, namely, methenyltetrahydrofolate or the flavin/deazaflavin compounds F_o, FMN, or FAD (100–103). Crystal structures reveal that the F_o-utilizing CPD photolyase (76, 77)

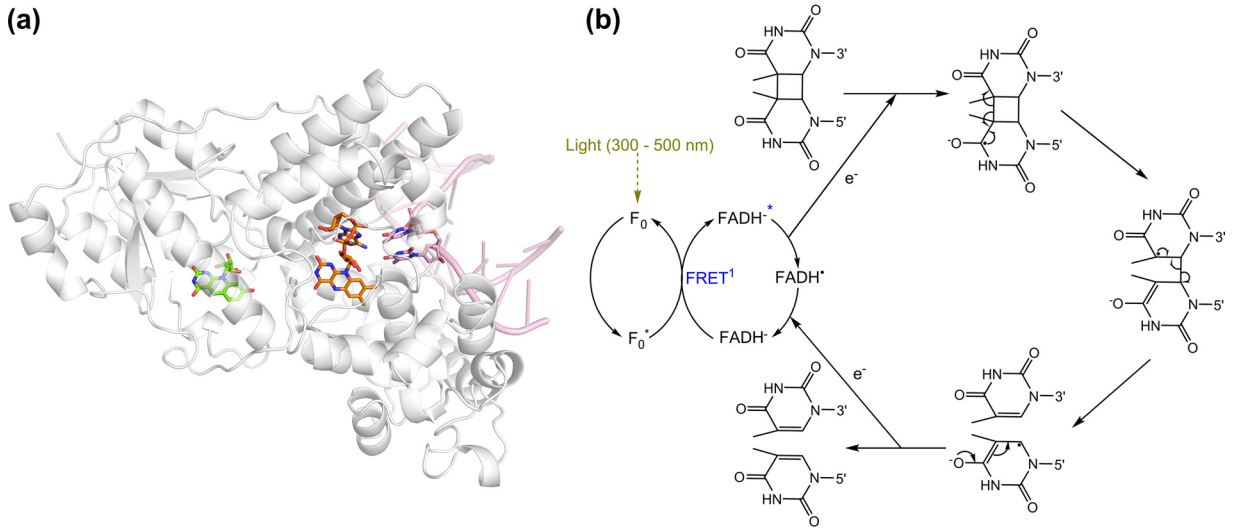

FIG 4 Structure and function of the F_o-utilizing DNA photolyases. (a) Crystal structure of the F_o-utilizing CPD photolyase of *Synechococcus elongatus* (PDB ID 1TEZ) (106). (b) Catalytic cycle of the enzyme. FRET is an acronym for Förster resonance energy transfer. The blue asterisk after $FADH^-$ indicates that the molecule is in the excited state.

from *Synechococcus elongatus* (Protein Data Bank [PDB] identifiers [IDs] 1QNF, 1TEZ, and 1OWL) (57, 104–106) is a single-subunit enzyme containing an N-terminal α/β domain and a C-terminal α-helical domain. Both chromophores are deeply buried, with F_o located in a cleft between the domains and $FADH^-$ embedded in the α-helical domain (Fig. 4) (57, 106). The ~17-Å distance between the chromophores enables efficient FRET while potentially preventing competitive electron transfer reactions between the cofactors (74).

The catalytic cycle of F_o-utilizing CPD photolyases has been elucidated through extensive spectroscopic and structural studies on the *S. elongatus* photolyase (Fig. 4). In the light-independent initial reaction, the enzyme recognizes and binds to damaged duplex DNA on the basis of its bent orientation (106). The antennal chromophore F_o thereafter captures a photon of blue light with an absorbance peak at 437 nm (red-shifted due to the strong interaction of the chromophore with the protein) (77). Femtosecond-scale spectroscopic studies show that F_o then transfers the energy to $FADH^-$ through FRET (107). The excited catalytic chromophore ($FADH^{-*}$) thereafter transfers an electron to the pyrimidine dimer, leading to its cleavage, and back-electron transfer restores the catalytic chromophore to an active form ready for a second catalytic cycle (108, 109). As reviewed in detail elsewhere (75, 110), similar reaction cycles facilitate light capture by other antennal chromophores and cleavage of pyrimidine-pyrimidone dimers. F_o-dependent photolyases are generally more efficient than methenyltetrahydrofolate-dependent ones, and the quantum yields of the energy transfer and electron transfer steps have been shown to be at near-unity (58, 107).

2.3. Cofactor F_{420}

2.3.1. Biosynthesis

The chemical structure of F_{420}, a lactyloligoglutamyl phosphodiester of F_o, was inferred from spectroscopic analysis of its degradation products (6) and validated by chemical synthesis (111–113) (Fig. 1). Reflecting its modular molecular structure, F_{420} is synthesized from several precursors: F_o, lactate, the amino acid glutamate, and the nucleotide GTP (97, 114, 115). Through a combination of biochemical and genetic studies in methanogens and mycobacteria, the majority of the steps in the F_{420} biosynthetic pathway have been resolved (Fig. 5).

There are two major steps in the conversion of F_o to F_{420}. In the first, the lactate-derived intermediate L-lactyl-2-diphospho-5′-guanosine (LPPG) is condensed with F_o (116) to form the phosphodiester F_{420}-0 (i.e., F_{420} containing no glutamate side chain). This reaction is catalyzed by a 2-phospho-L-lactate transferase (named CofD in archaea and FbiA in actinobacteria) (117, 118). The structure of this enzyme (PDB ID 3C3D) demonstrates that the deazaflavin ring of F_o interacts with a hydrophobic pocket and two water molecules, while the nucleotide moiety of LPPG is accommodated in a Rossmann fold domain with a Mg^{2+} ion. It is proposed that, following conformational changes initiated by substrate binding, the condensation proceeds following the abstraction of a proton from the terminal hydroxyl group of F_o by the β-phosphate of LPPG (119).

Thereafter, the nonribosomal peptide synthase F_{420}:γ-L-glutamyl ligase (CofE/FbiB) catalyzes the GTP-dependent addition of an oligoglutamate tail (118, 120–122). L-Glutamate residues are added via γ-linkages to F_{420}-0 (F_{420}-0 + glutamate + GTP → F_{420}-1 + GDP + P_i) and glutamated derivatives thereof (F_{420}-*n* + glutamate + GTP → F_{420}-*n* + 1 + GDP + P_i) in a sequential manner. The X-ray crystallographic structure of the enzyme from *Archaeoglobus fulgidus* (PDB ID 2PHN) demonstrates that it forms a butterfly-like homodimer that accommodates GTP and Mn^{2+} at the dimer interface. It is proposed that the cofactor is activated by phosphorylation (at the terminal hydroxyl group of the lactate moiety of F_{420} and the terminal glutamate of F_{420}-*n* derivatives), and the resultant acyl-phosphate is subject to nucleophilic attack by the amino group of the incoming glutamate residue (123). The number of glutamate residues on F_{420} is highly species specific, ranging from two or three in methanogens without cytochromes (124), four or five in methano-

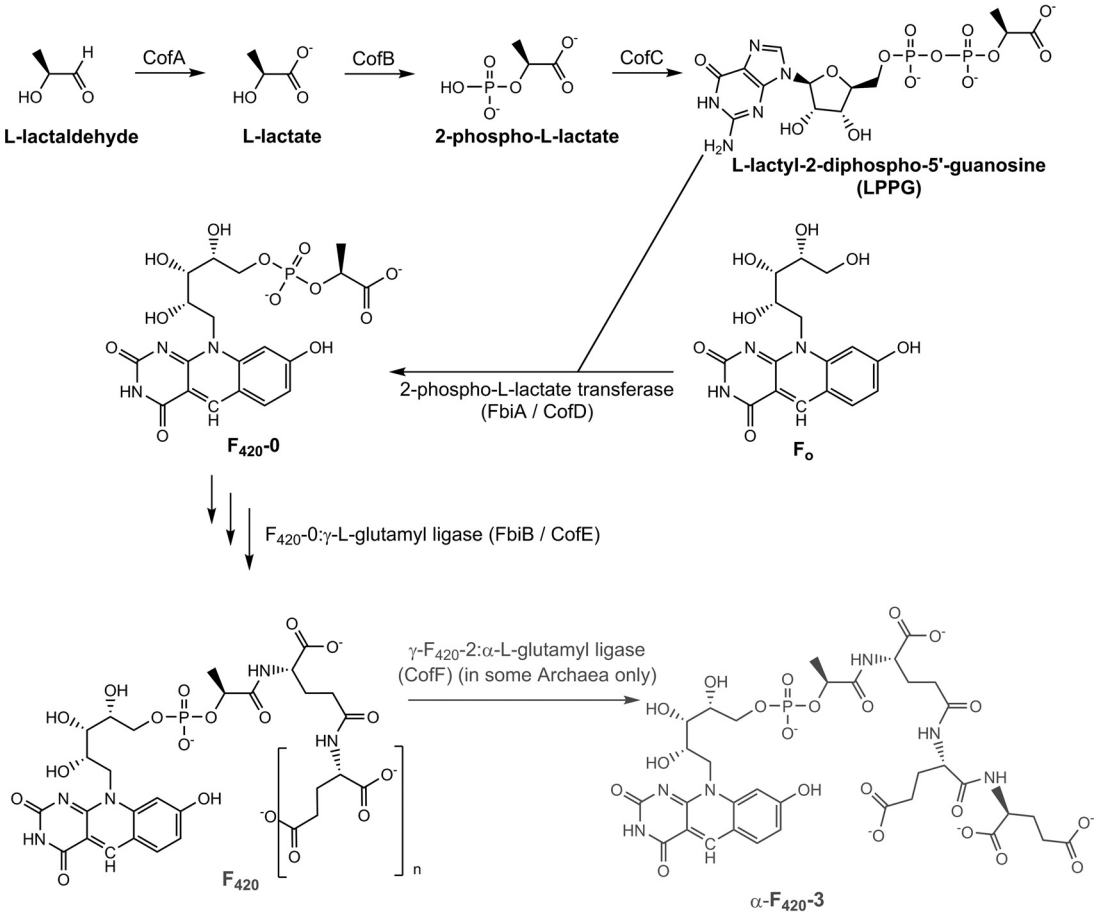

FIG 5 Summary of the F_{420} biosynthesis pathway from F_o.

gens with cytochromes (124), and five to seven in mycobacteria (125). The physiological significance and biochemical basis for these differences is not yet understood. In some archaea, a terminal α-linked glutamate residue (126, 127) is also added by γ-F_{420}-2:α-L-glutamate ligase (CofF) (128), an enzyme of the ATP-grasp superfamily.

The pathway that leads to the production of LPPG from the precursor L-lactate has only been partially resolved. Detailed studies on *Methanocaldococcus jannaschii* indicate that lactate is exclusively synthesized from L-lactaldehyde (129, 130); lactaldehyde is generated from the reduction of methylglyoxal or the aldol cleavage of fuculose-1-phosphate and is in turn oxidized to lactate by the NAD^+-dependent L-lactaldehyde dehydrogenase (CofA) (130). Though unconfirmed, it is assumed that lactate (synthesized from glycolytic pyruvate by L-lactate dehydrogenase) is also the precursor for LPPG in bacteria. It has been shown in methanogens that lactate can be phosphorylated to form 2-phospho-L-lactate in a GTP-dependent manner (116); however, the enzyme responsible (to be named CofB) has remained elusive in the 15 years since the reaction was discovered. Finally, the 2-phospho-L-lactate is converted to LPPG by the GTP-dependent enzyme 2-phospho-L-lactate guanylyltransferase (CofC) (PDB ID 2I5E) (116, 131). Homologous enzymes are required for F_{420} production in mycobacteria (132).

2.3.2. Distribution

F_{420} has a more restricted taxonomic distribution than F_o and the ubiquitous redox cofactors FAD, FMN, and NAD(P). The cofactor has been identified in a single phylum each of bacteria and archaea using analytical chemistry methods. Among the archaea, F_{420} is thought to be distributed in all methanogens, a group of strictly anaerobic methane-producing archaea (5, 15). In these organisms, F_{420} serves as a central catabolic cofactor and is also central to two of the three main methanogenesis pathways. While present in low levels in some methanogens (e.g., *Methanosarcinales*), it is present at concentrations between 100 to 400 mg per kg in many hydrogenotrophs (15, 61, 62). F_{420} has also been identified in several nonmethanogenic euryarchaeota, including three species of the sulfate-reducing genus *Archaeoglobus* (19, 133–135) and seven species of the photosynthetic genera *Halobacteria* and *Halococcus* (20, 136). The cofactor is also proposed to be central to the metabolism of the various lineages of the anaerobic methanotrophic archaea (ANME) (21, 137). Comparative genomics indicate that the genes required for F_{420} biosynthesis are also distributed in the *Thaumarchaeota*, *Aigarchaeota*, *Geoarchaeota*, *Bathyarchaeota*, and *Lokiarchaeota* (138–142). The absorbance spectra of single cells of the ammonia- and cyanate-oxidizing thaumarchaeon *Nitrososphaera gargensis* are also consistent with the presence of F_{420} (143, 144). It is unclear whether F_{420} is pro-

TABLE 2 Activity, role, and distribution of F_{420}-dependent oxidoreductases[a]

Oxidoreductase and domain	Physiological role[b]	Taxonomic distribution[c]	Description	EC no.	PDB ID	Reference(s)
F_{420}-reducing dehydrogenases						
Archaea						
Frh: F_{420}-reducing hydrogenase	Hydrogenotrophic methanogenesis. Couples oxidation of H_2 to reduction of F_{420}. May be physiologically reversible.	All orders of methanogens	Section 3.2.1	1.12.98.1	4OMF, 4CI0, 3ZFS	11, 16, 150, 219, 224, 227
Ffd: F_{420}-reducing formate dehydrogenase	Formatotrophic methanogenesis. Couples oxidation of formate to reduction of F_{420}. May be part of the electron-bifurcating complex.	*Methanobacteriales*, *Methanococcales*, *Methanopyrales*, *Methanomicrobiales*, *Methanocellales*	Section 3.2.2	1.2.99.9		17, 185, 190, 242, 259
Adf: F_{420}-reducing secondary alcohol dehydrogenase	Growth on secondary alcohols. Couples oxidation of secondary alcohols (e.g., isopropanol) to reduction of F_{420}.	*Methanomicrobiales*, *Methanocellales*	Section 3.2.3	1.1.98.5	1RHC	49, 271, 272
Bacteria						
Fno: F_{420}-reducing NADPH dehydrogenase	Exchanges electrons between NADP and F_{420}. F_{420} reduction important in bacteria, as F_{420} is the secondary cofactor.	Many *Actinomycetes* (e.g., *Streptomyces*, *Rhodococcus*, *Nocardia*, *Nocardioides*), *Alpha-* or *Betaproteobacteria*?	Section 4.2.1	1.5.1.40		12, 155
Fgd: F_{420}-reducing glucose-6-phosphate dehydrogenase	Heterotrophic growth. Couples oxidation of glucose-6-phosphate to reduction of F_{420} via the pentose phosphate pathway.	Many *Actinomycetes* (e.g., *Mycobacterium*, *Actinoplanes*, *Microbacterium*, *Amycolatopsis*), *Chloroflexi*?	Section 4.2.2	1.1.98.2	3B4Y	163
fHMAD: F_{420}-reducing hydroxymycolic acid dehydrogenase	Cell wall biosynthesis. Catalyzes F_{420}-dependent oxidation of hydroxymycolic acids to ketomycolic acids.	Few *Mycobacterium* (primarily pathogenic species)	Section 4.2.3			364, 365
$F_{420}H_2$-dependent reductases						
Archaea						
Mtd: F_{420}-reducing methylene-H_4MPT dehydrogenase	Reduces $CH{\equiv}H_4MPT$ to $CH_2{=}H_4MPT$ with $F_{420}H_2$ in methanogenesis. Reaction physiologically reversible.	All orders of methanogens, *Archaeoglobales*, ANME	Section 3.3.1	1.5.98.1	1QV9, 1U6I, 3IQF, 3IQE	18, 47, 166, 275, 284, 285
Mer: $F_{420}H_2$-dependent methylene-H_4MPT reductase	Reduces $CH_2{=}H_4MPT$ to CH_3-H_4MPT with $F_{420}H_2$ in methanogenesis. Reaction physiologically reversible.	All orders of methanogens, *Archaeoglobales*, ANME, *Halobacteriales*	Section 3.3.1	1.5.98.2	1F07, 1EZW, 1Z69	48, 159, 166, 284
Fpo: $F_{420}H_2$-dependent methanophenazine reductase	Proton-translocating primary dehydrogenase in respiratory chain transferring electrons from $F_{420}H_2$ to heterodisulfide	*Methanosarcinales*	Section 3.3.2	1.1.98.4		162, 304–306, 327
Fqo: $F_{420}H_2$-dependent quinone reductase	Proton-translocating primary dehydrogenase in respiratory chain transferring electrons from $F_{420}H_2$ to sulfate	*Archaeoglobales*, ANME	Section 3.3.2	1.1.98.4		21, 198–200
Fpr: $F_{420}H_2$-dependent oxidase	Detoxifies O_2 by mediating the four-electron reduction of O_2 to H_2O with $F_{420}H_2$	*Methanobacteriales*, *Methanococcales*, *Methanomicrobiales*, *Methanocellales*	Section 3.3.3	1.5.3.22	2OHH, 2OHI, 2OHJ	161, 192
Fsr: $F_{420}H_2$-dependent sulfite reductase	Detoxifies sulfite by mediating the six-electron reduction of sulfite to sulfide with $F_{420}H_2$. Also enables use of sulfite as an S source.	*Methanobacteriales*, *Methanococcales*	Section 3.3.4	1.8.98.3		51, 191

Fno: $F_{420}H_2$-dependent NADP reductase	Exchanges electrons between NADP and F_{420}. NADP reduction important in archaea, as NADP is the secondary cofactor.	All orders of methanogens, *Archaeoglobales*, ANME	Section 3.3.5	1.5.1.40	1JAY, 1JAX	16, 22, 160, 201
Bacteria						
Ddn: $F_{420}H_2$-dependent nitroreductases	May serve to detoxify redox cycling agents and other exogenous compounds. Also catalyze nitroimidazole activation.	Most *Actinomycetes* (e.g., *Mycobacterium*, *Streptomyces*, *Rhodococcus*), *Chloroflexi*?, *Methanosarcinales*?	Section 4.3.1		3H96, 4Y9I, 3R5R, 3R57	28, 30, 32, 164
Fbr: $F_{420}H_2$-dependent biliverdin reductases	Reduce the heme degradation product biliverdin to bilirubin. May also reduce mycobillins. FDOR-B3 and -B4 family.	Most *Actinomycetes* (e.g., *Mycobacterium*, *Streptomyces*, *Rhodococcus*), *Chloroflexi*?, *Halobacteriales*?	Section 4.3.1		2ASF, 4QVB, 1W9A	30, 165, 418, 419
Fts: $F_{420}H_2$-dependent tetracycline synthases	Reduce dehydrotetracyclines during streptomycete antibiotic synthesis. Role in mycobacteria unknown. FDOR-B1 family.	Most *Actinomycetes* (e.g., *Mycobacterium*, *Streptomyces*, *Rhodococcus*), *Chloroflexi*?, *Halobacteriales*?	Section 4.3.1		3F7E, 1RFE	28–30
Other $F_{420}H_2$-dependent flavin/deazaflavin oxidoreductases	Activities of A2-A4, B1, B2, B5, B6, AA1-AA5 families unknown. AA1s may be fatty acid saturases.	Most *Actinomycetes* (e.g., *Mycobacterium*, *Streptomyces*, *Rhodococcus*), *Chloroflexi*?, *Halobacteriales*?	Section 4.3.1		4ZKY	30, 55
Fht: $F_{420}H_2$-dependent picrate reductases	Reduces 2,4,6-trinitrophenol (picrate) for use as a C and N source through hydride transfer to the nitroaromatic ring	Few *Actinomycetes* (*Rhodococcus*, *Nocardia*, *Nocardioides*)	Section 4.3.2			54, 155
Fps: $F_{420}H_2$-dependent tetrahydropyrrole synthases	Reduces 4-propylidene-3,4-dihydropyrrole-2-carboxylate during biosynthesis of pyrrolobenzodiazepines antibiotics	Few *Actinomycetes* (*Streptomyces*, *Streptosporangium*)	Section 4.3.2			50, 389
Other $F_{420}H_2$-dependent luciferase-like hydride transferases	Unknown. Likely to have diverse roles in endogenous and exogenous redox metabolism of organic compounds.	Most *Actinomycetes* (e.g., *Mycobacterium*, *Streptomyces*, *Rhodococcus*)	Section 4.3.2			

[a] For more information about the enzymes, see the sections in the text where the enzymes are described, Enzyme Commission (EC) entries, Protein Data Bank structures, and key primary references.

[b] Note that several of F_{420}-dependent reactions are physiologically reversible, including those catalyzed by Fno, Mtd, Mer, and possibly Frh. Fno is primarily an $F_{420}H_2$-dependent NADP reductase in methanogens and a F_{420}-reducing NADPH dehydrogenase in bacteria; the enzyme appears to be similar in archaea and bacteria but is used in a different physiological context.

[c] *Euryarchaeota* are listed by order, namely, six methanogenic orders (*Methanobacteriales*, *Methanococcales*, *Methanopyrales*, *Methanomicrobiales*, *Methanocellales*, and *Methanosarcinales*) and two nonmethanogenic orders (*Archaeoglobales* and *Halobacteriales*). The various lineages of the uncultured anaerobic methanotrophic archaea are denoted as ANME. Actinobacteria are listed by genus (*Mycobacterium*, *Streptomyces*, *Rhodococcus*, *Nocardia*, *Nocardioides*, *Streptosporangium*, *Microbacterium*, *Actinoplanes*, and *Amycolatopsis*).

duced by *Crenarchaeota*; while the cofactor was reported to be present at low levels in representatives of the *Sulfolobus* and *Thermoplasma* (20), the genomes of these organisms suggest that in fact they lack the capacity to synthesize this deazaflavin by any currently understood biosynthetic mechanism.

It is assumed that F_{420} has a more restricted distribution among bacteria. The cofactor has been identified in representatives of the actinobacterial genera *Mycobacterium* (23, 27, 125, 145), *Streptomyces* (25, 27, 29, 146), *Nocardia* (27, 145), and *Nocardioides* (54). Most of these representatives are saprophytic soil bacteria that adopt a heterotrophic, aerobic lifestyle. The cofactor has also been reported in several mycobacterial pathogens, namely, the major obligate pathogens *Mycobacterium tuberculosis*, *Mycobacterium bovis*, and *Mycobacterium leprae*, as well as several opportunistic species (145). Comparative genomic analyses show that the genes involved in F_{420} biosynthesis and utilization are also found in representatives of the *Chloroflexi*, *Alphaproteobacteria*, *Betaproteobacteria*, and *Gammaproteobacteria* (30, 37), which constitute some of the most dominant taxa in aerated soil ecosystems (147). The occasional references to F_{420}-dependent processes in *Cyanobacteria* are erroneous; these have emerged from authors misattributing F_o-dependent processes to F_{420} (72, 148) or relying on incorrect automated sequence predictions (149). Indeed, F_{420} has yet to be chemically identified in any species outside the phyla *Euryarchaeota* and *Actinobacteria*.

2.3.3. Enzymology

In most archaea and some actinobacteria, F_{420} is reduced through coupled steps in central catabolic pathways (Table 2). Methanogens are able to oxidize their substrates for growth using F_{420}, i.e., H_2 (via the F_{420}-reducing hydrogenase [Frh]) (150), formate (via the F_{420}-reducing formate dehydrogenase [Ffd]) (17), or secondary alcohols (via the F_{420}-reducing secondary alcohol dehydrogenase [Adf]) (49). This facilitates the entry of electrons into the CO_2-reducing pathway of methanogenesis and generates $F_{420}H_2$ to drive cellular redox reactions (151). Note that, contrary to historical reports (152, 153), carbon monoxide dehydrogenase, pyruvate dehydrogenase, and α-ketoglutarate dehydrogenase of methanogens are not F_{420} dependent in methanogens (151, 154). Mycobacteria also reduce F_{420} via their central catabolic pathways by using the F_{420}-reducing glucose-6-phosphate dehydrogenase (Fgd), one of two entry points to the reductive pentose phosphate pathway. However, pathways also exist to reduce F_{420} using other redox cofactors depending on external and internal redox states, i.e., NADP (via the F_{420}-NADP oxidoreductase [Fno]) in many actinomycetes (12, 155) and tetrahydromethanopterin (via methylene tetrahydromethanopterin dehydrogenase [methylene-H_4MPT dehydrogenase {Mtd} and methylene-H_4MPT reductase {Mer}]) in methylotrophic methanogens (156, 157). As emphasized by the central placement of F_{420} in the redox ladder of Table 1, many of these reactions are physiologically reversible. The physiology and biochemistry of the F_{420}-reducing dehydrogenases is discussed in detail in sections 3.2 and 4.2.

The physiological roles of F_{420} are primarily elicited by the coupling of the oxidation of $F_{420}H_2$ to the reduction of other compounds (Table 2). In methanogens, $F_{420}H_2$ oxidation sustains a wide range of processes. $F_{420}H_2$ is used to reduce one-carbon units bound to tetrahydromethanopterin, the central one-carbon carrier in methanogenesis pathways (158), and NADP, the central cofactor for anabolic processes (16). This depends on the aforementioned reactions catalyzed by Mtd (47), Mer (159), and Fno (160). The cofactor can additionally be used to detoxify O_2 (via $F_{420}H_2$-dependent oxidase [Fpr]) (161), mobilize sulfite (via $F_{420}H_2$-dependent sulfite reductase [Fsr]) (51), and in methanogens with cytochromes, reduce methanophenazine for respiratory energy conservation (via $F_{420}H_2$-dependent methanophenazine reductase [Fpo]) (162). $F_{420}H_2$ can be used to reduce diverse organic compounds in actinomycetes, including endogenous metabolites (e.g., quinones, porphyrins, fatty acids) (30, 32) and exogenous compounds (e.g., tetracyclines, picrate, aflatoxins) (28, 29, 54). These activities depend on two diverse superfamilies distinguished by their split β-barrel (flavin/deazaflavin oxidoreductases [FDORs]) (30, 37) or TIM barrel (luciferase-like hydride transferases [LLHTs]) protein folds (Fig. 6) (37). The $F_{420}H_2$-dependent reductase enzymes are discussed in more detail in sections 3.3 and 4.3.

The majority of F_{420}- and $F_{420}H_2$-binding proteins bind the cofactor within either TIM barrel (Adf, Mer, F_{420}-reducing hydroxymycolic acid dehydrogenase [fHMAD], Fgd, and other LLHTs) (48, 49, 163), FrhB-like (Frh, Fpo, Ffd, and Fsr) (150), or split β-barrel (FDORs) (28, 30, 164, 165) folds (Fig. 6). Exceptions to this are the structures of Mtd (novel Mtd-like fold) (166), Fno (Rossmann fold) (160), and Fpr (interface of β-lactamase and flavodoxin folds) (52). Of these known F_{420} binding architectures, the F_{420}-binding TIM barrel and split β-barrel proteins share structural homology with related FMN- and FAD-binding proteins (30, 48). In contrast, the Mtd-like and FrhB-like folds have been found only in F_{420}- or $F_{420}H_2$-dependent proteins (150, 166). All of the proteins carry out hydride transfer on the *Si*-face of F_{420} (48, 49, 150, 160, 163, 166, 167), with the exception of the FDORs that catalyze the reaction on the *Re*-face (28, 165). These proteins are adapted for F_{420} binding by the presence of a positively charged channel or region that associates with the phospholactate and polyglutamate chain. In FDORs, LLHTs, Mtd, and Fno, hydrogen bonding interactions at the pyrimidine and hydroxyl of the deazaflavin moiety anchor the cofactor, along with hydrophobic interactions to the *Re*-face (*Si*-face for FDORs) that is not involved in the enzyme reaction (28, 48, 49, 150, 160, 161, 163–166). In FrhB, Fno, and Fpr, stability is also provided by aromatic interactions with the enzyme-bound FAD, NADP, or FMN (52, 150, 160).

3. F_{420} IN METHANOGENS AND OTHER ARCHAEA

3.1. Physiological Roles

3.1.1. Methanogens

F_{420} is a catabolic redox cofactor in both methanogenic and nonmethanogenic archaea. Methanogens are microorganisms that produce methane as the end product of their anaerobic pathways of energy generation (168). These organisms encompass at least six phylogenetically distinct, metabolically diverse orders of the archaeal phylum *Euryarchaeota*: *Methanobacteriales*, *Methanococcales*, *Methanopyrales*, *Methanomicrobiales*, *Methanocellales*, and *Methanosarcinales* (169–173). F_{420} is synthesized in all of these orders, where it serves as a redox cofactor in both methanogenesis pathways and wider cellular processes (5, 15). In fact, the characteristic fluorescence of many methanogens is due to the presence of this cofactor (5, 59, 60).

Methanogens can generate methane through three major routes, the CO_2-reducing, methylotrophic, and aceticlastic path-

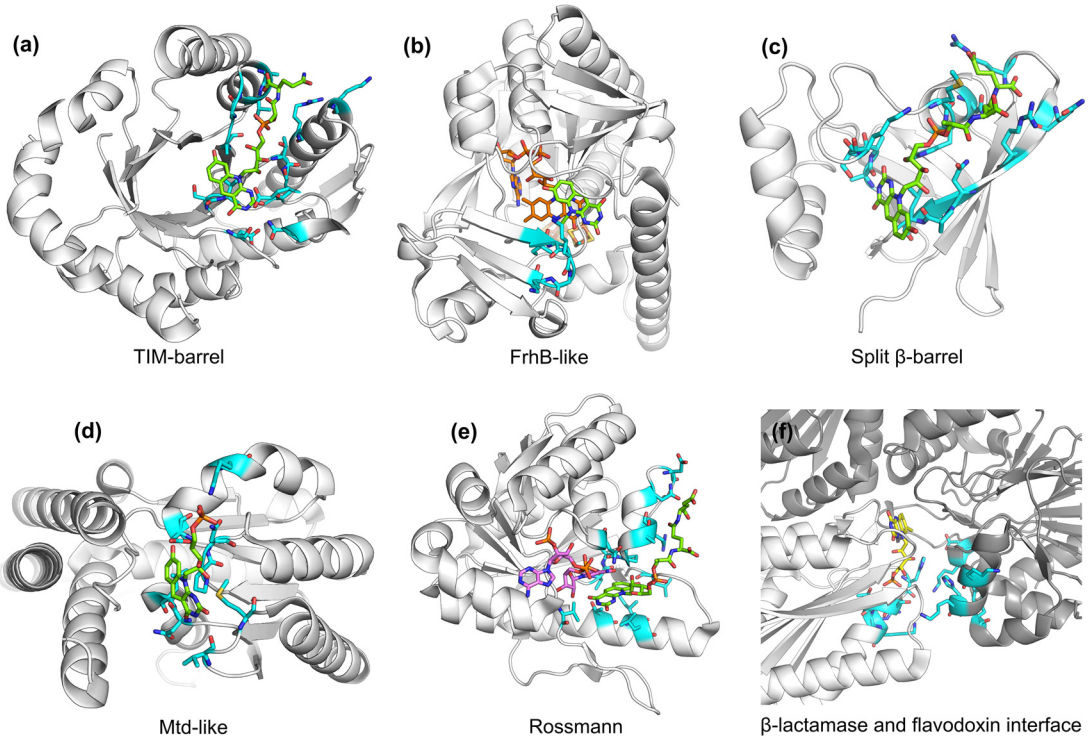

FIG 6 Structures of F_{420}-binding protein domains. (a) TIM barrel fold of Fgd (PDB ID 3B4Y [163]), (b) structure of Frh subunit B (PDB IDs 4OMF [150] and 3ZFS [167]), (c) split β-barrel fold of Ddn (PDB ID 3R5R [164]), (d) novel protein fold of Mtd (PDB ID 3IQE [166]), (e) Rossmann fold of Fno (PDB ID 1JAY [160]) and (f) the interface between β-lactamase and flavodoxin folds in Fpr (PDB ID 2OHJ [161]). Where available, the F_{420} molecule is shown in green, and key residues at the F_{420}-binding site are highlighted in cyan. In panels b, d, and f, the positions of the FAD (orange), NADP (purple), and FMN (yellow) molecules required for F_{420} binding are also shown.

ways (174–177) (Fig. 7). In the CO_2-reducing pathway, CO_2 is progressively reduced to methane using exogenously derived electrons (151, 168, 178). This pathway sustains hydrogenotrophic growth using H_2-derived electrons (16), formatotrophic growth using formate-derived electrons (17), and in some organisms, growth on secondary alcohols (179). In the methylotrophic pathway, the methyl groups of methanol, methylated amines, and methylated sulfides are converted into CH_4 (reductive route) and CO_2 (oxidative route), with the oxidative reactions occurring through a reverse arm of the CO_2-reducing pathway (157, 175, 180). In the aceticlastic pathway, acetate is fermented to methane (through reduction of the methyl group) and CO_2 (through oxidation of the carboxy group) (175, 180, 181). Most methanogens are capable of hydrogenotrophic growth, with cytochrome-containing methanogens (i.e., the *Methanosarcinales*) primarily respiring H_2 and the other five orders conserving energy through electron-bifurcating pathways (182, 183). Formatotrophic growth is also widespread (17, 184, 185), but it does not occur in the *Methanosarcinales* (186). In contrast, only a few taxa are capable of methylotrophic growth (the family *Methanosarcinaceae* and genus *Methanosphaera*) (176, 187) and aceticlastic growth (the families *Methanosarcinaceae* and *Methanosaetaceae*) (176, 188). These pathways are nevertheless quantitatively important, with the aceticlastic pathway responsible for up to two-thirds of global net methane production. The biochemistry, physiology, and ecology of methanogenesis will be discussed further only in the context of F_{420} metabolism; readers requiring further background on this topic are referred to several excellent reviews (151, 154, 168, 178, 182, 189).

F_{420} is central to the CO_2-reducing and methylotrophic pathways of methanogenesis. Dedicated F_{420}-dependent hydrogenases/dehydrogenases oxidize H_2 (Frh) (17, 150), formate (Ffd) (17, 190), and secondary alcohols (Adf) (49, 179) for entry into the CO_2-reducing pathway. F_{420} also serves as the redox cofactor for the Mtd and Mer reactions, which mediate the fourth and fifth steps of the CO_2-reducing pathway, reducing methenyl-tetrahydromethanopterin (methenyl-H_4MPT) to methyl-H_4MPT with $F_{420}H_2$ (47, 159). They operate in the reverse direction in the methylotrophic pathway, oxidizing methyl-H_4MPT to methenyl-H_4MPT. However, F_{420} is not involved in the aceticlastic pathway, which depends on a largely distinct set of enzymes (175, 181). In addition to mediating methanogenesis, dedicated F_{420}-dependent enzymes mediate a wide array of other cellular reactions in methanogens, including reduction of NADP for biosynthetic pathways (Fno) (22), mobilization of sulfite as a sulfur source (Fsr) (51, 191), and detoxification of atmospheric O_2 (Fpr) (161, 192). Methanogens with cytochromes can use $F_{420}H_2$ generated through the methylotrophic pathway as an input to the respiratory chain using the proton-translocating $F_{420}H_2$-reducing methanophenazine reductase (Fpo) (162, 193). Interestingly, F_{420} is still present in acetate-grown *Methanosarcina* (194) and the obligately aceticlastic genus *Methanosaeta* (195, 196), reinforcing the idea that the cofactor has been selected for roles well beyond methanogenesis. On the basis of metagenomic studies, it was recently reported that members of the newly defined phylum *Bathyarchaeota* may also be F_{420}-dependent methylotrophic methanogens (141).

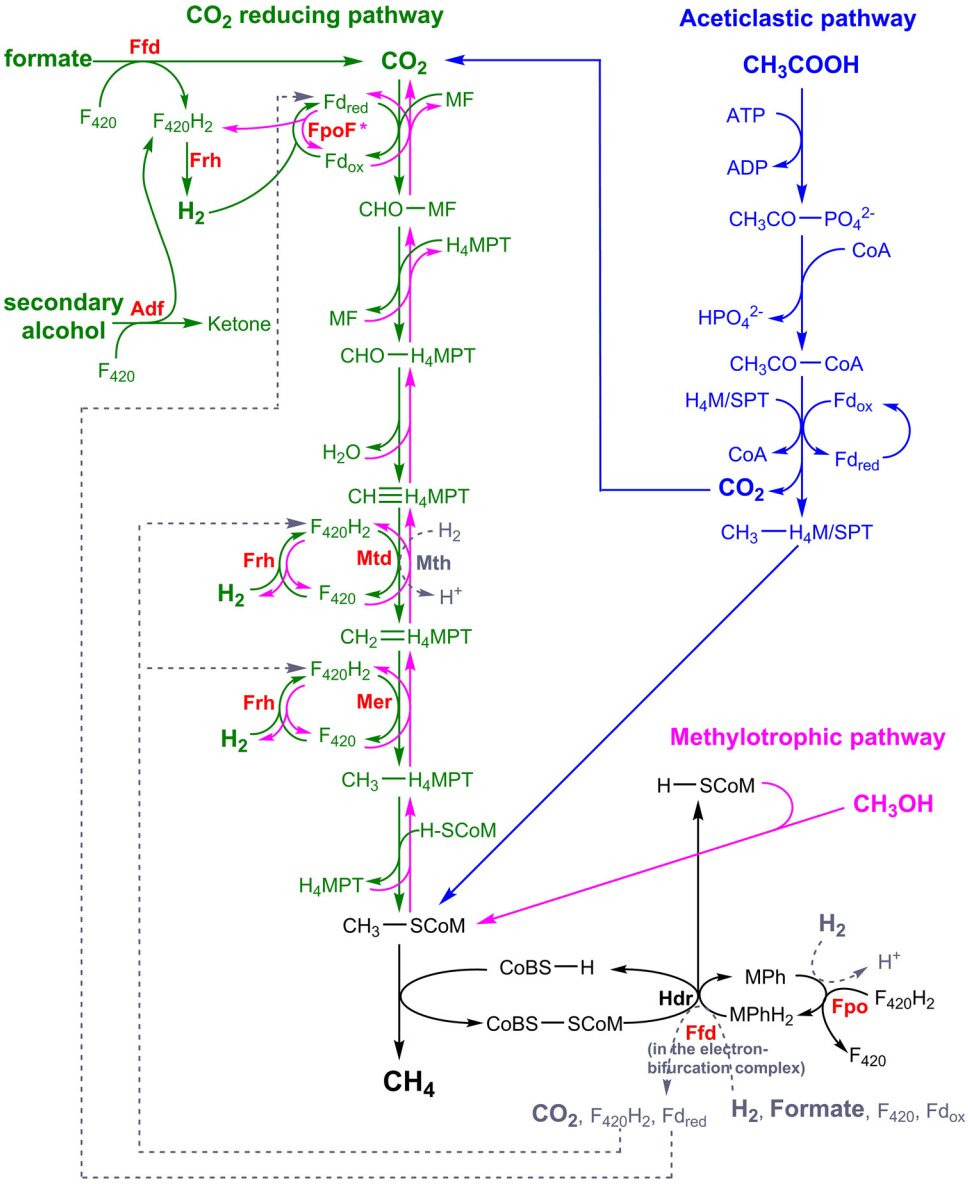

FIG 7 CO_2-reducing (green), methylotrophic (pink), and aceticlastic (blue) pathways of methanogenesis. The routes for energy generation from H_2/CO_2, formate, secondary alcohols, methanol, and acetate are shown. Processes common to all pathways are shown in black, and dashed arrows in gray show alternative pathways. F_{420}-dependent oxidoreductases are highlighted in red and catalyze both forward and reverse reactions, except for FpoF which is known to catalyze only $F_{420}H_2$ reoxidation. Abbreviations: $Fd_{red/ox}$, reduced/oxidized ferredoxin; MF, methanofuran; H_4MPT, tetrahydromethanopterin; H_4SPT, tetrahydrosarcinapterin; H-SCoM, 2-mercaptoethanesulfonate (reduced coenzyme M); CoBS-H, N-7-mercaptoheptanoylthreonine phosphate (reduced coenzyme B); MPh/$MPhH_2$, reduced/oxidized methanophenazine.

3.1.2. Sulfate-reducing archaea

F_{420} is also known to be synthesized by two orders of nonmethanogenic archaea, the *Archaeoglobales* and *Halobacteriales* (20, 136). *Archaeoglobi* are primarily heterotrophic, sulfate-reducing thermophiles that inhabit deep-sea vents (19), whereas *Halobacteria* are primarily phototrophic, facultatively aerobic halophiles that dominate hypersaline waters (197). While the two orders have very different metabolisms, both to methanogens and to each other, they are closely phylogenetically related to the *Methanomicrobiales*, *Methanosarcinales*, and *Methanocellales* (169, 171, 172). It is likely that F_{420} was synthesized in the common ancestor of each of these five orders prior to their metabolic divergence. While little is known about the role of F_{420} in *Halobacteria* (20, 136), a range of biochemical studies indicate that $F_{420}H_2$ is a central catabolic electron donor in *Archaeoglobus fulgidus* (133). $F_{420}H_2$ donates electrons to the sulfate-reducing respiratory chain via the proton-translocating $F_{420}H_2$-dependent quinonereductase (Fqo) (198–200). Additionally, the $F_{420}H_2$-dependent NADP reductase (Fno) is proposed to generate NADPH for various biosynthetic pathways (160, 201). F_{420} appears to be reduced through distinct routes depending on whether the growth substrate is H_2/CO_2 or lactate. It is well-established that, during the anaerobic oxidation of lactate to CO_2, F_{420} can be reduced by Mtd and Mer (133, 200, 202). Given that the organism lacks Frh, it

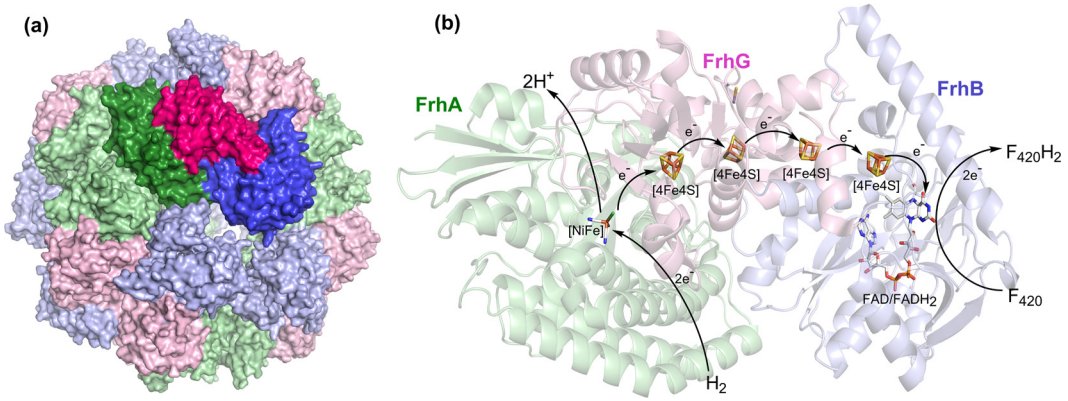

FIG 8 (a) Structure of the dodecameric complex of Frh (PDB ID 4OMF [150]), where a single protomer (identified with darker shades) contains three subunits: FrhA (green), FrhB (blue), and FrhG (pink). (b) Electron transfer route from H_2 to F_{420} within the Frh subunits during hydrogenotrophic methanogenesis.

remains to be resolved how *A. fulgidus* generates $F_{420}H_2$ during hydrogenotrophic growth (203); possible routes include electron transfer from reduced ferredoxin (Fd_{red}) (via a hypothetical complex), quinols (via reverse electron transfer), or NADPH (via Npo) (135, 200).

3.1.3. Methanotrophic archaea

There is strong evidence that F_{420} is also central to the metabolism of anaerobic methanotrophic archaea (ANME). In contrast to methanogens, these archaea consume, rather than produce, methane and use the electrons liberated from methane to drive sulfate- and nitrate-reducing respiratory chains (204–207). While these organisms have yet to be successfully cultured, they are of enormous ecological and geochemical significance; it is predicted that 90% of the methane produced by methanogens in marine sediments is immediately recycled by ANME (189, 208, 209). Extensive studies of microbial ecology have demonstrated that these organisms are closely related to two orders of methanogens (*Methanosarcinales* and *Methanomicrobiales*), and form at least three major phylogenetic clades (ANME-1, ANME-2, and ANME-3) (210, 211). A range of genomic and biochemical evidence suggests that these archaea predominantly grow through a reverse methanogenesis pathway (similar to the methylotrophic pathway; Fig. 7), through which $F_{420}H_2$ is generated via the Mer and Mtd reactions (137, 212–215). The $F_{420}H_2$ that is produced from this pathway is proposed to be reoxidized by the proton-translocating Fqo complex, with sulfate or nitrate serving as the terminal respiratory electron acceptor (21, 215). This proposal was recently supported by a metagenomic/metatranscriptomic study that showed that the nitrate-reducing methanotroph *Methanoperedens nitroreducens* (part of the ANME-2 lineage) expresses a complete reverse methanogenesis pathway, along with all the F_{420} biosynthesis genes and a putative Fqo complex (137). Environmental sequencing has also inferred a role for F_{420} in other ANME lineages (21, 215, 216). Also consistent with the presence of F_{420}, ANME, like methanogens, are autofluorescent under UV light (217, 218).

3.2. F_{420}-Reducing Dehydrogenases

3.2.1. Frh: F_{420}-reducing hydrogenase

The F_{420}-reducing hydrogenase directly couples H_2 to F_{420} reduction (9, 11, 219, 220). The enzyme is encoded by genes in all classes of methanogens (183) and is the preferred route to F_{420} reduction during hydrogenotrophic methanogenesis (Fig. 7) (221–223). This hydrogenase is essential for growth on H_2/CO_2 in *Methanosarcina barkeri* (*Ms. barkeri*) (224), but it appears to be dispensable in methanogens with genes that encode an alternative pathway for F_{420} reduction such as *Methanococcus maripaludis* (*Mc. maripaludis*) (225). The enzyme complex, encoded by the transcriptional subunit *frhADGB* (222), is a product of the association of an F_{420} reductase subunit of the F_{420}-binding protein family (functionally analogous to F_{420} reductase domains of Fsr, Fpo, and Ffd) with a H_2-oxidizing [NiFe]-hydrogenase of the group 3a family (226). Structural characterization of this complex from *Methanothermobacter marburgensis* through cryo-electron microscopy (167, 227) and X-ray crystallography (150) revealed a large dodecameric complex of heterotrimers (FrhABG), arranged as a shell with a solvent-filled core (Fig. 8). Each heterotrimeric protomer (FrhABG) contains a [NiFe]-hydrogenase large subunit (FrhA; matured by the endopeptidase FrhD), a [NiFe]-hydrogenase small subunit (FrhG), and an F_{420} reductase subunit (FrhB). While the complex is located in the cytoplasm (150), it is often purified from the membrane fraction due to its high molecular mass of 1.2 MDa (228–230).

During the H_2-dependent reduction of F_{420}, H_2 binding and oxidation occur at the buried [NiFe] center of FrhA, which is facilitated by a hydrophobic channel that extends from the [NiFe] center to the outer surface of the enzyme complex (150). On the basis of structural and spectroscopic studies, it is proposed that H_2 is heterolytically cleaved in a mechanism similar to other [NiFe]-hydrogenases (150, 219, 231–233). As with other [NiFe]-hydrogenases, the protons generated are relayed from the [NiFe] center to the outer surface of the complex, where they are released to the bulk solvent near a covalently bound FAD molecule on the FrhB subunit of a neighboring protomer (150). Concomitantly, electrons from the H_2 cleavage reaction are individually transferred via four [4Fe4S] clusters (three on FrhG and one on FrhB) to the FAD molecule bound to FrhB of the same protomer, generating $FADH_2$ (Fig. 8). The terminal step involves hydride transfer from $FADH_2$ to F_{420}, which binds reversibly at a solvent-accessible pocket on FrhB, with the 5-deazaflavin rings (*Si*-face) next to the isoalloxazine of the FAD cofactor (*Si*-face) (150, 234). Kinetic and structural data suggest that hydride transfer to F_{420} occurs rapidly and is rate limited by diffusion, rather than conformational change (227, 235). The remarkable oligomerization of the com-

plex does not appear to influence the reaction kinetics of the hydrogenase and instead may serve to protect metal centers from redox-active compounds of the cytosol (150).

It has been proposed that Frh is physiologically active in both the forward and reverse directions (224, 225). While Frh primarily sustains H_2-mediated F_{420} reduction during hydrogenotrophic growth, it may mediate $F_{420}H_2$-mediated H_2 production during methylotrophic methanogenesis and formate-dependent growth (224, 225). This is consistent with the observations of severe defects of *Ms. barkeri* Δ*frh* mutants during growth on methanol and on H_2 production during formate-dependent growth of *Mc. maripaludis* (225). While F_{420} reduction is more thermodynamically favorable (E_0 F_{420} = −340 mV; E_0 H_2 = −410 mV), the reverse reaction may occur when $F_{420}H_2$ accumulates and H_2 partial pressure [pH_2] is low. This is supported by biochemical data that Frh purified from *Methanobacterium formicum* can sustain a moderate rate of $F_{420}H_2$-mediated H_2 evolution (230). However, genetic dissection experiments will be required to definitively confirm whether Frh-mediated H_2 evolution can occur *in vivo* at physiologically relevant rates.

Several variants of Frh can be encoded by genes in the same genome. Many methanogens carry genes that encode both a selenium-containing F_{420}-reducing hydrogenase (Fru) in addition to a selenium-free one (Frh) (183, 221, 222). Studies on the purified [NiFeSe]-hydrogenase from *Methanococcus voltae* suggest that the selenium-containing isozymes are faster acting and more oxygen tolerant than the selenium-free variant (236, 237). Hence, transcription of Fru over Frh occurs in selenium-containing conditions in this organism (221, 238, 239). In addition, variants of Frh were recently found to be encoded by genes of several non-F_{420}-producing species of the archaeal order *Thermococci* and the bacterial family *Desulfobacteriaceae* (183). Biochemical and sequence analyses indicate that these enzymes cannot reduce F_{420} and instead couple to another electron acceptor, such as a flavin (240); these enzymes and their F_{420}-reducing relatives are capable of reducing FAD and FMN *in vitro* (16, 240).

3.2.2. Ffd: F_{420}-reducing formate dehydrogenase

Many hydrogenotrophic methanogens can also grow using formate as the sole electron donor, including species from the genera *Methanococcus* (241, 242), *Methanobacterium* (243), and *Methanospirillum* (184). This process is especially ecologically significant, given that formate produced by fermentative bacteria can be consumed by methanogens through interspecies transfer (244). It is well established that formatotrophic growth is linked to F_{420} metabolism (17) and that it depends on F_{420}-reducing formate dehydrogenases (called Ffd or Fdh) (242). Although Ffd has not been structurally characterized, biochemical studies on the enzyme from *Methanobacterium formicicum* (*Mb. formicicum*) have revealed its core architecture. Ffd is a membrane-bound heterodimeric enzyme containing several redox centers (190, 245, 246). The large subunit is homologous with the structurally characterized bacterial formate dehydrogenases (247), and it is predicted to contain a molybdopterin guanine nucleotide cofactor (MGD) (248–252) and a [4Fe4S] center (190). The small subunit is unique to methanogenic archaea and is predicted to contain two [4Fe4S] clusters (190), an FAD cofactor (190, 253, 254), and an F_{420}-binding site that is homologous to FrhB (150). It has been proposed that formate is oxidized at the molybdopterin center and that electrons are shuttled via the FeS clusters to the electron gate FAD

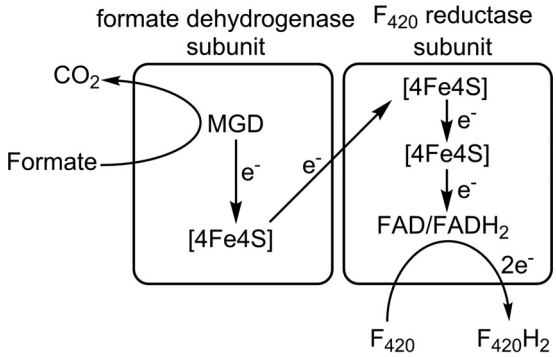

FIG 9 Proposed architecture of Ffd and electron transfer route from formate to F_{420}.

and finally to F_{420} (254) (Fig. 9). Like most other F_{420}-dependent enzymes (255), hydride transfer to C-5 of F_{420} is *Si*-face stereospecific (254).

Two pathways that facilitate formate-dependent methanogenesis have been elucidated (Fig. 7). In the first pathway, it has been proposed that electrons derived from formate are funneled through the hydrogenotrophic pathway, with $F_{420}H_2$ and H_2 serving as intermediates (225, 256). First, formate is disproportionated through the combined activity of Ffd (formate + F_{420} → CO_2 + $F_{420}H_2$) and Frh ($F_{420}H_2$ → F_{420} + H_2) (257). Subsequently, the H_2 and CO_2 produced are converted to methane through the hydrogenotrophic pathway (225). More recently, it was proposed that Ffd can form an electron-bifurcating complex with heterodisulfide reductase; in this model, the oxidation of formate simultaneously drives the exergonic reduction of heterodisulfide and endergonic reduction of ferredoxin (258, 259). This pathway is supported through analysis of protein-protein interactions, which indicate that Ffd forms a membrane-bound supercomplex with a heterodisulfide reductase (Hdr) and a hydrogenase subunit (VhuD) (259, 260). Genetic dissection studies likewise show that Ffd but not Frh is essential for formatotrophic growth of *Mc. maripaludis* (259, 261–263). In fact, a suppressor mutant of *Mc. maripaludis* sustains formatotrophic growth when all of its seven hydrogenases are deleted (261). Costa et al. proposed that, in addition to providing electrons to Hdr, Ffd must also provide $F_{420}H_2$ to sustain the central reactions catalyzed by Mer and Mtd in the methanogenesis pathway (259).

As with Frh, methanogens have evolved selenium-free and selenium-containing variants of the Ffd. Whereas *Mb. formicicum* carries a gene that encodes a single Ffd, *Methanococcus vannielii* carries genes that encode both selenium-free and selenium-containing variants of the Ffd (185, 264). Selenium supplementation markedly stimulates formate-driven growth of the organism, suggesting that the selenocysteine-containing Ffd may be the more efficient variant (265). In contrast, both Ffd variants in *Mc. maripaludis* are selenoproteins (266); hence, the organism requires the presence of selenium to grow on formate (267, 268). Genetic dissection has demonstrated that each homolog confers a competitive growth advantage, with single mutants impaired and double mutants unviable for formatotrophic growth (242). Interestingly, while some *Methanosarcina* species carry genes that encode Ffd homologs (269), methanogens with cytochromes cannot sustain formate-dependent growth. Thauer et al. rationalize that the high H_2 threshold of these organisms compared to other methanogens

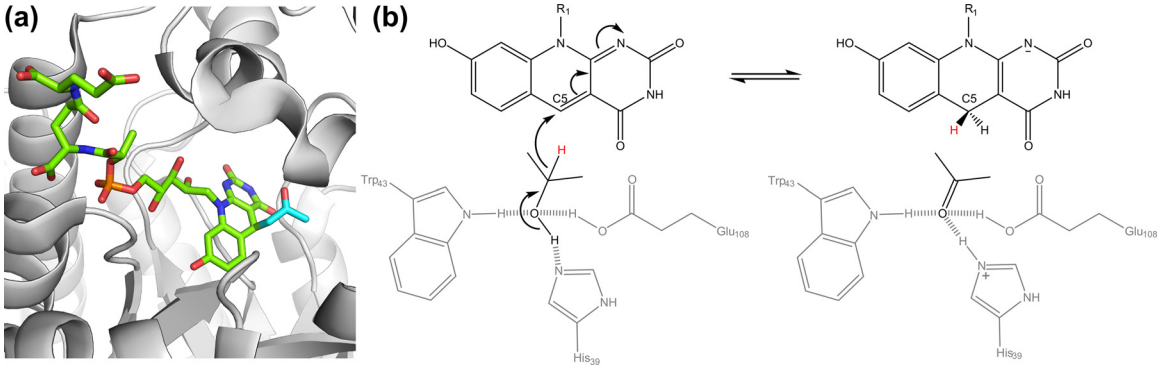

FIG 10 Structure of the active site of Adf. (a) Cartoon representation of the protein (PDB ID 1RHC [49]) showing the bound F_{420}-acetone adduct. (b) Proposed mechanism of isopropanol reduction to acetone (49). R_1 is the ribitylphospholactyl-oligoglutamate chain of F_{420}.

means that they would not be able to competitively oxidize H_2 produced from formate metabolism (182). An alternative explanation is that they lack the electron-bifurcating systems required to efficiently couple formate oxidation to growth (259).

3.2.3. Adf: F_{420}-reducing secondary alcohol dehydrogenase

Some methanogens are capable of low-yield growth using alcohols as electron donors. Whereas methanogens oxidize primary alcohols (e.g., ethanol) using standard NADP-reducing alcohol dehydrogenases (Adh) (22, 270), some can also metabolize secondary and cyclic alcohols using a phylogenetically unrelated class of F_{420}-dependent secondary alcohol dehydrogenases (Adf) (271, 272). The enzymes that mediate this are sparsely distributed, encoded by genes on just six sequenced methanogens in the NCBI database, all of the class *Methanomicrobia*. The $F_{420}H_2$ generated from the reduction of secondary alcohols (e.g., isopropanol, butan-2-ol) to ketones (e.g., acetone, butanone) is, in turn, used to sustain the CO_2-reducing pathway of methanogenesis and other cellular reductive processes (271, 272). Adf belongs to the bacterial luciferase superfamily (TIM barrel protein fold), which also includes other F_{420}-dependent enzymes Fgd (163), Mer (48), and Fht (155). As with other enzymes of the luciferase superfamily, crystallographic analysis shows that Adf from *Methanoculleus thermophilicus* is dimeric, containing a nonprolyl *cis* peptide bond toward the *Re*-face of F_{420} that keeps the 5-deazaflavin rings in a bent "butterfly" conformation (49). The structure contains the inactive F_{420}-acetone adduct (Fig. 10) (thought to form due to acetone accumulation in the presence of oxidized F_{420} in a reductive environment); small secondary alcohol substrates, such as isopropanol, bind in the same pocket in the active enzyme (49). Hydride transfer occurs on the *Si*-face of the cofactor, facilitated by the abstraction of a proton from the alcohol by a catalytic histidine residue and the stabilization of the alcoholate anion transition state by nearby tryptophan and glutamate residues (49, 273).

3.3. $F_{420}H_2$-Dependent Reductases

3.3.1. Mtd: F_{420}-reducing methylene-H_4MPT dehydrogenase/Mer: $F_{420}H_2$-dependent methylene-H_4MPT reductase

In all methanogenesis pathways, tetrahydromethanopterin (H_4MPT) serves as the carrier of one-carbon (1C) units (158, 274). 1C units can be conjugated to H_4MPT in various oxidation states, including formyl (CHO-H_4MPT), methenyl (CH≡H_4MPT), methylene (CH_2=H_4MPT), and methyl (CH_3-H_4MPT). In hydrogenotrophic and formatotrophic methanogenesis, CO_2 is activated through three F_{420}-independent initial steps (Fig. 7). The resultant methenyl-H_4MPT adduct is reduced to methylene-H_4MPT and methyl-H_4MPT via two successive F_{420}-dependent steps. The first is catalyzed by the F_{420}-reducing methylene-H_4MPT dehydrogenase (Mtd; $CH{\equiv}H_4MPT^+ + F_{420}H_2 \rightarrow CH_2 = H_4MPT + F_{420} + H^+$) (18, 275–278). The second is catalyzed by the $F_{420}H_2$-dependent methylene-H_4MPT reductase (Mer; $CH_2 = H_4MPT + F_{420}H_2 \rightarrow CH_3\text{-}H_4MPT + F_{420}$) (279–284). Reflecting the standard redox potentials of F_{420}, methylene-H_4MPT, and methenyl-H_4MPT (Table 1), these reactions are physiologically reversible. Hence, Mer and Mtd can also be used to oxidize CH_3-H_4MPT to $CH{\equiv}H_4MPT^+$ with the concomitant reduction of two mole equivalents of F_{420} (156, 157). This is particularly important in the oxidative arm of the methylotrophic methanogenesis pathway, which generates reducing agents ($F_{420}H_2$, Fd_{red}) through the oxidation of CH_3-S-CoM (coenzyme M) to CO_2 (Fig. 7) (157).

A succession of crystal structures of Mtd and Mer have revealed much about their architectures and mechanisms. The structure of Mtd from *Methanopyrus kandleri* revealed a unique protein fold compared to other F_{420}-binding proteins (47, 166, 285, 286). Whereas most F_{420}-binding proteins adopt bacterial luciferase-like (TIM barrel) (163), FDOR-like (split β-barrel) (30), or FdrB-like (novel αβ fold) (150) protein folds, Mtd folds into a unique tertiary structure (47, 166) (Fig. 6). Each protein chain of the homohexameric complex of Mtd (a trimer of dimers) contains an αβ domain, a smaller helical bundle domain, and a C-terminal sheet segment (47). Methenyl-H_4MPT and $F_{420}H_2$ bind opposite each other at the active site, which is located between the two domains and capped by the loop segment of the adjacent chain (Fig. 11) (166). The reaction is catalyzed through a ternary complex mechanism (276, 284), wherein hydride transfer occurs between C-14a of methylene-H_4MPT (*Re*-face stereospecific) and C-5 of $F_{420}H_2$ (*Si*-face stereospecific) (166, 287–289). Crystal structures of Mer homologs have been solved from three organisms, *Methanoplanus kandleri* (159), *Methanothermobacter marburgensis* (159), and *Methanosarcina barkeri* (48). As a member of the bacterial luciferase superfamily, Mer contains a characteristic TIM barrel fold and a nonprolyl *cis*-peptide bond close to the F_{420}-binding site (48, 159). Modeling studies indicate that methylene-H_4MPT and $F_{420}H_2$ are likely to bind opposite each other to

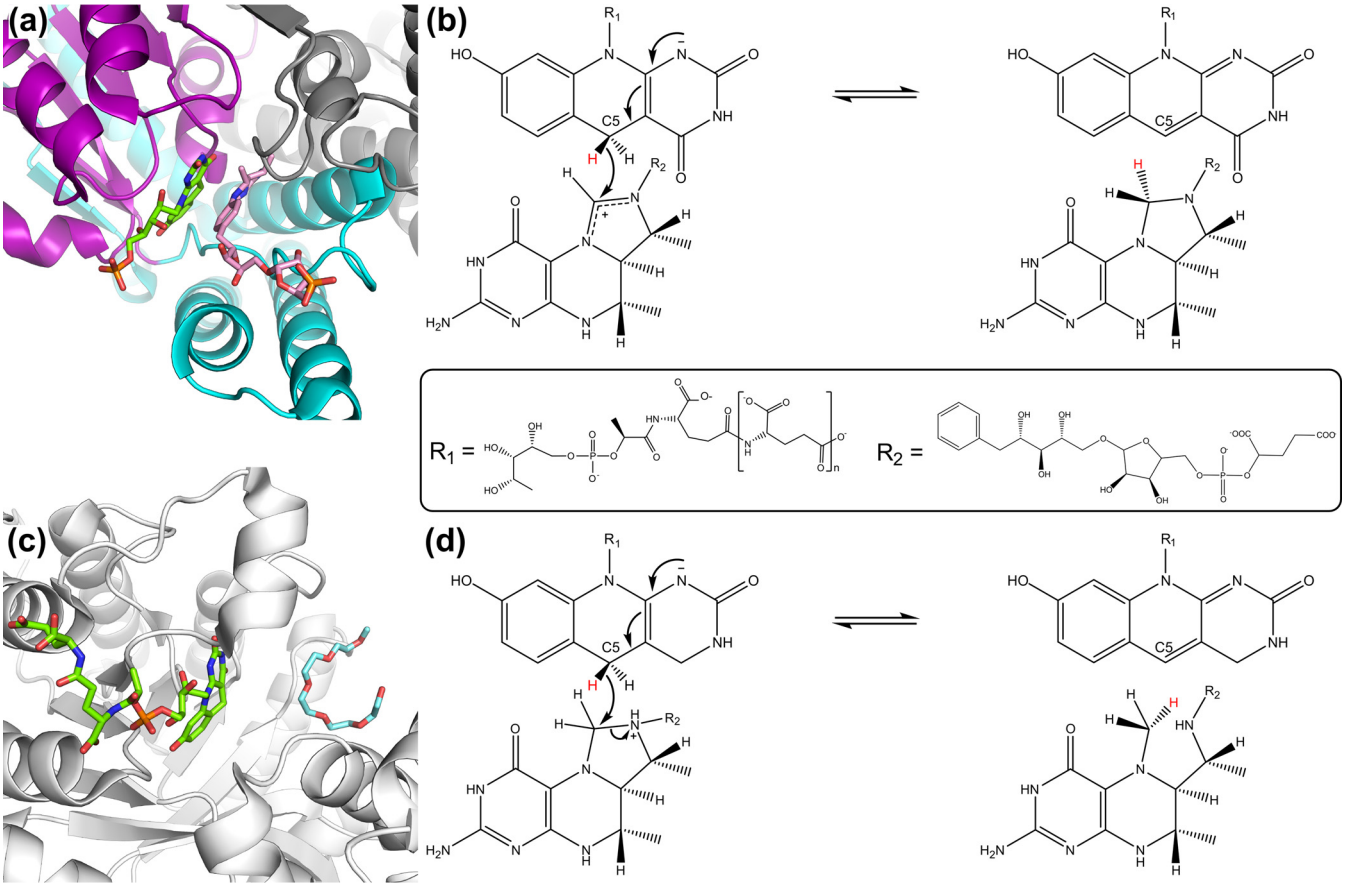

FIG 11 Structure and mechanism of $F_{420}H_2$-dependent hydride transfers to one-carbon compounds conjugated to tetrahydromethanopterin. (a) Structure of Mtd (PDB ID 3IQE [166]) as a ternary complex with F_{420} (green) and methenyl-H_4MPT$^+$ (pink). The large αβ-domain of a single subunit is shown in purple, and the helical bundle domain is shown in cyan. The secondary subunit in the dimer is shown in gray. (b) Mechanism of hydride transfer between $F_{420}H_2$ (*Si*-face) and methenyl-H_4MPT$^+$ (*Re*-face) leading to methylene-H_4MPT production (166). (c) Structure of Mer (PDB ID 1Z69 [48]) as a ternary complex with F_{420} (green) and polyethylene glycol (blue) occupying the methylene-H_4MPT-binding site. (d) Inferred mechanism of hydride transfer between $F_{420}H_2$ (*Si*-face) and methylene-H_4MPT (*Re*-face) leading to methyl-H_4MPT production (166).

form a ternary complex like in Mtd (48), enabling direct hydride transfer in a stereospecific manner (289) (Fig. 11).

In four of the methanogenic orders, the fourth step in the CO_2 reduction pathway can be effected using H_2 instead of F_{420} (Fig. 7) (183). The methylene-H_4MPT hydrogenase (Mth; also known as the [Fe]-hydrogenase, the H_2-forming methylenetetrahydromethanopterin dehydrogenase, and Hmd) directly reduces methenyl-H_4MPT to methylene-H_4MPT using H_2 ($CH{\equiv}H_4MPT^+ + H_2 \rightarrow CH_2{=}H_4MPT + H^+$) (290–292). Several transcriptome analyses have indicated that, while the F_{420}-dependent route is constitutive, the H_2-dependent route predominates at high H_2 partial pressures (pH_2) that induce rapid growth (293–295). Consistently, Mtd mutants of *Methanobacter thermoautotrophicus* are unable to grow at low pH_2 (296). Methanogens can also reduce F_{420} using H_2 through the combined action of Mth ($CH{\equiv}H_4MPT^+ + H_2 \rightarrow CH_2{=}H_4MPT + H^+$) and Mtd ($CH_2{=}H_4MPT + F_{420} + H^+ \rightarrow CH{\equiv}H_4MPT^+ + F_{420}H_2$) (the net reaction is $H_2 + F_{420} \rightarrow F_{420}H_2$) (225, 297). Hendrickson and Leigh demonstrated through genetic dissection in *Mc. maripaludis* that this Mth-Mtd cycle can fully compensate for Frh during hydrogenotrophic growth; the pathways could be eliminated separately, but not together (225). Transcriptional and biochemical studies on *Methanothermobacter marburgensis* (*Mt. marburgensis*) have suggested that the Mth-Mtd cycle is particularly important during nickel-limiting conditions when the F_{420}-reducing [NiFe]-hydrogenase cannot be synthesized (297, 298).

Homologs of Mtd and Mer are also present in sulfate-reducing archaea (299, 300). *Archaeoglobus fulgidus* converts lactate to three molecules of carbon dioxide using an Mtd/Mer-facilitated 1C pathway similar to methylotrophic methanogenesis (133, 300). The $F_{420}H_2$ produced by Mtd and Mer can be subsequently respired through a sulfate-reducing electron transport chain (200). It has also been proposed that these enzymes operate during the reverse methanogenesis pathway of anaerobic methanotrophic archaea (ANME). In support of this, genes encoding homologs of Mtd and Mer have been found in some reconstructed ANME metagenomes (21, 137, 215). Heterologously expressed Mtd from an ANME-1 archaeon catalyzed the same reaction as Mtd from methanogens, with similar catalytic specificity and cofactor dependence (214). In addition to F_{420}-dependent enzymes, NAD(P)-dependent methylenetetrahydromethanopterin dehydrogenases have been characterized that have central roles in the formaldehyde assimilation pathways of aerobic methylotrophic bacteria (301, 302).

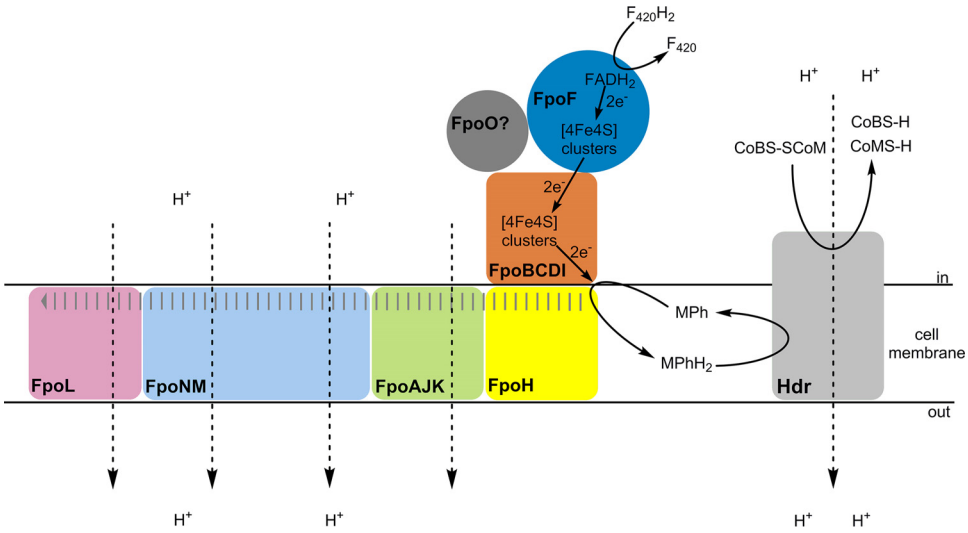

FIG 12 Model of respiration in *Methanosarcina mazei* using $F_{420}H_2$ as an electron donor and heterodisulfide as an electron acceptor. In this system, the primary dehydrogenase is the proton-translocating $F_{420}H_2$-dependent methanophenazine reductase (Fpo) and the terminal reductase is methanophenazine-dependent heterodisulfide reductase (Hdr). Arrangement of Fpo subunits and the proposed electron and proton transfer pathways are inferred from the homology of the system to bacterial complex I (Nuo) (317, 319, 320). Gray lines show the propagation of conformational change in the E-channel (FpoAJKH) and antiporter (FpoNML) modules upon electron transfer to methanophenazine (MPh/$MPhH_2$), and dashed arrows show possible routes for proton transfer based on structural analysis of complex I. The protein topology of Hdr is not shown in detail.

3.3.2. Fpo: $F_{420}H_2$-dependent methanophenazine reductase/Fqo: $F_{420}H_2$-dependent quinone reductase

The single order of methanogens containing cytochromes, i.e., the *Methanosarcinales*, can translocate protons by coupling the oxidation of $F_{420}H_2$ to the reduction of heterodisulfide (CoM-S-S-CoB). It was initially thought that this activity was mediated by a single hypothetical enzyme complex, the $F_{420}H_2$:heterodisulfide oxidoreductase (303). However, it is now appreciated that this system is in fact formed from two respiratory complexes (304–306), the $F_{420}H_2$-dependent methanophenazine reductase (Fpo) (162) and the methanophenazine-dependent heterodisulfide reductase (Hdr) (307), which are linked by the redox-active membrane-diffusible cofactor methanophenazine (305, 308–310) (Fig. 10). Constituting the primary dehydrogenase, Fpo is a respiratory proton pump exclusive to the order *Methanosarcinales* (162). Serving as the terminal reductase, Hdr is anchored to the membrane by a *b*-type cytochrome (307, 311, 312). Together, these enzymes translocate four protons (two each through Fpo and Hdr) per molecule of $F_{420}H_2$ that is oxidized (303). In contrast, the Hdr-linked complexes of methanogens without cytochromes are primarily cytosolic and do not serve a respiratory role (182).

The complete Fpo complex has been purified from only a single species, *Methanosarcina mazei* (*Ms. mazei*) (162, 313–315). The complex is very similar to bacterial NADH:ubiquinone oxidoreductase I (Nuo; also known as complex I) in both overall subunit composition and amino acid sequence (316, 317). The Fpo complex is formed of 13 subunits that associate into a hydrophilic portion (FpoFBCDIO) and a transmembrane portion (FpoAHJKNML) (162, 318). The hydrophilic electron input (FpoF) and electron output (FpoBCDI) modules catalyze electron transfer from $F_{420}H_2$ to methanophenazine and are largely conserved with Nuo. However, there are several key differences: an $F_{420}H_2$-oxidizing subunit (FpoF) replaces the NADH-oxidizing module (NuoEFG), the phenazine-reducing subunit (FpoD) has a modified binding pocket compared to its quinone-reducing equivalent (NuoD), and a subunit of unknown function (FpoO) is present. The remaining hydrophobic portion of Fpo is embedded in the membrane, consisting of the proton-translocating E-channels (FpoAJKH) and Mrp antiporter-like channels (FpoNML) that are homologous to those in Nuo (316, 317, 319). Unlike Nuo, which pumps four protons per two input electrons, the Fpo complex is thought to translocate two protons per molecule of $F_{420}H_2$ (162). On the basis of the structure of bacterial Nuo (319, 320), a basic model for the mechanism of Fpo has be proposed (Fig. 12): electrons are transferred from $F_{420}H_2$ to methanophenazine, methanophenazine reduction propagates conformational changes to the E-channel and in turn the antiporter module, and two protons are subsequently translocated through half-channels via conserved lysine and glutamate residues.

During methylotrophic methanogenesis, it is proposed that the $F_{420}H_2$ formed serves as the major respiratory electron donor (Fig. 7). In this pathway, one-carbon compounds (e.g., methanol, methylamine) are activated to produce methyl-coenzyme M (methyl-S-CoM) and thereafter converted to CO_2 or methane; the oxidative branch yields $F_{420}H_2$ via the Mer and Mtd reactions, while the reductive branch generates proton motive force by coupling $F_{420}H_2$ oxidation to heterodisulfide reduction (318, 321). Consistently, trimethylamine-cultured Δ*fpo* mutants of *Ms. mazei* are severely compromised in growth and methane formation compared to the wild-type strain (193). Surprisingly, these findings do not extend to *Ms. barkeri*; in this organism, Fpo appears to be dispensable for methylotrophic growth, whereas Frh is essential (224). On this basis, Kulkarni et al. (224) in Metcalf's laboratory have proposed that H_2 is an intermediate during methylotrophic growth wherein electrons from the $F_{420}H_2$ produced by Mer and Mtd may be used to drive H_2 production by Frh. The H_2 produced is in turn reoxidized via a hydrogenase (Vhu) that can reduce methanophenazine to facilitate heterodisulfide reduction by Hdr,

thereby bypassing the need for Fpo (224). Frh activity is consistently 10-fold higher in *Ms. barkeri* than in *Ms. mazei*; hence, Frh may be able to fully substitute or compensate for loss of Fpo activity only in the former organism (193). Fpo is also likely to be dominant during methylotrophic growth in *Methanosarcina acetivorans*, which exhibits low levels of hydrogenase expression and activity (322, 323).

Beyond methylotrophic methanogenesis, several other roles have been proposed for the Fpo system. For example, the proton gradient generated by Fpo is thought to contribute to ATP synthesis during hydrogenotrophic methanogenesis, while H_2 oxidation can be coupled to methanophenazine reduction directly (via the methanophenazine-reducing hydrogenase), F_{420} is also sometimes preferentially used as an intermediate (through the combined activities of Frh and Fpo) (182, 224). There is also evidence that Fpo contributes to the growth of *Methanosarcina barkeri* on carbon monoxide (324). More recent work also suggests that FpoF may sometimes function as a cytosolic enzyme independently of the other membrane-bound Fpo components in certain methanogens (193, 325). Consistently, the *fpoF* gene is genomically separated from the rest of the *fpo* operon in several *Methanosarcina* species (269, 326), and the protein is expressed at high levels in the cytosolic fraction of *Ms. mazei* cells (193). FpoF from *Ms. mazei* can slowly, but specifically, catalyze electron transfer from Fd_{red} to F_{420} (Fig. 7), which may help to maintain redox balance among methanogenic cofactors (193). Interestingly, members of the genus *Methanosaeta* (part of the order *Methanosarcinales*) contain a variant of Fpo (*fpoABCDHIJKLMNO*) that lacks the $F_{420}H_2$-oxidizing subunit FpoF and instead may be dependent on another reducing agent, e.g., Fd_{red} (196, 327).

A related multimeric membrane-bound proton-translocating complex is also present in some nonmethanogenic archaea (198). The enzyme appears to serve as an $F_{420}H_2$-dependent menaquinone reductase (Fqo) during sulfate respiration of *Archaeoglobi* (198, 199). Transcriptome analysis has shown that Fqo is constitutively expressed at high levels in *Archaeoglobus fulgidus* together with the other respiratory chain components (200). The enzyme is composed of 11 subunits that assemble in a manner similar to Fpo in methanogenic archaea, but it likely reduces menaquinone rather than methanophenazine via the FqoD subunit (199). Homologous enzymes are also encoded by some ANME archaea (e.g., *Methanoperedens nitroreducens*) and are proposed to input electrons derived from methane oxidation into sulfate- and nitrate-reducing respiratory chains (21, 215, 328).

3.3.3. Fpr: $F_{420}H_2$-dependent oxidase

Among the more recently discovered F_{420}-binding proteins, the physiological role of the $F_{420}H_2$-dependent oxidases (Fpr/FprA) is to catalyze the four-electron reduction of dioxygen (O_2) to water (H_2O) in methanogens (161, 192). In contrast to terminal oxidases, these enzymes are not linked to respiratory chains and instead appear to have evolved to detoxify O_2. Encoded in the genomes of five of the six presently recognized orders of methanogens (173), the $F_{420}H_2$ oxidases are part of the flavodiiron protein family, which have been implicated in O_2 and/or NO detoxification in microorganisms across all three domains of life. The methanogen enzymes share particularly high sequence identity (~40%) to the reductases in the anaerobic bacteria *Moorella thermoacetica* and *Desulfovibrio vulgaris* (52, 329), but they use $F_{420}H_2$ rather than an additional rubredoxin domain containing $FMNH_2$ as the reductant. Fpr has been correlated with the ability of methanogens such as *Methanobrevibacter arboriphilus* and *Methanothermobacter marburgensis* (*Mt. marburgensis*) to efficiently scavenge micromolar concentrations of O_2 in their environment (192). Although yet to be confirmed through genetic dissection, it has been hypothesized that such enzymes are responsible for the surprising and potentially ecologically significant aerotolerance of many members of the methanogens (all obligate anaerobes) (192, 330, 331). Some methanogens carry genes that encode multiple isozymes (e.g., *Mt. marburgensis* encodes three FprA homologs) (332), though it has yet to be resolved whether they are differentially regulated and kinetically distinct.

X-ray crystal structures of Fpr from *Methanothermobacter marburgensis* have been determined. They reveal that each monomer of this homotetrameric enzyme binds a diiron center, an FMN cofactor, and a solvent-diffusible $F_{420}H_2$ molecule (161, 192, 255). The enzyme forms a functional homodimer, with the diiron center of one subunit associating with the FMN cofactor of another (161). The structure of this enzyme has been solved in three conformational states (reduced-active, oxidized-active, and oxidized-inactive states) by altering the oxygen exposure of the protein crystals prior to data collection (161). This has enabled the elucidation of the probable catalytic mechanism for this protein (Fig. 13). Dioxygen binding occurs at the reduced-active state [Fe(II)Fe(II)$FMNH_2$], where the $F_{420}H_2$-binding site adjacent to FMN is in a "closed" conformation. The oxygen molecule forms a peroxo intermediate that bridges the diiron center and is reduced to release two water molecules through a diferric transition state. This forms the oxidized-active state of the enzyme [Fe(III)Fe(III)FMN], inducing conformational changes to "open" the $F_{420}H_2$-binding site. Two subsequent $F_{420}H_2$ molecules can then bind in a *Si-Si* conformation adjacent to the oxidized FMN, reducing both the diiron center and FMN to regenerate the reduced-active state. The enzyme also adopts a third oxidized-inactive state where the iron ion closest to FMN is displaced. An additional iron ion is also present, which locks the $F_{420}H_2$-binding site in the "open" state, preventing oxygen binding. This is hypothesized to occur in the presence of excess oxygen to prevent loss of reducing power (161).

3.3.4. Fsr: $F_{420}H_2$-dependent sulfite reductase

The $F_{420}H_2$-dependent sulfite reductase (Fsr) catalyzes the six-electron reduction of sulfite to sulfide (51). Discovered by Johnson and Mukhopadhyay, the enzyme appears to have a dual role in methanogens: detoxification of sulfite and growth on sulfite as the sole sulfur source (51, 191). While sulfite is generally inhibitory for growth of methanogens (e.g., *Methanococcus maripaludis*) (191, 333), diverse species are able to utilize it as a sole sulfur source (e.g., *Methanocaldococcus jannaschii*) (51, 334, 335). *Mc. maripaludis* can be rendered sulfite tolerant through recombinant expression of *Mc. jannaschii* Fsr (191). Fsr purified from *Mc. jannaschii* rapidly catalyzes sulfite reduction using $F_{420}H_2$ (51). The single-subunit enzyme appears to have arisen through the fusion of an $F_{420}H_2$-binding protein with a sulfite reductase (336, 337): the N-terminal domain is homologous to the FhrB-like domains of other $F_{420}H_2$ dehydrogenases, while the C-terminal domain is similar to siroheme-containing dissimilatory sulfite reductases (51). It is therefore proposed that, as in Frh, Ffd, and Fpo (Fig. 8, 9, and 12), $F_{420}H_2$ is oxidized at the N-terminal domain and electrons are funneled to the C-terminal domain via a possible flavin,

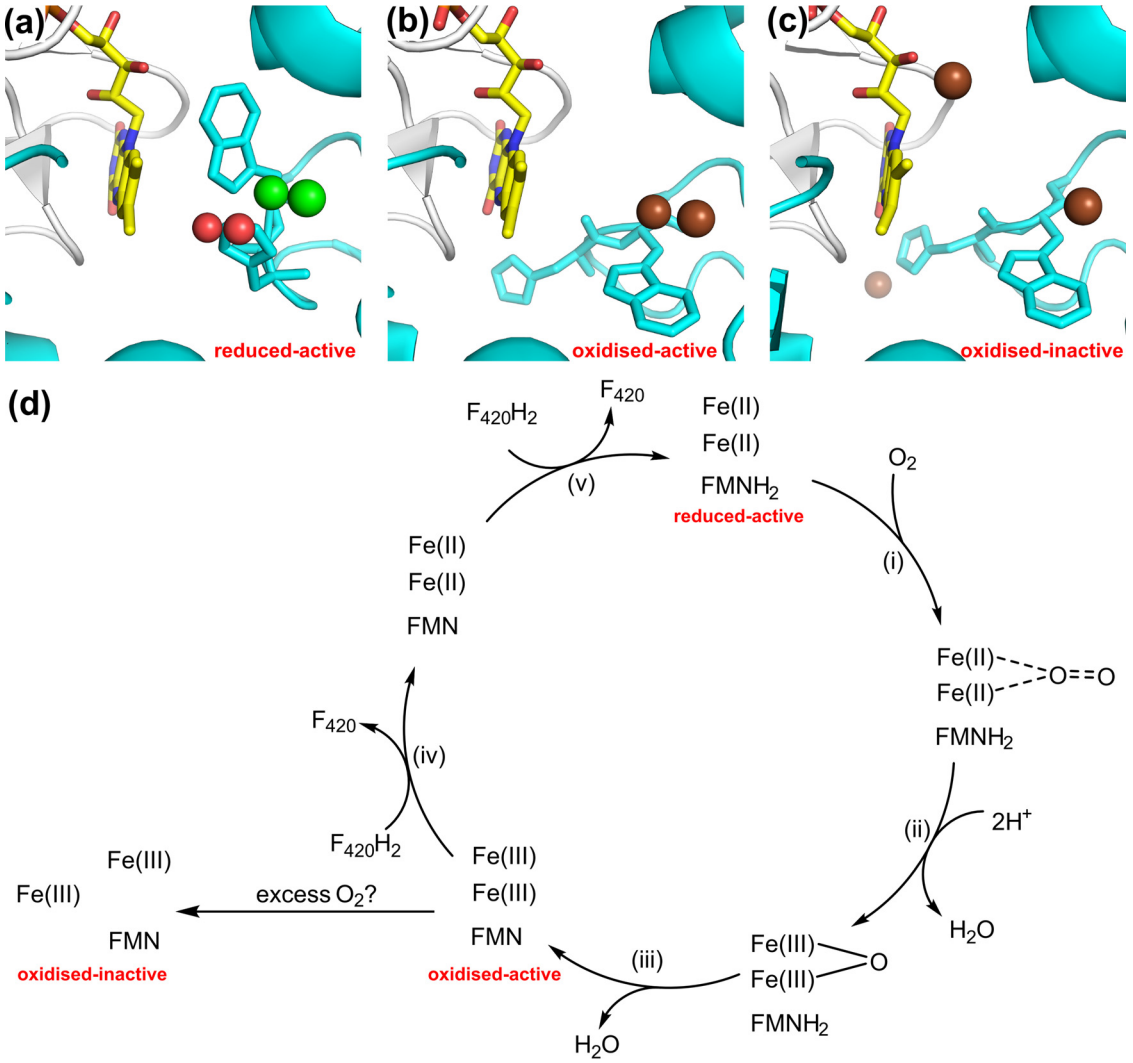

FIG 13 Summary of $F_{420}H_2$-dependent oxygen detoxification by Fpr. The mechanism was inferred based on the three crystallographic states of the active site (161): (a) the reduced-active state where the $F_{420}H_2$-binding site adjacent to FMN is "closed" by a loop with bulky aromatic residues (PDB ID 2OHI), (b) the oxidized-active state where the $F_{420}H_2$-binding site is "open" due to conformational changes in the loop (PDB ID 2OHH), and (c) the oxidized-inactive state where one iron atom in the diiron center is displaced and an additional third iron is present locking the loop in the "open" state (PDB ID 2OHJ). Fe(III) is shown in green, Fe(II) is shown in brown, water molecules at the predicted dioxygen-binding site are red, and FMN is in yellow. (d) Catalytic mechanism of Fpr. The five steps are shown as follows. (i) Transient binding of dioxygen to the reduced-active state; (ii) oxidation of the diiron center with the release of a water molecule; (iii) oxidation of FMN to release the second water molecule; (iv) reduction of the diiron center via FMN at the oxidized-active state, which binds $F_{420}H_2$ as an electron donor; (v) reduction of FMN by a second $F_{420}H_2$ molecule.

an [4Fe4S] cluster, and siroheme, where the sulfite is subsequently reduced (337). The enzyme appears to be sensitive to oxygen, but it can be reactivated by cellular thioredoxins (338). Other than Fsr, some methanogens can also mobilize sulfite using the P_{590}-type sulfite reductases (339), the physiological role of which are still incompletely resolved (336).

3.3.5. Fno: $F_{420}H_2$-dependent NADP reductase

In most cases, the catabolic pathways of methanogens reduce F_{420} and ferredoxin, but not nicotinamides. In order to generate NADPH for biosynthetic processes, methanogens instead transfer electrons from $F_{420}H_2$ to NADP (151). This process depends on $F_{420}H_2$:NADP oxidoreductase (Fno), a physiologically reversible enzyme that primarily acts as an $F_{420}H_2$-dependent NADP reductase in methanogens and an F_{420}-reducing NADPH dehydrogenase in bacteria. Fno is present in all six orders of methanogens and can reduce NADP using electrons derived from $F_{420}H_2$ during hydrogenotrophic, formatotrophic, and methylotrophic growth (16, 152, 340). An exception is those methanogens that grow on primary alcohols (e.g., *Methanoculleus thermophilicus*), which instead use an NADP-reducing primary alcohol dehydrogenase (272); in such organisms, Fno serves as an F_{420}-reducing NADPH dehydrogenase that generates sufficient $F_{420}H_2$ to drive the fourth and fifth steps in the CO_2-reducing pathway of methanogenesis (22). In contrast, methanogens that harbor an F_{420}-reducing secondary alcohol dehydrogenase use Fno in the typical NADP-reducing direction (22). Homologous enzymes also appear to bridge catabolic and anabolic processes in *Archaeoglobi* (201) and *Halobacteria* (136).

One of the best-understood F_{420}-dependent enzymes, Fno has

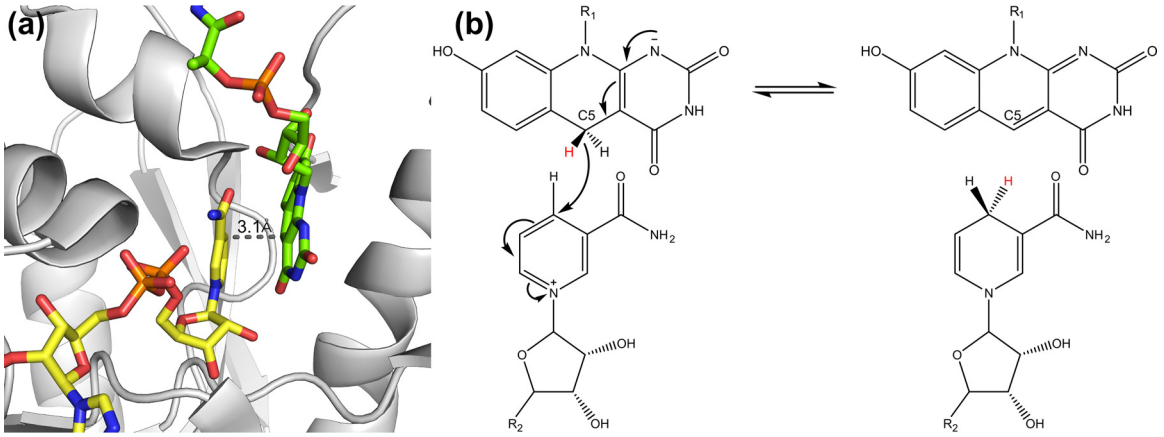

FIG 14 Structure and catalytic mechanism of Fno. (a) Structure of the active site of Fno (PDB ID 1JAY [160]), showing F_{420} and NADP positioned for electron transfer. (b) Hydride transfer mechanism from the *Si*-face of F_{420} to the *Si*-face of $NADP^+$ (160). R_1 is the ribitylphospholactyl-oligoglutamate chain of F_{420}, and R_2 is 2-phosphoadenosine 5-diphosphate.

been purified and characterized from methanogens of the genera *Methanococcus* (341, 342), *Methanothermobacter* (343, 344), *Methanosphaera* (345), and *Methanogenium* (22). The structure of Fno from *Archaeoglobus fulgidus* complexed with F_{420} and NADP gives direct structural insight into its hydride transfer mechanism (Fig. 14). The single-subunit enzyme contains a small C-terminal domain and an N-terminal domain characteristic of a dinucleotide-binding Rossmann fold. The nicotinamide and deazaflavin moieties of the cofactors are bound roughly parallel to each other (*Si*-face to *Si*-face) in a hydrophobic pocket between the domains (160). The aromatic groups are laterally shifted relative to each other, such that the C-4 atom of NADP is positioned exactly above the C-5 atom of F_{420} (201, 346) to allow for hydride transfer at an optimal distance of 3.1 Å. The affinity of F_{420} for Fno increases in the presence of NADP, suggesting that NADP binding facilitates F_{420} binding (160). Consistently, structural comparison between apo- and holoenzymes indicates that NADP binding facilitates a conformational change that induces $F_{420}H_2$ binding and generates a catalytically active ternary complex (160).

3.4. Cofactor F_{390}

Two purinated derivatives of F_{420} are formed in methanogens under certain conditions, and these two derivatives of F_{420} are collectively referred to as F_{390} (347, 348). F_{390}-A and F_{390}-G are formed when F_{420} forms a phosphodiester linkage with AMP and GMP, respectively, via the 8-hydroxy group of the 5-deazaflavin ring (348, 349). Seemingly exclusive to methanogens, F_{390} has been identified in genera as diverse as *Methanothermobacter* (347, 350), *Methanobacterium* (351), *Methanobrevibacter* (330), and *Methanosarcina* (352). Owing to their electron-donating groups, F_{390} compounds have a higher standard redox potential (−320 mV) than F_{420} (−340 mV) and hence may be ideal for sensing or catalytic roles under oxidizing conditions (353). These derivatives are synthesized when methanogens are exposed to oxygen and are hydrolyzed back to F_{420} and AMP/GMP upon reestablishment of anaerobiosis (349). Production depends on an ATP/GTP-dependent F_{390} synthetase of the adenylate-forming superfamily (354–356), while a hydrolase mediates the AMP/GMP-forming hydrolysis reaction (356, 357). As F_{390} synthesis appears to be sensitive to both redox state and oxygenation levels (296, 355), it has been proposed that the cofactor derivative is part of a redox-sensing system that regulates metabolic activity of methanogens. It has been consistently demonstrated that F_{390} synthetase transcription and F_{390} cellular expression levels are correlated with the availability of reductant in *Methanobacterium thermoautotrophicum* (358, 359). However, no genetic or phenotypic studies have been performed to resolve its physiological role. In fact, there has been an almost complete absence of literature on this molecule over the last 2 decades.

4. F_{420} IN MYCOBACTERIA AND OTHER BACTERIA

4.1. Physiological Roles

4.1.1. Mycobacteria

Relatively little is known about the roles of F_{420} in bacteria. The cofactor has been experimentally shown to be synthesized in only one bacterial phylum thus far, *Actinobacteria*, where it has mainly been studied for its roles in secondary, rather than primary, metabolism. Nevertheless, a number of recent phenotypic and biochemical studies have shed light on the endogenous roles of F_{420} in mycobacteria, an actinobacterial genus of major medical and environmental significance (360, 361). F_{420} is synthesized and reduced by all members of the genus *Mycobacterium*, including saprophytes (e.g., *M. smegmatis*, *M. fortuitum*), opportunistic pathogens (e.g., *M. avium*, *M. kansasii*), and the causative agents of tuberculosis (*M. tuberculosis* complex) and leprosy (*M. leprae*) (20, 125, 145). The observation that F_{420} is synthesized even in *M. leprae*, rendered an unculturable, host-dependent organism through massive genome decay (362), suggests that it has an evolutionarily conserved central role in mycobacterial metabolism. In contrast to methanogens, F_{420} is not essential for the viability of mycobacteria under ideal conditions: F_{420} biosynthesis (*fbiC*) and reduction (*fgd*) genes have been successfully deleted or disrupted in *M. smegmatis* (28, 31, 132, 363), *M. tuberculosis* (32, 35), and *M. bovis* (72). However, there is a range of evidence that F_{420} contributes to the notorious ability of mycobacteria to persist in deprived and challenging environments (56). Mycobacteria that are unable to synthesize F_{420} are unable to survive oxygen deprivation, oxi-

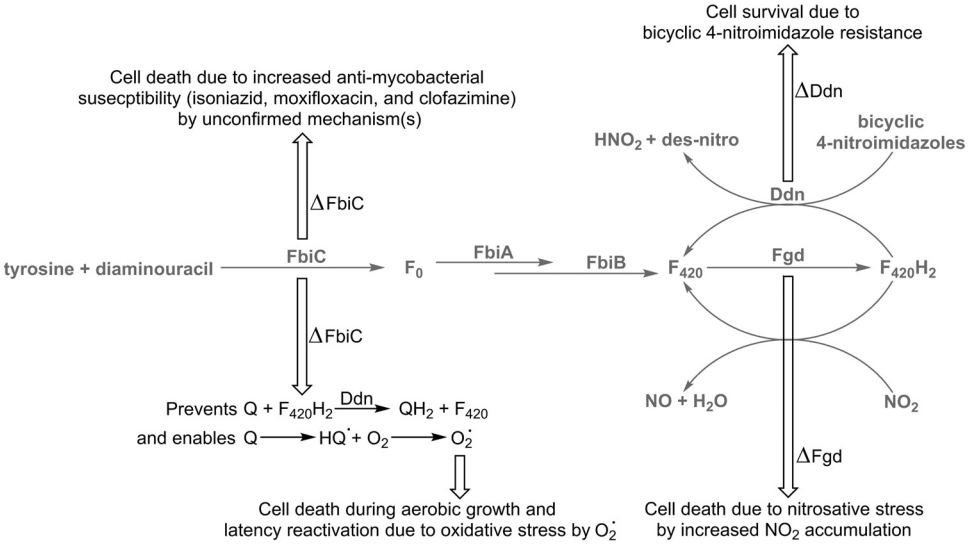

FIG 15 Pleiotropic phenotypes associated with loss of function of F_{420} in mycobacteria. Relevant reactions in the F_{420} biosynthesis and utilization pathway are shown in gray. Hollow arrows show observed chemical and phenotypic effects due to loss-of-function mutations in specific enzymes in the pathway. Q, quinone; QH_2, dihydroquinone; $HQ^{\bullet}$, semiquinone.

dative stress, nitrosative stress, or antibiotic treatment (Fig. 15) (31, 32, 363).

Several F_{420}-dependent enzymes have been functionally annotated in mycobacteria. Pathogenic mycobacteria such as *M. tuberculosis* encode F_{420}-reducing hydroxymycolic acid dehydrogenases (fHMAD) that oxidize hydroxymycolic acids to ketomycolic acids in the cell wall (364, 365). These mycolic acid derivatives appear to influence the integrity and permeability of the cell envelope, which renders them less sensitive to cytotoxic agents such as antibiotics (366–368). Preliminary data indicate that a subgroup of the flavin/deazaflavin oxidoreductase superfamily (FDOR-AAs) may also be involved in fatty acid modification (30). Other members of this superfamily (FDOR-Bs) reduce the degradation products formed during heme oxygenation (30): biliverdin (produced by host heme oxygenase-1 and mycobacterial HugZ in the CO-generating pathway) and possibly mycobilin (produced by mycobacterial MhuD in the CO bypass pathway) (369–371). Our biochemical studies have shown that *M. smegmatis* carries a gene that encodes a conserved $F_{420}H_2$-dependent biliverdin reductase that rapidly reduces biliverdin to bilirubin (30), a potent antioxidant (372, 373).

There is also evidence that F_{420} contributes to an oxidative stress response system in mycobacteria. The survival rate of Δ*fbiC* strains of *M. tuberculosis* is 100- to 1,000-fold lower than wild-type cells following challenge with redox cycling agents (i.e., menadione, plumbagin) and antibiotics (i.e., isoniazid, clofazimine) (32). Δ*fgd* strains of *M. smegmatis* are similarly impaired (363). One explanation is that mycobacteria store electrons as glucose-6-phosphate (G6P) and mobilize them using Fgd (F_{420}-dependent glucose-6-phosphate dehydrogenase) in response to oxidative stress; G6P levels in *M. smegmatis* are consistently approximately 100-fold higher than those of *E. coli* during preferential growth conditions, but the levels become depleted following challenge with redox cycling agents (363). $F_{420}H_2$-derived electrons may be used in endogenous redox processes to prevent or reverse damage from reactive oxygen species. For example, it has been proposed that a subgroup of the flavin/deazaflavin oxidoreductase superfamily (FDOR-As) are $F_{420}H_2$-dependent menaquinone reductases that maintain the respiratory chain in a reduced state in response to oxidative stress (32). Several previous reports have demonstrated that the mycobacterial respiratory chain can be remodeled in response to environmental changes (374, 375), and the ability of $F_{420}H_2$ to serve as a respiratory electron donor has already been demonstrated for respiratory archaea (162, 199). However, this hypothesis has yet to be supported with data on phenotypes or energy, and it remains unclear whether purified FDOR-As are capable of reducing menaquinone (30, 32). There is also evidence that mycobacteria instead use electrons liberated from G6P by Fgd to directly detoxify exogenous agents (363). Two independent studies have demonstrated that FDOR-As rapidly reduce menadione and plumbagin using $F_{420}H_2$ (30, 32), and it is also plausible that these highly promiscuous proteins (28, 55) can directly detoxify certain antibiotics too. However, genetic studies have yet to definitively link FDORs to antibiotic resistance and oxidative stress responses.

The potentially related role of F_{420} in nitrosative stress resistance is also perplexing. *M. tuberculosis* transposon mutants of *fbiC* are hypersusceptible to acidified nitrite (376); this was shown through an *in vitro* screen designed to simulate the environment of an activated macrophage, in which inducible nitric oxide synthase (iNOS)-derived NO is oxidized to NO_2^-, acidified into HNO_2, and dismutated into NO and NO_2 (377), which have antimycobacterial properties (378). One study showed that NO_2 is rapidly nonenzymatically reduced to NO by $F_{420}H_2$ under aerobic conditions (31). However, it is likely that F_{420}-dependent enzymatic mechanisms also contribute to nitrosative stress resistance, either through direct detoxification or indirect mechanisms. Indeed, it is possible that F_{420} may confer protection against cytotoxic agents in multiple ways: enhancing physical barriers through cell wall synthesis, direct detoxification by reducing exogenous agents, and maintaining redox balance through endogenous metabolism. Given the diverse roles of

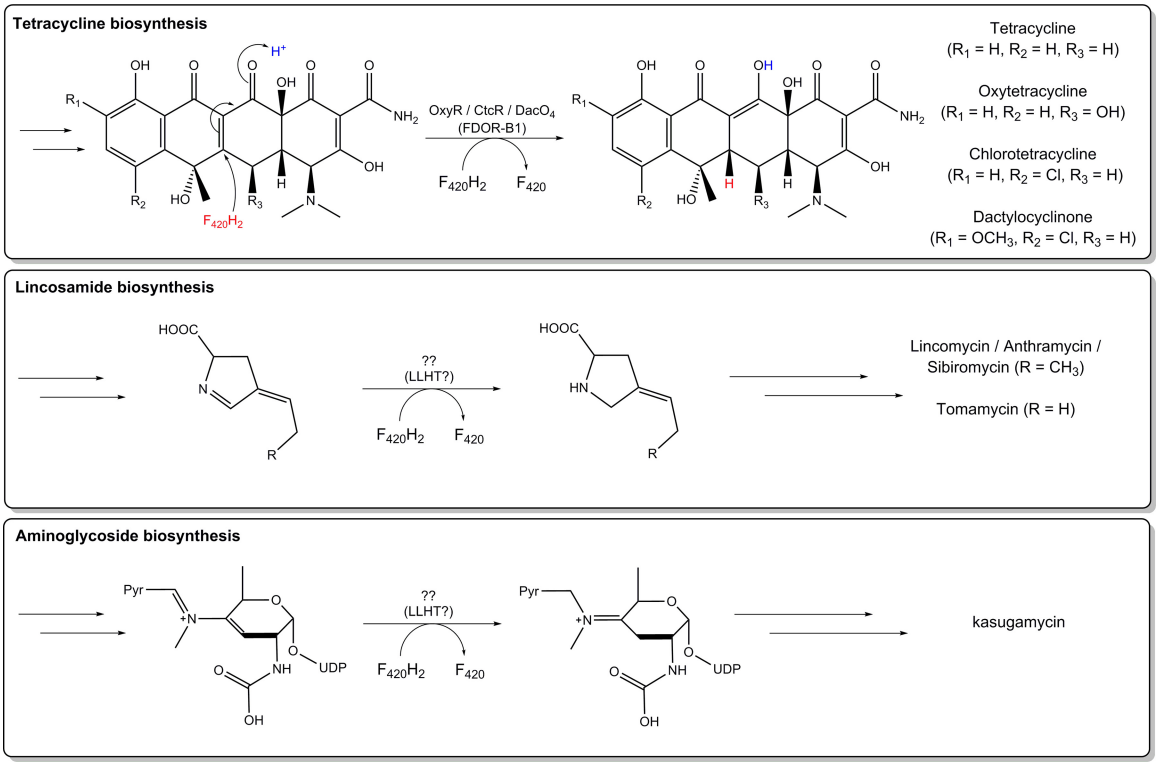

FIG 16 Reactions catalyzed by $F_{420}H_2$-dependent reductases in the biosynthesis pathways of tetracyclines (26), lincosamides (146, 388, 389), and aminoglycosides (394).

F_{420} in mycobacterial metabolism and the pleiotropic phenotypes associated with the cofactor's absence, it seems likely that F_{420} is required for latent tuberculosis infection *in vivo*, though this has yet to be definitively confirmed. In line with this, *M. tuberculosis* strains incapable of synthesizing ketomycolic acids are attenuated in macrophages and mice (366–368). One study surprisingly indicated that transposon mutants of *fbiC* are viable *in vivo* in the murine model of acute infection (379), though it is unclear whether such mutants would be capable of establishing a chronic infection.

4.1.2. Streptomycetes

It is well established that F_{420} is required for the synthesis of tetracycline antibiotics, a group of broad-spectrum aromatic polyketide antibiotics produced by streptomycetes (380). As far back as 1960, McCormick et al. isolated a hydride-transferring cofactor mediating tetracycline biosynthesis (24, 381–383), now known to be F_{420} (29, 122, 384). A combination of genetic and biochemical studies have since shown that an $F_{420}H_2$-dependent reductase (OxyR) catalyzes the final step of oxytetracycline biosynthesis (385), namely, reduction of the C-5a=C-11a double bond of dehydrooxytetracycline (Fig. 16) (29). This enzyme can also perform the equivalent reaction for tetracycline. Closely related enzymes are involved in the same step during biosynthesis of chlorotetracycline (CtcR) and dactylocyclinone (DaCO4) in *Streptomyces aureofaciens* and *Streptomyces rimosus* (29, 386). Encoded by the oxytetracycline (*oxy*), chlorotetracycline (*ctc*), and dactylocyclinone (*dac*) gene clusters (29), these enzymes are members of the flavin/deazaflavin oxidoreductase (FDOR) superfamily (30) and utilize $F_{420}H_2$ reduced through the action of Fno (387).

F_{420} is also required for the synthesis of lincosamide antibiotics by *Streptomyces lincolnensis* strains (146, 388, 389), including lincomycin, the precursor of the clinical semisynthetic antibiotic clindamycin (390). On the basis of the accumulation of 4-propylidene-3,4-dihydropyrrole-2-carboxylic acid by strains unable to biosynthesize F_{420}, it is proposed that an $F_{420}H_2$-dependent reductase catalyzes the reduction of the imine moiety of the dihydropyrrole to tetrapyrrole (Fig. 16) (389, 391). The biosynthesis of other pyrrolobenzodiazepine antibiotics (392) are facilitated by equivalent $F_{420}H_2$-dependent imine reduction steps, namely, tomaymycin (*Streptomyces achromogenes*) (50), sibiromycin (*Streptosporangium sibiricum*) (393), kasugamycin (*Streptomyces kasugaensis*) (394), and anthramycin (*Streptomyces rifuineus*) (395). However, biochemical studies have yet to definitively identify which enzymes are responsible for these reactions. The strongest candidates are the putative $F_{420}H_2$-dependent luciferase-like hydride transferases (LLHTs) encoded in the sequenced antibiotic synthesis gene clusters (50, 391, 393–395) of each of these organisms. Because all research thus far has focused on the roles of F_{420} in the secondary metabolism of streptomycetes, little is known about the roles of this cofactor in central metabolism of this genus; it is likely that streptomycetes use F_{420} to support some important metabolic pathways, as they carry genes that encode homologs of mycobacterial enzymes such as the $F_{420}H_2$-dependent biliverdin reductase (30).

4.1.3. Other actinobacteria

It is established that F_{420} is synthesized in multiple other actinobacterial genera, including *Rhodococcus*, *Nocardia*, and *Nocardioides* (27, 54, 145). However, all studies of such genera have focused on the roles of F_{420} in exogenous substrate reduction, and very little is known about the endogenous roles of F_{420}-dependent processes. The richest literature is on the degradation of picrate (2,4,6-trinitrophenol) and related compounds (e.g., 2,4-dinitrophenol, 2,4-dinitroanisole) (396, 397). A number of actinobacteria, including *Rhodococcus opacus* and *Nocardioides simplex*, are able to mobilize picrate as their sole carbon and nitrogen source (396, 398). This depends on reductive activation of these particularly electron-deficient aromatic compounds using two $F_{420}H_2$-dependent hydride transferases (hydride transferase I [HTI] and hydride transferase II [HTII]) (section 4.3.2) (155). Fno supplies the reductant for this process and is expressed from the same operon as the hydride transferases (54, 155, 396). While polynitroaromatic compounds are anthropogenic, actinobacteria may have evolved the capacity to degrade them from preexisting pathways that metabolize naturally occurring nitroaromatic compounds (e.g., chloramphenicol) (399, 400). It has also been demonstrated that $F_{420}H_2$-dependent oxidoreductases of the flavin/deazaflavin oxidoreductase superfamily have broad substrate specificity; enzymes purified from genera as diverse as *Mycobacterium*, *Frankia*, *Nocardia*, and *Rhodococcus* are capable of reducing coumarin natural products (28, 55). F_{420} may also contribute to the well-reported abilities of soil actinomycetes to biodegrade a wide variety of other polycyclic aromatic hydrocarbons (401). While the physiological advantage of this promiscuity is unclear, it might provide actinobacteria an adaptive or selective advantage to consume or detoxify the wide range of natural products in their respective environments (402, 403).

4.2. F_{420}-Reducing Dehydrogenases

4.2.1. Fno: F_{420}-reducing NADPH dehydrogenase

Fno is the only redox-active F_{420}-dependent protein proven to be conserved between archaea and bacteria. Whereas Fno primarily serves to reduce NADP in methanogens ($F_{420}H_2$-dependent NADP reductases), its homologs generally act in the reverse direction to reduce F_{420} in bacteria (F_{420}-reducing NADPH dehydrogenases) (219); this reflects that, whereas F_{420} is a central catabolic cofactor in methanogens, it is of secondary importance to NADP in the central metabolism of most bacteria (168). While Fno has yet to be structurally characterized in actinobacteria, the enzyme is expected to have a similar structure and mechanism: sequence comparisons and biochemical studies (12) indicate that the overall architecture and cofactor-binding sites are conserved with the archaeal enzyme (section 3.3.5) (160). The $F_{420}H_2$ generated by Fno in bacteria is used for various reductive processes, for example, biosynthesis of tetracycline antibiotics by *Streptomyces* (387) and the mobilization of picrate by *Rhodococcus* and *Nocardioides* species (54, 155).

4.2.2. Fgd: F_{420}-reducing glucose-6-phosphate dehydrogenase

While Fno appears to be the enzyme primarily responsible for F_{420} reduction in most actinobacteria, it is replaced by the F_{420}-reducing glucose-6-phosphate dehydrogenase in several genera, including *Mycobacterium* (Table 2). This enzyme directly links central carbon catabolism in actinobacteria to F_{420} reduction (glucose-6-phosphate + $F_{420} \rightarrow$ 6-phosphogluconolactone + $F_{420}H_2$) (163, 404). First identified in the soil bacterium *M. smegmatis* (148, 404), Fgd has since been identified in multiple other environmental actinobacteria and the obligate pathogens *M. tuberculosis* and *M. leprae* (145). Fgd is either the sole or main source of $F_{420}H_2$ in mycobacteria; neither Δ*fbiC* and Δ*fgd* strains are capable of activating exogenous substrates through $F_{420}H_2$-dependent reactions in *M. tuberculosis* (33, 35) and *M. smegmatis* (28, 363). Fgd therefore appears to have evolved principally as a mechanism to generate $F_{420}H_2$. As elaborated above, there is also evidence that glucose-6-phosphate serves as an electron store in mycobacteria that is mobilized by Fgd in response to oxidative stress (32, 363). The role of Fgd in generating flux through the pentose phosphate pathway appears to be supplementary, given that most mycobacteria also encode conventional NADP-dependent glucose-6-phosphate dehydrogenases (145). An interesting exception may be *M. leprae*, as genome analysis and biochemical studies indicate that it employs F_{420}, but not NADP, for G6P oxidation (145, 362, 405).

The F_{420}-reducing and NADP-reducing glucose-6-phosphate dehydrogenases are not phylogenetically related (148). Fgd is a member of the bacterial luciferase family (163) with a similar TIM barrel structure and catalytic mechanism reminiscent of Adf (49) and Mer (159). The cofactor is accommodated in the active site, with the isoalloxazine rings innermost and the oligoglutamate tail extending into the solvent (Fig. 6), where the isoalloxazine is in a bent butterfly-like conformation due to steric interactions with the protein backbone, including the nonprolyl *cis*-peptide bond behind its *Re*-face (163). The glucose-6-phosphate has been modeled to bind in a positively charged pocket adjacent to the *Si*-face of the deazaflavin (163), similar to what was observed in the ternary complex of the related Adf (Fig. 10). Hydride transfer is thought to occur similarly to Adf (Fig. 17) and is mediated by conserved histidine, tryptophan, and glutamate residues (49, 163): proton abstraction is initiated by the histidine, tryptophan stabilizes the resulting anion transition state, and glutamate is likely to serve as the proton donor for N-2 of the deazaflavin for $F_{420}H_2$ formation (49, 163).

4.2.3. fHMAD: F_{420}-reducing hydroxymycolic acid dehydrogenase

The F_{420}-reducing hydroxymycolic acid dehydrogenase (fHMAD) is responsible for oxidizing hydroxymycolic acids to ketomycolic acids during cell wall biosynthesis (365). A member of the bacterial luciferase family, the enzyme shares 36% sequence identity with Fgd (364). However, in contrast to its original annotation, the enzyme cannot oxidize glucose-6-phosphate (364) and is specific for hydroxymycolic acids (365). The enzyme is translocated through the cell membrane by the Tat pathway and is anchored to the outside of the cell membrane, where it can function in cell wall modification (364). Reflecting the taxonomic distribution of fHMAD (364, 365), ketomycolic acids are distributed in pathogenic mycobacteria (e.g., *M. tuberculosis* complex, *M. avium* complex) but are absent from most soil species (e.g., *M. smegmatis*) (406). Ketomycolic acids appear to be critical for the virulence of *M. tuberculosis*; strains lacking oxygenated mycolic acids have profoundly altered envelope permeability, are hypersusceptible to antibiotics, and are attenuated in macrophages and mice (366–368). Consistent with the synthesis of ketomycolic acids in response to

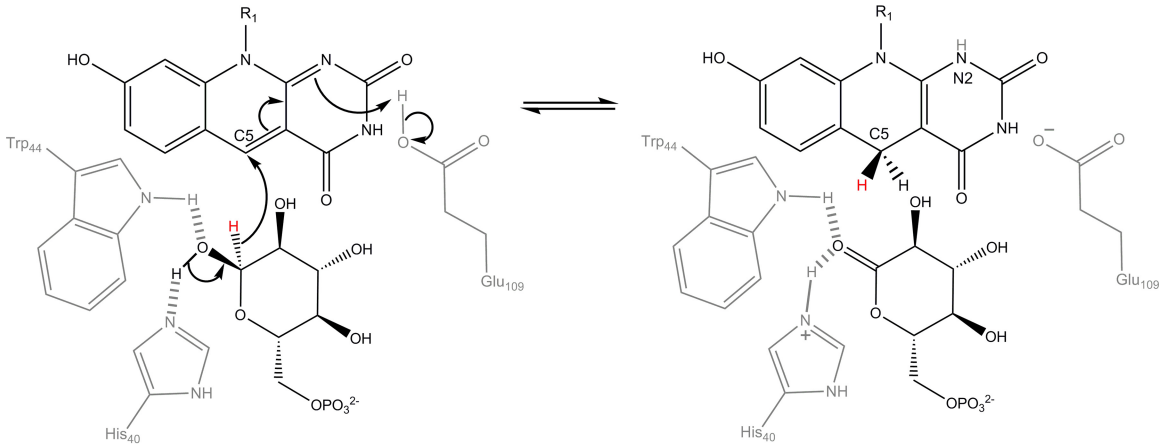

FIG 17 Proposed catalytic mechanism of Fgd (163). F_{420} is reduced to $F_{420}H_2$, and glucose-6-phosphate is oxidized to 6-phosphogluconate.

stress, the gene encoding fHMAD is under the control of the alternative sigma factor SigF in *M. tuberculosis* (407, 408). It was recently confirmed that fHMAD is inhibited by the nitroimidazopyran prodrug pretomanid (PA-824) (365); this interaction may be responsible for the altered mycolic acid composition of pretomanid-treated cells and may contribute to the mode of action of this next-generation bactericidal agent (33).

4.3. $F_{420}H_2$-Dependent Reductases

4.3.1. FDORs: flavin/deazaflavin oxidoreductase superfamily

$F_{420}H_2$-dependent reductases elicit the physiological roles of F_{420} in actinobacteria. They are split into two superfamilies, the flavin/deazaflavin oxidoreductases (FDORs) (30) and the luciferase-like hydride transferases (LLHTs; section 4.3.2) (37). FDORs are small (~150-residue) enzymes that accommodate a cofactor-binding channel and substrate-binding pocket into a split β-barrel fold (30). This superfamily is highly diverse in terms of catalytic activity (reductases, oxidases, and oxygenases), cofactor specificity (F_{420}, FMN, FAD, and heme), and substrate range (30, 409). We have shown that they have diversified into two major families, FDOR-As and FDOR-Bs, that share less than 30% sequence similarity but share the same protein fold (28, 30) (Fig. 18). Proteins from the FDOR-A family are exclusively F_{420}-binding proteins (28, 35, 55, 164, 410) restricted to the phyla *Actinobacteria* and *Chloroflexi* (28, 30, 37). In contrast, FDOR-B proteins are widely distributed, including in bacteria that do not synthesize F_{420}. They include the ubiquitous FMN-dependent pyridoxine/pyridoxamine 5′-phosphate oxidases (PnPOx) involved in vitamin B_6 biosynthesis (411–413), heme oxygenases (HugZ) involved in heme catabolism (414–416), and several groups of uncharacterized FAD-binding proteins (30, 417). *Actinobacteria* and *Chloroflexi* also carry genes that encode multiple $F_{420}H_2$-dependent reductases of the FDOR-B family, which are broadly divided into six subgroups (28, 30, 165, 418, 419). Structural and sequence analyses demonstrate that conserved motifs define cofactor specificity (30); in the case of $F_{420}H_2$-dependent reductases, deazaflavin binding is stabilized by a large hydrophobic groove complementary to the isoalloxazine ring and a positively charged groove that interacts with the oligoglutamate tail (28, 30, 164, 165). Interestingly, unlike all other F_{420}-binding proteins characterized thus far, the most likely substrate-binding pocket of the F_{420}-binding FDORs appears to be toward the *Re*-face of the cofactor (30, 164, 165), similar to the FMN-dependent members of the superfamily (420).

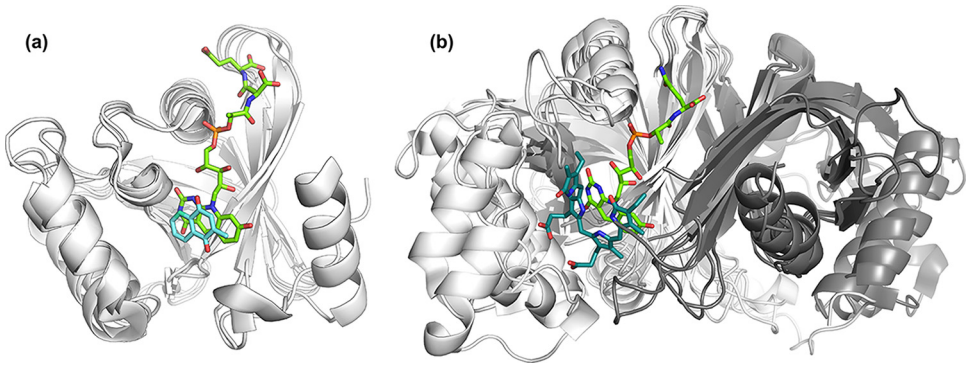

FIG 18 Representative crystal structures of FDOR-A (monomers) and FDOR-B (dimers) proteins. (a) Structures of the quinone-reducing FDOR-A1 proteins MSMEG_2027 (PDB ID 4Y9I [30]) and MSMEG_3356 (PDB ID 3H96 [28]) overlaid with the complex of rv3547 with F_{420} (PDB ID 3R5R [164]) with menadione docked into the active site. (b) Overlay of solved structures of $F_{420}H_2$-dependent FDOR-B proteins. These proteins include the FDOR-B1 proteins rv2991 (PDB ID 1RFE) and MSMEG_3380 (PDB ID 3F7E [28]), FDOR-B2 protein MSMEG_6526 (PDB ID 4ZKY [30]), FDOR-B3 protein rv1155 complexed with F_{420} (PDB ID 4QVB [165]) and FDOR-B4 protein rv2074 (PBD ID 2ASF [419]). Biliverdin, a substrate of FDORs B3 and B4, is docked at the active site (30).

In mycobacteria, there is a multiplicity of $F_{420}H_2$-dependent reductases of the FDOR family: 30 in *M. smegmatis*, 15 in *M. tuberculosis*, and 3 in *M. leprae* (30). As most of these enzymes remain to be functionally annotated, the reasons behind the extreme expansion and diversification of this superfamily remain unclear. The highly diverse architecture of the substrate-binding sites of these proteins, concurrent with a high degree of conservation of the F_{420}-binding site, suggests that they have evolved to catalyze the $F_{420}H_2$-dependent reduction of a variety of substrates (30). Some subgroups (e.g., FDOR-B2s, FDOR-B4s) are tightly phylogenetically clustered and have probably been constrained for a specific function (30). In contrast, representatives of the manifold subgroup FDOR-A1 exhibit broad and overlapping substrate specificities (28, 30). Such enzymes are capable of reducing a wide range of exogenous substrates, including coumarin natural products such as fungus-derived aflatoxins and plant-derived furanocoumarins (e.g., angelicin, methoxsalen) (28, 55). They also show potent activity against redox cycling agents such as menadione and plumbagin (30, 32). The physiological role of these enzymes may therefore be to detoxify a wide range of oxidizing agents in their environment using electrons channeled from G6P. The absence of such detoxification systems may contribute to the profound sensitivity of Δ*fbiC* and Δ*fgd* mutants to redox cycling agents and antibiotics, as discussed in section 4.1.1 (32, 363). Consistent with a role in detoxification or biodegradation, there is some evidence from expression studies (28, 30, 164) and proteome analyses (421, 422) that these enzymes are bound to the membrane through their N termini. Another enzyme of this class, rv3547 (Ddn; deazaflavin-dependent nitroreductase) has also attracted much attention for its role in the activation of nitroimidazole prodrugs (e.g., pretomanid, delamanid) by *M. tuberculosis* (section 5.1) (34, 35, 164).

The endogenous roles of the FDOR-type $F_{420}H_2$-dependent reductases in mycobacteria are presently being resolved. We have shown that a structurally characterized (419) subgroup of this family (FDOR-B4s) are efficient $F_{420}H_2$-dependent biliverdin reductases (30). They convert the heme degradation product biliverdin—produced by HugZ in environmental mycobacteria (30) and host heme oxygenase 1 (HO1) (369) during tuberculosis infection—to bilirubin via hydride transfer to C-10 (30). This may be advantageous for survival of oxidative stress, given that bilirubin is a potent antioxidant that can compensate for 10,000-fold excess in peroxide radicals (372, 373). A recent study showed that addition of bilirubin enhanced the survival of *Mycobacterium abscessus* in HO1-inhibited macrophages, possibly via modulation of intracellular reactive oxygen species (ROS) levels (423). These proteins may also reduce mycobilins (30), the product of the CO bypass pathway of heme oxygenation by mycobacterial MhuD (370). This FDOR group is only the second family of biliverdin reductases to be identified; a previously characterized family of mammalian and cyanobacterial biliverdin reductases employs nicotinamides as an electron source (424, 425). We also observed low-level biliverdin reductase activity in the structurally related FDOR-B3s (30). However, their low catalytic efficiency and suboptimal active site structure for biliverdin binding suggests that this promiscuous activity may result from a common evolutionary origin to the FDOR-B4s; FDOR-B3 enzymes are therefore likely to have a different, currently unidentified physiological substrate (30).

Among other FDORs, there is preliminary evidence that FDOR-AAs are $F_{420}H_2$-dependent fatty acid reductases; these membrane-bound enzymes may contribute to cell wall modification and host invasion, although their substrate specificity has yet to be defined (30). While it has been proposed that FDOR-A proteins are $F_{420}H_2$-dependent menaquinone reductases (32), to date, activity has been observed only with nonphysiological quinones (e.g., menadione), rather than with menaquinone (30, 32); hence, it is unclear whether these enzymes have primarily evolved to input electrons into the respiratory chain or instead detoxify exogenous redox cycling agents (section 4.1.1). Finally, it was recently shown that the $F_{420}H_2$-dependent step in the biosynthesis of antibiotics of the tetracycline, oxotetracycline, and chlortetracycline classes (122, 381, 382, 384) is mediated by enzymes of the FDOR-B1 subgroup in streptomycetes (section 4.1.2) (29).

4.3.2. LLHTs: luciferase-like hydride transferase superfamily

Luciferase-like hydride transferases (LLHTs) are another diverse superfamily of flavin/deazaflavin enzymes. These enzymes were previously defined as luciferase-like monooxygenases (LLMs), but this is inappropriate given that their reaction mechanisms are O_2 independent. Like the FDORs, members of this superfamily vary in their cofactor preferences (F_{420}, FMN, FAD) and catalytic activities (oxidases, reductases, oxygenases) (163, 426–428). F_{420}-binding LLHTs can be distinguished by a conserved glycine residue that binds the phosphate group without steric hindrance, which is not conserved in the FMN-binding proteins of this family (48). The best-characterized F_{420}-dependent LLHTs are the three aforementioned dehydrogenases: F_{420}-reducing methylene-H_4MPT dehydrogenase (Mtd), F_{420}-reducing glucose-6-phosphate dehydrogenase (Fgd), and F_{420}-reducing hydroxymycolic acid dehydrogenase (fHMAD). However, comparative genome analysis indicates that there are numerous other F_{420}-dependent LLHTs in actinomycetes, the majority probably serving as reductases (37). These have been implicated in a variety of roles, ranging from pyrrolobenzodiazepene antibiotic synthesis in streptomycetes (50, 393, 394, 429) to cell wall metabolism in mycobacteria (37) and exogenous substrate mobilization by rhodococci (155). A bioinformatics analysis predicted that there are some 45 F_{420}-binding LLHTs in *M. smegmatis* and 17 in *M. tuberculosis*, though this has yet to be validated experimentally (37). In contrast to the FDOR superfamily (30), to date, no comprehensive analysis of the phylogeny, structure, and function of these enzymes has been performed.

The best-characterized $F_{420}H_2$-dependent reductases of this superfamily are the hydride transferases involved in the biodegradation of the explosive picrate and related compounds (54, 155). In *Rhodococcus opacus*, two LLHTs known as hydride transferase I (HTI) and hydride transferase II (HTII) catalyze the reduction of picrate into hydride-Meisenheimer and dihydride-Meisenheimer complexes (430–432). Subsequent tautomerization, nitrite elimination, reduction, and hydrolysis steps lead to the production of 4,6-dinitrohexanoate, which can then be oxidatively degraded (432). The complete pathway involved is shown in Fig. 19. This pathway enables such organisms to grow using picrate and related compounds as the sole carbon and nitrogen sources (396, 398). The genes encoding the hydride transferases are organized in an operon together with genes encoding other enzymes in the pathway, including Fno which supplies reductant to the pathway (155, 433). Consistent with these genes having a physiological role in the biodegradation of nitroaromatic compounds, the repressor NpdR

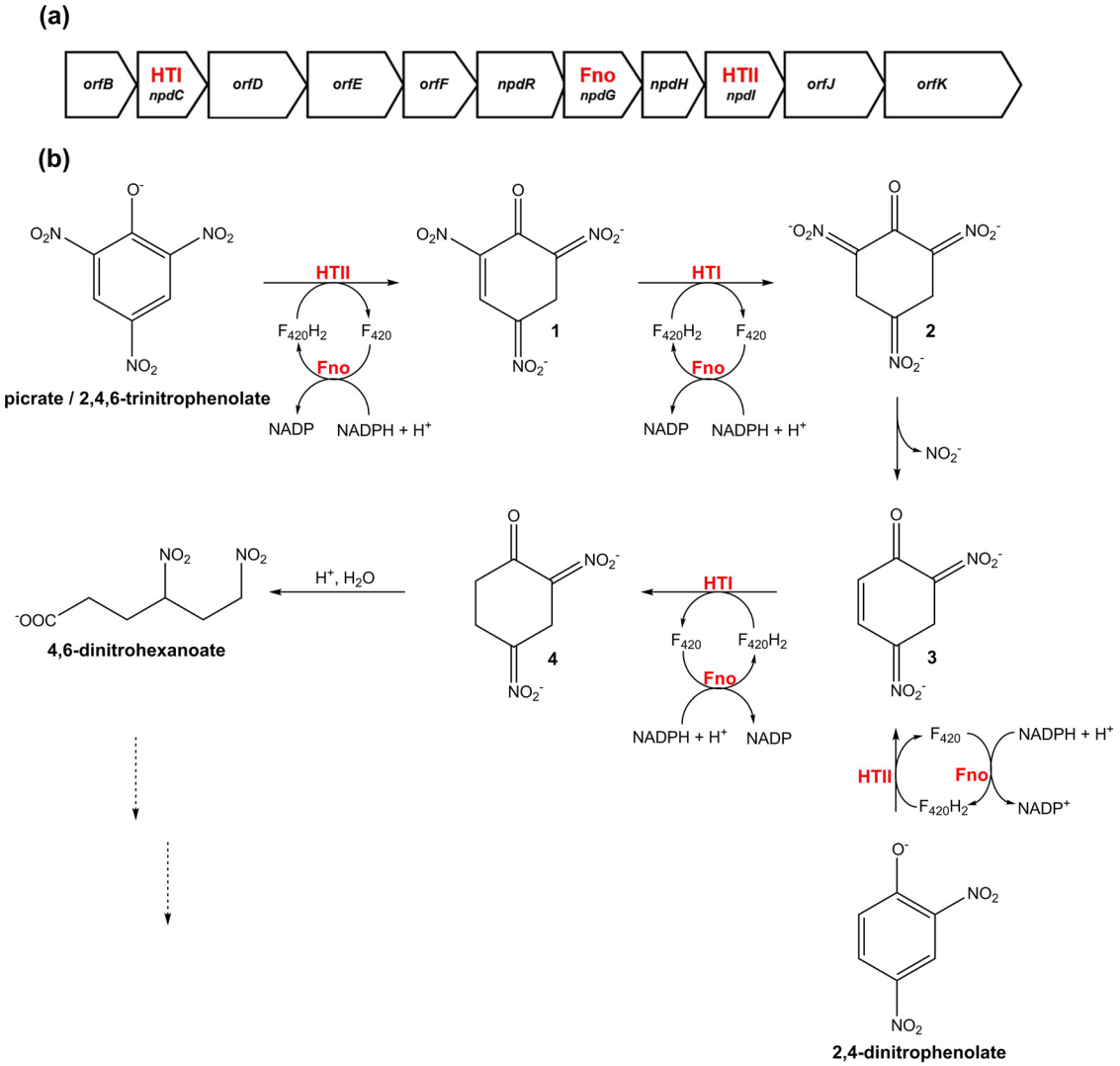

FIG 19 F_{420}-dependent degradation of picrate. (a) Genetic determinants of picrate degradation in *Rhodococcus opacus*. F_{420}-utilizing oxidoreductases are highlighted in gray, namely, two luciferase-like hydride transferases (HTI and HTII) and the F_{420}-reducing NADPH dehydrogenase (Fno) (155). Translation of the operon is silenced by the transcription factor NpdR, which is inactivated in the presence of nitroaromatic compounds (434). (b) Mechanism of picrate and 2,4-dinitrophenolate mobilization by *Rhodococcus opacus*. Hydride transfer from $F_{420}H_2$ is catalyzed by HTI and HTII, while $F_{420}H_2$ is regenerated by the F_{420}-reducing NADPH dehydrogenase Fno. The combined action of these enzymes generate hydride-Meisenheimer complex (compound 1 [shown as boldface 1 in the figure]) and dihydride-Meisenheimer complex (compound 2) of picrate and hydride-Meisenheimer complex (compound 3) and dihydride-Meisenheimer complex (compound 4) of 2,4-dinitrophenolate (394, 422).

usually silences these genes, but it is inactivated in the presence of nitroaromatics (434).

The hydride transferases that mediate these reactions share approximately 30% amino acid sequence identity with Mtd of methanogens (435). The results of comparative genomics suggest that homologs of these proteins are exclusively encoded by the genera *Nocardioides*, *Rhodococcus*, and *Nocardia* among presently sequenced organisms. Empirical studies consistently indicate that equivalent enzymatic pathways can degrade nitroaromatic compounds in five additional *Rhodococcus* species (398, 436–438) and three *Nocardioides* species (54, 396, 397, 432, 439). Beyond picrate and 2,4-dinitrophenol, LLHTs are involved in the biodegradation of other nitroaromatic compounds. We recently reported a *Nocardioides* strain that is able to mineralize 2,4-dinitroanisole (DNAN) through an initial O-demethylation step (catalyzed by a novel hydrolase) followed by degradation of the resultant 2,4-dinitrophenol by LLHTs (397). 2,4,6-Trinitrotoluene (TNT) can also be initially reduced to an equivalent hydride-Meisenheimer complex in *Rhodococcus* and *Mycobacterium* strains (440, 441); however, this is unproductive, as the complex cannot be further metabolized to yield carbon or nitrogen sources (441).

5. APPLICATIONS AND IMPLICATIONS

5.1. Tuberculosis Treatment

Globally, tuberculosis (TB) is the most significant bacterial disease in terms of morbidity and mortality, infecting approximately 2 billion individuals and causing approximately 1.5 million deaths in 2013 (442). The standard treatment for tuberculosis relies on a 6-month, four-drug combination therapy (isoniazid, rifampin,

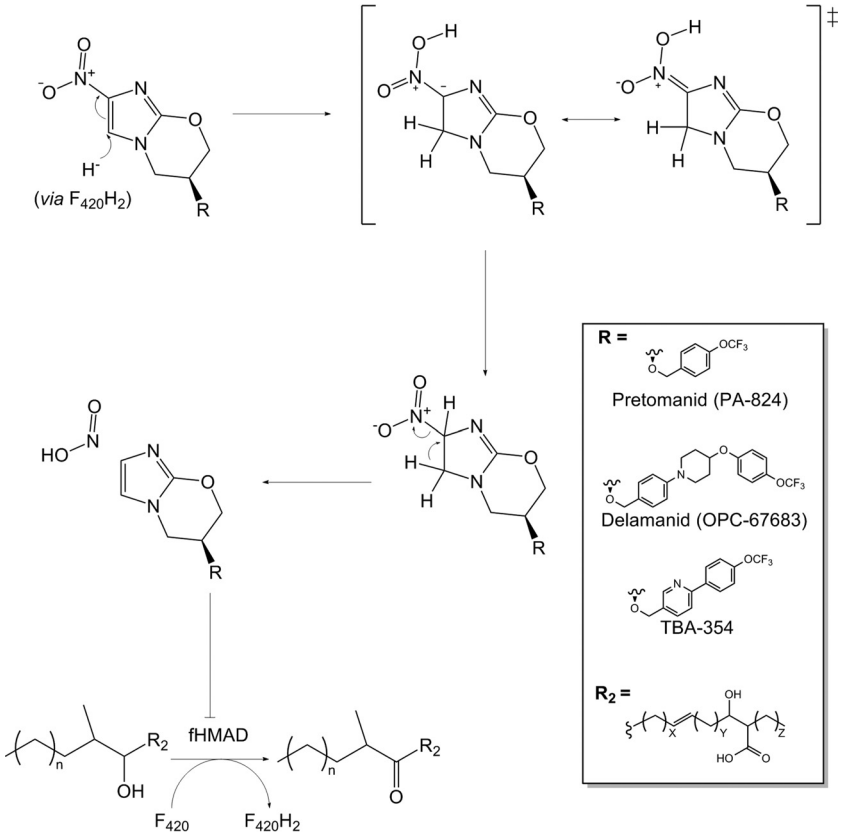

FIG 20 Reductive activation and mode of action of the prodrug pretomanid by the $F_{420}H_2$-dependent reductase rv3547 (FDOR-A1) (33, 34, 365).

pyrazinamide, and ethambutol) (443). There are major issues with this therapy: high cost per patient, poor compliance and management, growing worldwide drug resistance, and extensive drug-drug interactions (444). These problems are a reflection of the extraordinary biology of *M. tuberculosis*, which can transition between chronic and latent infection states that can evade the immune system and resist drug treatment (56), necessitating potent drug regimens to eliminate all tubercle bacilli from infected patients. There is thus an urgent need to develop new antimycobacterials to supplement or replace the current first-line drugs. F_{420} is implicated in the abilities of *M. tuberculosis* to maintain nonreplicating persistent states and resist antibiotic treatment, oxidative stress, and nitrosative stress (section 4.1). Hence, there may be particular promise in developing small-molecule inhibitors of F_{420} biosynthesis and enzymatic pathways in order to target persistent mycobacteria. The pleiotropic importance of F_{420} in *M. tuberculosis* (31, 32), combined with its absence from human cells and commensal microflora, suggest that a specific inhibitor would be highly potent while having few off-target effects. Such an inhibitor is likely to have a synergistic effect if used with existing drug regimens (with the exception of nitroimidazole prodrugs that require $F_{420}H_2$ for activation [33, 34]), given that strains unable to synthesize F_{420} are hypersusceptible to first-line and second-line antimycobacterials (32, 363). There are opportunities to use our knowledge of the F_{420} biosynthesis pathways for fragment-based drug screening and structure-based drug design (445), although no significant progress has been reported in this area thus far. The F_{420} system might also be exploited for the treatment of other serious mycobacterial diseases (145), for example those caused by *M. bovis*, *M. ulcerans*, *M. marinum*, and *M. leprae* (360).

However, there may be even more promise in exploiting the F_{420} system to activate prodrugs. Delamanid (OPC-67683; approved for multidrug-resistant TB [MDR-TB]) (446), pretomanid (PA-824; phase III clinical trials) (33), and the next-generation TBA-354 (phase I clinical trials) (447, 448) are recently developed nitroimidazole prodrugs that are activated by hydride transfer from $F_{420}H_2$ (Fig. 20). These compounds have been shown to inhibit *M. tuberculosis* growth at submicromolar levels and exhibit no cross-resistance with current clinical drugs *in vitro* due to their novel mode of action (33, 34, 446, 449–451). In particular, delamanid shows great promise in the treatment of multi- and extensively drug-resistant TB (MDR-TB and XDR-TB, respectively) (452–454), while combination therapies that incorporate pretomanid exhibited highly promising 14-day bactericidal activity with minimal side effects (455, 456). The mechanism of activation of these prodrugs has been studied primarily with pretomanid (Fig. 20). A member of the FDOR-A1 family (28, 30), rv3547 (deazaflavin-dependent nitroreductase [Ddn]), mediates the hydride transfer from $F_{420}H_2$ to the nitroimidazole (35, 164, 457). Hydride addition leads to the formation of an unstable intermediate, which decomposes into three primary metabolites (predominantly a des-nitro compound) (33–35). During the decomposition, the nitro group is eliminated, resulting in accumulation of reactive nitrogen species (nitric oxide, nitrous acid) in a dose-dependent manner (34, 458). Transcriptome profiling indicates that the prodrug has a dual bactericidal mode of action as a

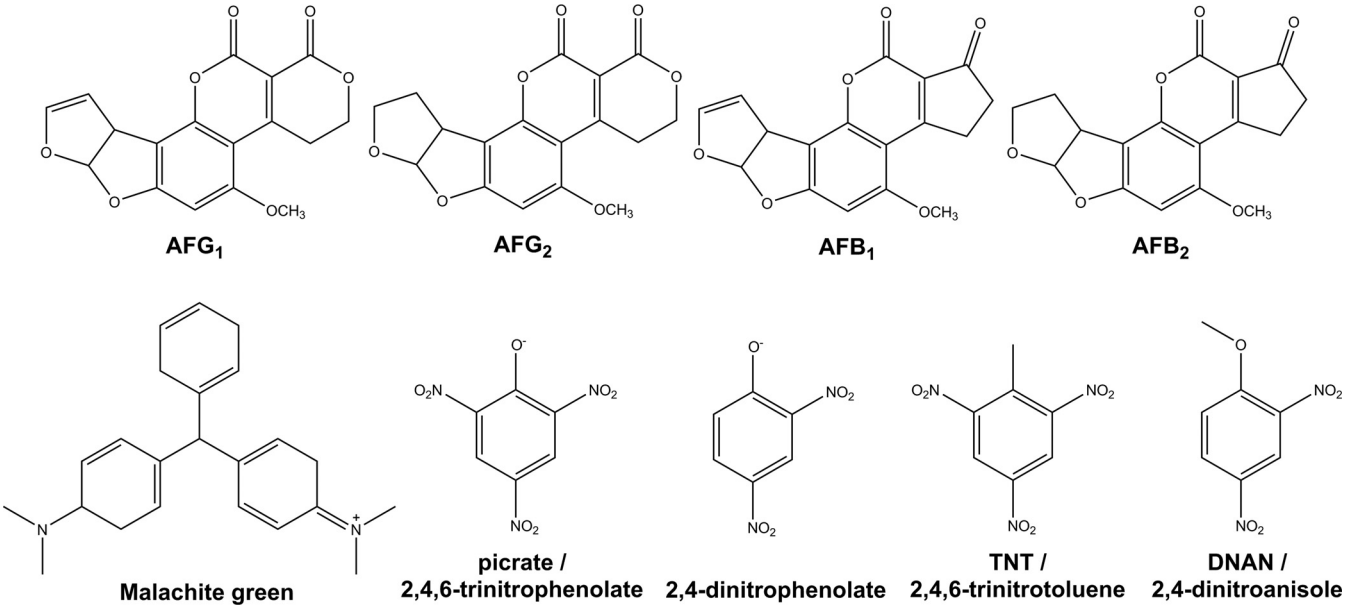

FIG 21 Chemical structures of xenobiotics reduced by actinobacterial $F_{420}H_2$-dependent reductases of the FDOR and LLHT superfamilies. The structures shown are of carcinogenic aflatoxins (aflatoxin G_1 [AFG_1], AFG_2, $AFGB_1$, and $AFGB_2$) (28), nitroaromatic explosives (picrate, 2,4-dinitrophenol, 2,4,6-trinitrotoluene, and 2,4-dinitroanisole) (396), and the toxin malachite green (132).

result of the products formed (33, 459): the primary decomposition products prevent mycolic acid biosynthesis (possibly by inhibiting fHMAD [365, 446]), while reactive nitrogen species (RNS) release causes respiratory poisoning (34). Other mycobacteria are thought to be resistant to pretomanid because they either lack homologs of the activating enzyme rv3547 (i.e., *M. leprae*) (460) or carry genes that encode homologous enzymes with mutations in the nitroimidazole-binding site (e.g., *M. smegmatis*) (30, 164).

There are, however, concerns that *M. tuberculosis* will rapidly develop resistance against nitroimidazoles (35, 461). Point mutations in Ddn may be able to prevent pretomanid activation without inhibiting the protein's native quinone reductase activity (30, 32). Likewise, loss of function of rv3547, *fbiC*, or *fgd* result in cross-resistance to delamanid and pretomanid (458). In the clinic, it was recently reported that an XRD-TB patient rapidly acquired delamanid resistance through loss of function of the F_{420} system (462). Interestingly, the original lead nitroimidazole compound for combating *M. tuberculosis*, CGI-17341 (now abandoned due to safety concerns) (463), depends on the presence of F_{420} but not Ddn for antimicrobial activity (458). As CGI-17341 lacks the hydrophobic tail and phenyloxazole residues of delamanid and pretomanid, it is likely to be activated by a wider range of FDORs (458). It may therefore be possible to develop next-generation nitroimidazoles that are broadly activated by FDORs and hence will have more promising antimicrobial resistance profiles.

5.2. Methane Mitigation

Methane is the second most important anthropogenic greenhouse gas and contributes to about 20% of total anthropogenic climate forcing. Approximately 70% of methane emissions result from the activity of methanogens, the abundance of which has increased as a result of ruminant animal farming, rice paddy agriculture, and solid and liquid waste production (464). As a dominant catabolic cofactor in methanogens, as well as a central mediator in hydrogenotrophic, formatotrophic, and methylotrophic methanogenesis, F_{420} facilitates these emissions. One strategy targeted at reducing methane emissions from ruminant animals and rice paddy fields is to administer methanogen inhibitors (465–467). Economical methanogenesis inhibitors may be particularly attractive in livestock agriculture, as they may simultaneously reduce greenhouse gas emissions while enhancing ruminant productivity (468). Highlighting the potential in this area, a recent study demonstrated that administration of the methyl-CoM reductase inhibitor 3-nitrooxypropanol to dairy cattle feed decreased methane production and increased body weight gain (468, 469). Other highly promising targets for methane mitigation include the F_{420} biosynthesis enzymes CofG/CofH and oxidoreductase Mer, given their presence and predicted essentiality in all methanogens, including obligately aceticlastic species (196). Given that these targets are absent from host cells and other ruminal microbiota (where ANME are not competitive), specific inhibitors are likely to have minimal off-target effects.

5.3. Bioremediation

Many $F_{420}H_2$-dependent reductases have broad substrate specificity and can reductively degrade diverse xenobiotic compounds. For example, mycobacterial flavin/deazaflavin oxidoreductases can degrade coumarin derivatives (28, 55), while rhodococcal luciferase-like hydride transferases can reduce polynitroaromatic compounds (438, 440). While the physiological advantage conferred by this promiscuity has not been fully resolved, it does provide a basis for the exploitation of F_{420} in bioremediation applications (470). It may be possible to deploy F_{420}-dependent organisms to remediate lands and waters contaminated with toxins and explosives. The most significant environmental contaminants that may be remediated through F_{420}-dependent processes are picrate, aflatoxins, and dyes such as malachite green (Fig. 21).

Among the most carcinogenic and hepatotoxic compounds known, aflatoxins are a group of mycotoxins produced by *Aspergillus flavus* and *Aspergillus parasiticus* that contaminate crops in tropical climates (471, 472). As coumarin derivatives, difurocoumarocyclopentenones (aflatoxins B1 and B2) and difurocoumarolactones (aflatoxins G1 and G2) can be efficiently degraded by mycobacterial $F_{420}H_2$-dependent reductases (28, 409). *Rhodococcus erythropolis* and *Nocardia corynebacterioides* can also degrade aflatoxin, possibly through using homologous enzymes (472–474). Environmental mycobacteria are also capable of decolorizing and detoxifying malachite green in an F_{420}-dependent manner (132, 475); while once extensively used as an antiparasitic in aquaculture, this compound has since become regulated against due to its toxicological properties (476).

Picrate and related nitroaromatic compounds are highly toxic explosives that extensively contaminate soils in current and former explosive manufacturing, processing, and storage facilities (477). Luciferase-like hydride transferases from certain actinomycetes can initiate mineralization of such compounds (438, 440). In the case of 2,4,6-trinitrotoluene (TNT), hydride transfer from LLHTs lead to the formation of dead-end products that cannot be further degraded (440, 441). However, multiple strains of *Rhodococcus*, *Nocardia*, and *Nocardioides* can completely mineralize picrate, 2,4-dinitrophenol (DNP), and 2,4-dinitroanisole (DNAP) as the sole carbon and nitrogen sources (396, 397). Administration of such bacteria to nitroaromatic-contaminated sites may be a cheaper and faster alternative to traditional physical remediation methods (477, 478). Consistently, there are reports of *Rhodococcus* sp. strain NJUST16 being used to biodegrade picrate from contaminated soils (437). As with bioremediation of aflatoxins and malachite green, administration of live bacteria is a more promising option than cell-free enzymatic systems, because F_{420} must be enzymatically reduced before it is utilized by $F_{420}H_2$-dependent reductases.

5.4. Industrial Biocatalysis

F_{420} may also prove a useful addition to the toolboxes of synthetic chemists. F_{420}-dependent processes already provide essential steps in some industrial processes, for example in the synthesis of some of the oldest-known antibiotic classes (29, 381), and there is considerable potential to expand the role of F_{420}-dependent enzymes as catalysts for synthetic chemistry. $F_{420}H_2$-dependent reductases of the FDOR and LLHT superfamilies can catalyze the stereospecific reduction of enones (28, 55, 291, 409) and imines (50, 388, 393) in diverse heterocycles. The broad substrate range of these enzymes may be particularly useful for catalyzing hydride addition to nonnatural compounds in a potentially stereospecific manner (479, 480). Such enzymes may be particularly useful in whole-cell biosynthetic cascades if coexpressed with cofactor recycling systems. A promising precedent in this regard is provided by the use of old yellow enzymes (OYEs) for the asymmetric reduction of enone moieties in yeast and bacteria (481). OYEs are mechanistically predisposed to *trans*-hydrogenation, whereby a hydride is delivered to the substrate from the cofactor and a proton is delivered to the opposite face of the substrate from an active site tyrosine (482). As $F_{420}H_2$-dependent reductases deliver hydrides from the cofactor, it is likely that they will provide access to *cis*-hydrogenation of enones for biocatalytic processes (including *in vivo*). Asymmetric imine reduction by enzymes is a promising area for development (483), not least because of the prominence of chiral amines in modern synthetic chemistry: ~40% of pharmaceuticals and ~20% of agrochemicals contain at least one chiral amine (484). However, the toolbox of enzymes available for use in such applications is still small and incomplete; there are few enzymes that will reduce a prochiral imine in a linear molecule, for example (483). The capacity of F_{420}-dependent enzymes to catalyze such imine reductions has, as yet, been explored only superficially (470).

A significant barrier to industrial application of F_{420}-dependent enzymes in biocatalytic applications is the commercial unavailability of F_{420}. While total chemical synthesis has been achieved (485), the most efficient and affordable way to obtain the cofactor is presently through extraction from F_{420} producers. Most laboratory-scale preparations of the cofactor currently rely on *Mycobacterium smegmatis*, a safe "fast"-growing aerobic bacterium that synthesizes micromolar quantities of F_{420} during fermenter growth (96). Bashiri et al. (486) were able to enhance F_{420} production in this organism by overexpressing the *fbiABC* genes in *trans* and inducing F_{420} production in a rich autoinduction medium. F_{420} can subsequently be purified from lysed cells by anion-exchange chromatography, followed by hydrophobic-interaction chromatography (96, 486). In the long-term, it would be preferable to metabolically engineer large-scale recombinant F_{420} production in *Escherichia coli*; however, this depends on the identification of the elusive enzyme responsible for production of 2-phospho-L-lactate (470). The capacity to produce F_{420} in heterologous organisms that do not naturally produce or use the cofactor also raises some interesting possibilities for synthetic biology. "Exotic" cofactors may enable wholly orthogonal synthetic pathways for chemical production in an organism, essentially divorcing the pathway from the central metabolic and regulatory background of the production organism.

6. CONCLUDING REMARKS

On first inspection, it seems surprising that 5-deazaflavins are involved in such disparate processes; very little seems to unify methanogenesis, tetracycline biosynthesis, and DNA photoreactivation other than this class of compounds. Underlying the selection of 5-deazaflavins across biology, however, are the unique properties conferred by the N-5 (flavin) to C-5 (deazaflavin) substitution. The photochemical properties of 5-deazaflavins are crucial for the role of F_o in light capturing and FRET. The electrochemical properties of F_{420} place it at the center of methanogenic redox metabolism and provide actinobacteria with a way of catalyzing low-potential hydride transfer reactions in their primary and secondary metabolism. The enzymes that synthesize 5-deazaflavins share conserved sequences and folds, suggesting that they were either present in the last universal common ancestor or were laterally transferred between archaea and bacteria. However, oxidoreductases appear to have evolved the capacity to utilize F_{420} on multiple occasions from related nicotinamide- or flavin-dependent proteins. Three types of F_{420}-binding sites are nevertheless conserved throughout biology, namely, those in FrhB-like, TIM barrel, and split β-barrel folds. Many F_{420}-dependent enzymes have a modular nature—as particularly evident in Frh, Fpo, and Fsr—suggesting that F_{420} is versatile enough to be accommodated in a wide range of redox enzyme systems.

For the future, there are numerous opportunities to both explore and exploit F_{420}. While we have a relatively rich understanding of the physiology and biochemistry of F_{420} in methanogenesis,

there are still conundrums to solve, for example in relation to the structurally unresolved Ffd, Fpo, and Fsr enzymes. Our understanding of the roles of F_{420} in actinobacteria is much less sophisticated, and there are multiple important questions to resolve. For example, why is F_{420} required for mycobacterial persistence and antibiotic resistance? Why do mycobacteria encode such a multiplicity of FDORs and LLHTs? What are the primary roles of F_{420} in the metabolism of streptomycetes and rhodococci? Looking at the bigger picture, it is still poorly understood how F_{420} biosynthesis pathways have evolved and why F_{420} is distributed in relatively few phyla. However, the finding that F_{420} is likely to be synthesized by ANME, *Chloroflexi*, and *Proteobacteria* indicates that the cofactor may be more important in oxic and anoxic communities than previously anticipated. There is also an urgent need to understand the role of F_{420} at the ecosystem level, particularly in relation to how F_{420}-dependent biodegradation processes influence the community structuring and chemical composition of soils. Fueled by the recent approval of delamanid for treatment of multidrug-resistant tuberculosis, there is also room to explore the application of F_{420} for medical, environmental, and industrial purposes. Half a century since their discovery by the Wolfe laboratory, 5-deazaflavins continue to surprise biologists and chemists alike.

ACKNOWLEDGMENTS

We thank Robyn Russell, Carol Hartley, Trevor Rapson, and the three anonymous reviewers for their useful comments on this review.

This work was supported by Australian Research Council research grants (DE120102673 and DP130102144) awarded to C.J.J., a CSIRO Office of the Chief Executive Postdoctoral Fellowship awarded to C.G., and Australian National University Higher Degree by Research PhD scholarships awarded to F.H.A., A.E.M., and B.M.L.

REFERENCES

1. **Hemmerich P, Nagelschneider G, Veeger C.** 1970. Chemistry and molecular biology of flavins and flavoproteins. FEBS Lett **8:**69–83. http://dx.doi.org/10.1016/0014-5793(70)80229-0.
2. **Walsh C.** 1980. Flavin coenzymes: at the crossroads of biological redox chemistry. Acc Chem Res **13:**148–155. http://dx.doi.org/10.1021/ar50149a004.
3. **O'Brien DE, Weinstock LT, Cheng CC.** 1967. 10-Deazariboflavin. Chem Ind **48:**2044–2045.
4. **O'Brien DE, Weinslock LT, Cheng CC.** 1970. Synthesis of 10-deazariboflavin and related 2,4-dioxopyrimido[4,5-b]quinolines. J Heterocycl Chem **7:**99–105. http://dx.doi.org/10.1002/jhet.5570070114.
5. **Cheeseman P, Toms-Wood A, Wolfe RS.** 1972. Isolation and properties of a fluorescent compound, Factor420, from Methanobacterium strain MoH. J Bacteriol **112:**527–531.
6. **Eirich LD, Vogels GD, Wolfe RS.** 1978. Proposed structure for coenzyme F_{420} from *Methanobacterium*. Biochemistry **17:**4583–4593. http://dx.doi.org/10.1021/bi00615a002.
7. **Walsh C.** 1986. Naturally occurring 5-deazaflavin coenzymes: biological redox roles. Acc Chem Res **19:**216–221. http://dx.doi.org/10.1021/ar00127a004.
8. **Jacobson F, Walsh C.** 1984. Properties of 7,8-didemethyl-8-hydroxy-5-deazaflavins relevant to redox coenzyme function in methanogen metabolism. Biochemistry **23:**979–988. http://dx.doi.org/10.1021/bi00300a028.
9. **de Poorter LMI, Geerts WJ, Keltjens JT.** 2005. Hydrogen concentrations in methane-forming cells probed by the ratios of reduced and oxidized coenzyme F_{420}. Microbiology **151:**1697–1705. http://dx.doi.org/10.1099/mic.0.27679-0.
10. **Friedrich W.** 1988. Vitamins. Walter de Gruyter & Co., Berlin, Germany.
11. **Jacobson FS, Daniels L, Fox JA, Walsh CT, Orme-Johnson WH.** 1982. Purification and properties of an 8-hydroxy-5-deazaflavin-reducing hydrogenase from *Methanobacterium thermoautotrophicum*. J Biol Chem **257:**3385–3388.
12. **Eker AP, Hessels JK, Meerwaldt R.** 1989. Characterization of an 8-hydroxy-5-deazaflavin:NADPH oxidoreductase from *Streptomyces griseus*. Biochim Biophys Acta **990:**80–86. http://dx.doi.org/10.1016/S0304-4165(89)80015-7.
13. **Hossain MS, Le CQ, Joseph E, Nguyen TQ, Johnson-Winters K, Foss FW.** 2015. Convenient synthesis of deazaflavin cofactor F_O and its activity in F_{420}-dependent NADP reductase. Org Biomol Chem **13:**5082–5085. http://dx.doi.org/10.1039/C5OB00365B.
14. **Wolin EA, Wolin MJ, Wolfe RS.** 1963. Formation of methane by bacterial extracts. J Biol Chem **238:**2882–2886.
15. **Eirich LD, Vogels GD, Wolfe RS.** 1979. Distribution of coenzyme F_{420} and properties of its hydrolytic fragments. J Bacteriol **140:**20–27.
16. **Tzeng SF, Wolfe RS, Bryant MP.** 1975. Factor 420-dependent pyridine nucleotide-linked hydrogenase system of *Methanobacterium ruminantium*. J Bacteriol **121:**184–191.
17. **Tzeng SF, Bryant MP, Wolfe RS.** 1975. Factor 420-dependent pyridine nucleotide-linked formate metabolism of *Methanobacterium ruminantium*. J Bacteriol **121:**192–196.
18. **Hartzell PL, Zvilius G, Escalante-Semerena JC, Donnelly MI.** 1985. Coenzyme F_{420} dependence of the methylenetetrahydromethanopterin dehydrogenase of *Methanobacterium thermoautotrophicum*. Biochem Biophys Res Commun **133:**884–890. http://dx.doi.org/10.1016/0006-291X(85)91218-5.
19. **Stetter KO, Lauerer G, Thomm M, Neuner A.** 1987. Isolation of extremely thermophilic sulfate reducers: evidence for a novel branch of archaebacteria. Science **236:**822–824. http://dx.doi.org/10.1126/science.236.4803.822.
20. **Lin XL, White RH.** 1986. Occurrence of coenzyme F_{420} and its γ-monoglutamyl derivative in nonmethanogenic archaebacteria. J Bacteriol **168:**444–448.
21. **Hallam SJ, Putnam N, Preston CM, Detter JC, Rokhsar D, Richardson PM, DeLong EF.** 2004. Reverse methanogenesis: testing the hypothesis with environmental genomics. Science **305:**1457–1462. http://dx.doi.org/10.1126/science.1100025.
22. **Berk H, Thauer RK.** 1997. Function of coenzyme F_{420}-dependent NADP reductase in methanogenic archaea containing an NADP-dependent alcohol dehydrogenase. Arch Microbiol **168:**396–402. http://dx.doi.org/10.1007/s002030050514.
23. **Cousins FB.** 1960. The prosthetic group of a chromoprotin from mycobacteria. Biochim Biophys Acta **40:**532–534. http://dx.doi.org/10.1016/0006-3002(60)91396-2.
24. **Miller PA, Sjolander NO, Nalesnyk S, Arnold N, Johnson S, Doerschuk AP, McCormick JRD.** 1960. Cosynthetic factor I, a factor involved in hydrogen-transfer in *Streptomyces aureofaciens*. J Am Chem Soc **82:**5002–5003. http://dx.doi.org/10.1021/ja01503a063.
25. **Eker APM, Pol A, van der Meyden P, Vogels GD.** 1980. Purification and properties of 8-hydroxy-5-deazaflavin derivatives from *Streptomyces griseus*. FEMS Microbiol Lett **8:**161–165. http://dx.doi.org/10.1111/j.1574-6968.1980.tb05071.x.
26. **Naraoka T, Momoi K, Fukasawa K, Goto M.** 1984. Isolation and identification of a naturally occurring 7, 8-didemethyl-8-hydroxy-5-deazariboflavin derivative from *Mycobacterium avium*. Biochim Biophys Acta **797:**377–380. http://dx.doi.org/10.1016/0304-4165(84)90260-5.
27. **Daniels L, Bakhiet N, Harmon K.** 1985. Widespread distribution of a 5-deazaflavin cofactor in *Actinomyces* and related bacteria. Syst Appl Microbiol **6:**12–17. http://dx.doi.org/10.1016/S0723-2020(85)80004-7.
28. **Taylor MC, Jackson CJ, Tattersall DB, French N, Peat TS, Newman J, Briggs LJ, Lapalikar GV, Campbell PM, Scott C, Russell RJ, Oakeshott JG.** 2010. Identification and characterization of two families of $F_{420}H_2$-dependent reductases from *Mycobacteria* that catalyse aflatoxin degradation. Mol Microbiol **78:**561–575. http://dx.doi.org/10.1111/j.1365-2958.2010.07356.x.
29. **Wang P, Bashiri G, Gao X, Sawaya MR, Tang Y.** 2013. Uncovering the enzymes that catalyze the final steps in oxytetracycline biosynthesis. J Am Chem Soc **135:**7138–7141. http://dx.doi.org/10.1021/ja403516u.
30. **Ahmed FH, Carr PD, Lee BM, Afriat-Jurnou L, Mohamed AE, Hong N-S, Flanagan J, Taylor MC, Greening C, Jackson CJ.** 2015. Sequence-structure-function classification of a catalytically diverse oxidoreductase superfamily in mycobacteria. J Mol Biol **427:**3554–3571. http://dx.doi.org/10.1016/j.jmb.2015.09.021.
31. **Purwantini E, Mukhopadhyay B.** 2009. Conversion of NO_2 to NO by reduced coenzyme F_{420} protects mycobacteria from nitrosative damage. Proc Natl Acad Sci U S A **106:**6333–6338. http://dx.doi.org/10.1073/pnas.0812883106.

32. **Gurumurthy M, Rao M, Mukherjee T, Rao SPS, Boshoff HI, Dick T, Barry CE, Manjunatha UH.** 2013. A novel F_{420}-dependent anti-oxidant mechanism protects *Mycobacterium tuberculosis* against oxidative stress and bactericidal agents. Mol Microbiol **87:**744–755. http://dx.doi.org/10.1111/mmi.12127.
33. **Stover CK, Warrener P, VanDevanter DR, Sherman DR, Arain TM, Langhorne MH, Anderson SW, Towell JA, Yuan Y, McMurray DN, Kreiswirth BN, Barry CE, Baker WR.** 2000. A small-molecule nitroimidazopyran drug candidate for the treatment of tuberculosis. Nature **405:**962–966. http://dx.doi.org/10.1038/35016103.
34. **Singh R, Manjunatha U, Boshoff HIM, Ha YH, Niyomrattanakit P, Ledwidge R, Dowd CS, Lee IY, Kim P, Zhang L, Kang S, Keller TH, Jiricek J, Barry CE.** 2008. PA-824 kills nonreplicating *Mycobacterium tuberculosis* by intracellular NO release. Science **322:**1392–1395. http://dx.doi.org/10.1126/science.1164571.
35. **Manjunatha UH, Boshoff H, Dowd CS, Zhang L, Albert TJ, Norton JE, Daniels L, Dick T, Pang SS, Barry CE.** 2006. Identification of a nitroimidazo-oxazine-specific protein involved in PA-824 resistance in *Mycobacterium tuberculosis*. Proc Natl Acad Sci U S A **103:**431–436. http://dx.doi.org/10.1073/pnas.0508392103.
36. **Lewis JM, Sloan DJ.** 2015. The role of delamanid in the treatment of drug-resistant tuberculosis. Ther Clin Risk Manag **11:**779–791. http://dx.doi.org/10.2147/TCRM.S71076.
37. **Selengut JD, Haft DH.** 2010. Unexpected abundance of coenzyme F_{420}-dependent enzymes in *Mycobacterium tuberculosis* and other actinobacteria. J Bacteriol **192:**5788–5798. http://dx.doi.org/10.1128/JB.00425-10.
38. **Hemmerich P, Massey V, Fenner H.** 1977. Flavin and 5-deazaflavin: a chemical evaluation of "modified" flavoproteins with respect to the mechanisms of redox biocatalysis. FEBS Lett **84:**5–21. http://dx.doi.org/10.1016/0014-5793(77)81047-8.
39. **Spencer R, Fisher J, Walsh C.** 1976. Preparation, characterization, and chemical properties of the flavin coenzyme analogues 5-deazariboflavin, 5-deazariboflavin 5′-phosphate, and 5-deazariboflavin 5′-diphosphate, 5′ leads to 5′-adenosine ester. Biochemistry **15:**1043–1053. http://dx.doi.org/10.1021/bi00650a015.
40. **Jorns MS, Hersh LB.** 1975. N-methylglutamate synthetase. Substrate-flavin hydrogen transfer reactions probed with deazaflavin mononucleotide. J Biol Chem **250:**3620–3628.
41. **Averill BA, Schonbrunn A, Abeles RH.** 1975. Studies on the mechanism of *Mycobacterium smegmatis* L-lactate oxidase. 5 deazaflavin mononucleotide as a coenzyme analogue. J Biol Chem **250:**1603–1605.
42. **Jorns MS, Hersh LB.** 1976. Nucleophilic addition reactions of free and enzyme-bound deazaflavin. J Biol Chem **251:**4872–4881.
43. **Fisher J, Spencer R, Walsh C.** 1976. Enzyme-catalyzed redox reactions with the flavin analogues 5-deazariboflavin, 5-deazariboflavin 5′-phosphate, and 5-deazariboflavin 5′-diphosphate, 5′→5′-adenosine ester. Biochemistry **15:**1054–1064. http://dx.doi.org/10.1021/bi00650a016.
44. **Edmondson DE, Barman B, Tollin G.** 1972. Importance of the N-5 position in flavin coenzymes. Properties of free and protein-bound 5-deaza analogs. Biochemistry **11:**1133–1138.
45. **Eker APM, Dekker RH, Berends W.** 1981. Photoreactivating enzyme from *Streptomyces griseus*-IV. On the nature of the chromophoric cofactor in *Streptomyces griseus* photoreactivating enzyme. Photochem Photobiol **33:**65–72.
46. **Xia K, Shen G-B, Zhu X-Q.** 2015. Thermodynamics of various F_{420} coenzyme models as sources of electrons, hydride ions, hydrogen atoms and protons in acetonitrile. Org Biomol Chem **13:**6255–6268. http://dx.doi.org/10.1039/C5OB00538H.
47. **Hagemeier CH, Shima S, Thauer RK, Bourenkov G, Bartunik HD, Ermler U.** 2003. Coenzyme F_{420}-dependent methylenetetrahydromethanopterin dehydrogenase (Mtd) from *Methanopyrus kandleri*: a methanogenic enzyme with an unusual quarternary structure. J Mol Biol **332:**1047–1057. http://dx.doi.org/10.1016/S0022-2836(03)00949-5.
48. **Aufhammer SW, Warkentin E, Ermler U, Hagemeier CH, Thauer RK, Shima S.** 2005. Crystal structure of methylenetetrahydromethanopterin reductase (Mer) in complex with coenzyme F_{420}: architecture of the F_{420}/FMN binding site of enzymes within the nonprolyl cis-peptide containing bacterial luciferase family. Protein Sci **14:**1840–1849. http://dx.doi.org/10.1110/ps.041289805.
49. **Aufhammer SW, Warkentin E, Berk H, Shima S, Thauer RK, Ermler U.** 2004. Coenzyme binding in F_{420}-dependent secondary alcohol dehydrogenase, a member of the bacterial luciferase family. Structure **12:**361–370. http://dx.doi.org/10.1016/j.str.2004.02.010.
50. **Li W, Chou S, Khullar A, Gerratana B.** 2009. Cloning and characterization of the biosynthetic gene cluster for tomaymycin, an SJG-136 monomeric analog. Appl Environ Microbiol **75:**2958–2963. http://dx.doi.org/10.1128/AEM.02325-08.
51. **Johnson EF, Mukhopadhyay B.** 2005. A new type of sulfite reductase, a novel coenzyme F_{420}-dependent enzyme, from the methanarchaeon *Methanocaldococcus jannaschii*. J Biol Chem **280:**38776–38786. http://dx.doi.org/10.1074/jbc.M503492200.
52. **Silaghi-Dumitrescu R, Kurtz DM, Jr, Ljungdahl LG, Lanzilotta WN.** 2005. X-ray crystal structures of *Moorella thermoacetica* FprA. Novel diiron site structure and mechanistic insights into a scavenging nitric oxide reductase. Biochemistry **44:**6492–6501.
53. **Thauer RK, Jungermann K, Decker K.** 1977. Energy conservation in chemotrophic anaerobic bacteria. Bacteriol Rev **41:**100–180.
54. **Ebert S, Rieger P-G, Knackmuss H-J.** 1999. Function of coenzyme F_{420} in aerobic catabolism of 2,4,6-trinitrophenol and 2,4-dinitrophenol by *Nocardioides simplex* FJ2-1A. J Bacteriol **181:**2669–2674.
55. **Lapalikar GV, Taylor MC, Warden AC, Scott C, Russell RJ, Oakeshott JG.** 2012. $F_{420}H_2$-dependent degradation of aflatoxin and other furanocoumarins is widespread throughout the Actinomycetales. PLoS One **7:**e30114. http://dx.doi.org/10.1371/journal.pone.0030114.
56. **Boshoff H, Barry C.** 2005. Tuberculosis - metabolism and respiration in the absence of growth. Nat Rev Microbiol **3:**70–80. http://dx.doi.org/10.1038/nrmicro1065.
57. **Tamada T, Kitadokoro K, Higuchi Y, Inaka K, Yasui A, de Ruiter PE, Eker AP, Miki K.** 1997. Crystal structure of DNA photolyase from *Anacystis nidulans*. Nat Struct Biol **4:**887–891. http://dx.doi.org/10.1038/nsb1197-887.
58. **Malhotra K, Kim ST, Walsh C, Sancar A.** 1992. Roles of FAD and 8-hydroxy-5-deazaflavin chromophores in photoreactivation by *Anacystis nidulans* DNA photolyase. J Biol Chem **267:**15406–15411.
59. **Edwards T, McBride BC.** 1975. New method for the isolation and identification of methanogenic bacteria. Appl Microbiol **29:**540–545.
60. **Doddema HJ, Vogels GD.** 1978. Improved identification of methanogenic bacteria by fluorescence microscopy. Appl Environ Microbiol **36:**752–754.
61. **van Beelen P, Dijkstra AC, Vogels GD.** 1983. Quantitation of coenzyme F_{420} in methanogenic sludge by the use of reversed-phase high-performance liquid chromatography and a fluorescence detector. Eur J Appl Microbiol Biotechnol **18:**67–69. http://dx.doi.org/10.1007/BF00508132.
62. **Dolfing J, Mulder J-W.** 1985. Comparison of methane production rate and coenzyme F_{420} content of methanogenic consortia in anaerobic granular sludge. Appl Environ Microbiol **49:**1142–1145.
63. **Reynolds PJ, Colleran E.** 1987. Evaluation and improvement of methods for coenzyme F_{420} analysis in anaerobic sludges. J Microbiol Methods **7:**115–130. http://dx.doi.org/10.1016/0167-7012(87)90032-7.
64. **Ashby KD, Casey TA, Rasmussen MA, Petrich JW.** 2001. Steady-state and time-resolved spectroscopy of F_{420} extracted from methanogen cells and its utility as a marker for fecal contamination. J Agric Food Chem **49:**1123–1127. http://dx.doi.org/10.1021/jf000689r.
65. **Kim YS, Westerholm M, Scherer P.** 2014. Dual investigation of methanogenic processes by quantitative PCR and quantitative microscopic fingerprinting. FEMS Microbiol Lett **360:**76–84. http://dx.doi.org/10.1111/1574-6968.12592.
66. **Rohde RA, Price PB.** 2007. Diffusion-controlled metabolism for long-term survival of single isolated microorganisms trapped within ice crystals. Proc Natl Acad Sci U S A **104:**16592–16597. http://dx.doi.org/10.1073/pnas.0708183104.
67. **Patiño S, Alamo L, Cimino M, Casart Y, Bartoli F, García MJ, Salazar L.** 2008. Autofluorescence of mycobacteria as a tool for detection of *Mycobacterium tuberculosis*. J Clin Microbiol **46:**3296–3302. http://dx.doi.org/10.1128/JCM.02183-07.
68. **Maglica Ž, Özdemir E, McKinney JD.** 2015. Single-cell tracking reveals antibiotic-induced changes in mycobacterial energy metabolism. mBio **6:**e02236-14. http://dx.doi.org/10.1128/mBio.02236-14.
69. **Fischer M, Bacher A.** 2006. Biosynthesis of vitamin B_2 in plants. Physiol Plant **126:**304–318. http://dx.doi.org/10.1111/j.1399-3054.2006.00607.x.
70. **Graham DE, Xu H, White RH.** 2003. Identification of the 7,8-didemethyl-8-hydroxy-5-deazariboflavin synthase required for coen-

zyme F_{420} biosynthesis. Arch Microbiol **180:**455–464. http://dx.doi.org/10.1007/s00203-003-0614-8.
71. **Decamps L, Philmus B, Benjdia A, White R, Begley TP, Berteau O.** 2012. Biosynthesis of F_0, precursor of the F_{420} cofactor, requires a unique two radical-SAM domain enzyme and tyrosine as substrate. J Am Chem Soc **134:**18173–18176. http://dx.doi.org/10.1021/ja307762b.
72. **Choi K-P, Kendrick N, Daniels L.** 2002. Demonstration that *fbiC* is required by *Mycobacterium bovis* BCG for coenzyme F_{420} and F_O biosynthesis. J Bacteriol **184:**2420–2428. http://dx.doi.org/10.1128/JB.184.9.2420-2428.2002.
73. **Philmus B, Decamps L, Berteau O, Begley TP.** 2015. Biosynthetic versatility and coordinated action of 5′-deoxyadenosyl radicals in deazaflavin biosynthesis. J Am Chem Soc **137:**5406–5413. http://dx.doi.org/10.1021/ja513287k.
74. **Epple R, Carell T.** 1998. Flavin- and deazaflavin-containing model compounds mimic the energy transfer step in type II DNA photolyases. Angew Chem Int Ed **37:**938–941. http://dx.doi.org/10.1002/(SICI)1521-3773(19980420)37:7<938::AID-ANIE938>3.0.CO;2-P.
75. **Sancar A.** 2003. Structure and function of DNA photolyase and cryptochrome blue-light photoreceptors. Chem Rev **103:**2203–2238. http://dx.doi.org/10.1021/cr0204348.
76. **Yasui A, Takao M, Oikawa A, Kiener A, Walsh CT, Eker AP.** 1988. Cloning and characterization of a photolyase gene from the cyanobacterium *Anacystis nidulans*. Nucleic Acids Res **16:**4447–4463. http://dx.doi.org/10.1093/nar/16.10.4447.
77. **Eker AP, Kooiman P, Hessels JK, Yasui A.** 1990. DNA photoreactivating enzyme from the cyanobacterium Anacystis nidulans. J Biol Chem **265:**8009–8015.
78. **Kelner A.** 1949. Effect of visible light on the recovery of *Streptomyces griseus* conidia from ultra-violet irradiation injury. Proc Natl Acad Sci U S A **35:**73–79. http://dx.doi.org/10.1073/pnas.35.2.73.
79. **Kobayashi T, Takao M, Oikawa A, Yasui A.** 1989. Molecular characterization of a gene encoding a photolyase from *Streptomyces griseus*. Nucleic Acids Res **17:**4731–4744. http://dx.doi.org/10.1093/nar/17.12.4731.
80. **Mayerl F, Piret J, Kiener A, Walsh CT, Yasui A.** 1990. Functional expression of 8-hydroxy-5-deazaflavin-dependent DNA photolyase from *Anacystis nidulans* in *Streptomyces coelicolor*. J Bacteriol **172:**6061–6065.
81. **Kiener A, Husain I, Sancar A, Walsh C.** 1989. Purification and properties of *Methanobacterium thermoautotrophicum* DNA photolyase. J Biol Chem **264:**13880–13887.
82. **Kiontke S, Gnau P, Haselsberger R, Batschauer A, Essen L-O.** 2014. Structural and evolutionary aspects of antenna chromophore usage by class II photolyases. J Biol Chem **289:**19659–19669. http://dx.doi.org/10.1074/jbc.M113.542431.
83. **Takao M, Kobayashi T, Oikawa A, Yasui A.** 1989. Tandem arrangement of photolyase and superoxide dismutase genes in *Halobacterium halobium*. J Bacteriol **171:**6323–6329.
84. **Eker APM, Hessels JKC, van de Velde J.** 1988. Photoreactivating enzyme from the green alga *Scenedesmus acutus*. Evidence for the presence of two different flavin chromophores. Biochemistry **27:**1758–1765.
85. **Glas AF, Maul MJ, Cryle M, Barends TRM, Schneider S, Kaya E, Schlichting I, Carell T.** 2009. The archaeal cofactor F_0 is a light-harvesting antenna chromophore in eukaryotes. Proc Natl Acad Sci U S A **106:**11540–11545. http://dx.doi.org/10.1073/pnas.0812665106.
86. **Petersen JL, Ronan PJ.** 2010. Critical role of 7,8-didemethyl-8-hydroxy-5-deazariboflavin for photoreactivation in *Chlamydomonas reinhardtii*. J Biol Chem **285:**32467–32475. http://dx.doi.org/10.1074/jbc.M110.146050.
87. **Selby CP, Sancar A.** 2012. The second chromophore in *Drosophila* photolyase/cryptochrome family photoreceptors. Biochemistry **51:**167–171. http://dx.doi.org/10.1021/bi201536w.
88. **Bennett CJ, Webb M, Willer DO, Evans DH.** 2003. Genetic and phylogenetic characterization of the type II cyclobutane pyrimidine dimer photolyases encoded by Leporipoxviruses. Virology **315:**10–19. http://dx.doi.org/10.1016/S0042-6822(03)00512-9.
89. **van Oers MM, Herniou EA, Usmany M, Messelink GJ, Vlak JM.** 2004. Identification and characterization of a DNA photolyase-containing baculovirus from *Chrysodeixis chalcites*. Virology **330:**460–470. http://dx.doi.org/10.1016/j.virol.2004.09.032.
90. **van Oers MM, Lampen MH, Bajek MI, Vlak JM, Eker APM.** 2008. Active DNA photolyase encoded by a baculovirus from the insect Chrysodeixis chalcites. DNA Repair (Amst) **7:**1309–1318. http://dx.doi.org/10.1016/j.dnarep.2008.04.013.
91. **Biernat MA, Ros VID, Vlak JM, van Oers MM.** 2011. Baculovirus cyclobutane pyrimidine dimer photolyases show a close relationship with lepidopteran host homologues. Insect Mol Biol **20:**457–464. http://dx.doi.org/10.1111/j.1365-2583.2011.01076.x.
92. **Xu F, Vlak JM, van Oers MM.** 2008. Conservation of DNA photolyase genes in group II nucleopolyhedroviruses infecting plusiine insects. Virus Res **136:**58–64. http://dx.doi.org/10.1016/j.virusres.2008.04.017.
93. **Xu F, Vlak JM, Eker APM, van Oers MM.** 2010. DNA photolyases of *Chrysodeixis chalcites* nucleopolyhedrovirus are targeted to the nucleus and interact with chromosomes and mitotic spindle structures. J Gen Virol **91:**907–914. http://dx.doi.org/10.1099/vir.0.018044-0.
94. **Adams MD, Celniker SE, Holt RA, Evans CA, Gocayne JD, Amanatides PG, Scherer SE, Li PW, Hoskins RA, Galle RF, George RA, Lewis SE, Richards S, Ashburner M, Henderson SN, Sutton GG, Wortman JR, Yandell MD, Zhang Q, Chen LX, Brandon RC, Rogers YH, Blazej RG, Champe M, Pfeiffer BD, Wan KH, Doyle C, Baxter EG, Helt G, Nelson CR, Gabor GL, Abril JF, Agbayani A, An HJ, Andrews-Pfannkoch C, Baldwin D, Ballew RM, Basu A, Baxendale J, Bayraktaroglu L, Beasley EM, Beeson KY, Benos PV, Berman BP, Bhandari D, Bolshakov S, Borkova D, Botchan MR, Bouck J, Brokstein P, Brottier P, et al.** 2000. The genome sequence of *Drosophila melanogaster*. Science **287:**2185–2195. http://dx.doi.org/10.1126/science.287.5461.2185.
95. **Peck MW.** 1989. Changes in concentrations of coenzyme F_{420} analogs during batch growth of *Methanosarcina barkeri* and *Methanosarcina mazei*. Appl Environ Microbiol **55:**940–945.
96. **Isabelle D, Simpson DR, Daniels L.** 2002. Large-scale production of coenzyme F_{420}-5,6 by using *Mycobacterium smegmatis*. Appl Environ Microbiol **68:**5750–5755. http://dx.doi.org/10.1128/AEM.68.11.5750-5755.2002.
97. **Kern R, Keller P, Schmidt G, Bacher A.** 1983. Isolation and structural identification of a chromophoric coenzyme F_{420} fragment from culture fluid of *Methanobacterium thermoautotrophicum*. Arch Microbiol **136:**191–193. http://dx.doi.org/10.1007/BF00409842.
98. **Weber S.** 2005. Light-driven enzymatic catalysis of DNA repair: a review of recent biophysical studies on photolyase. Biochim Biophys Acta **1707:**1–23. http://dx.doi.org/10.1016/j.bbabio.2004.02.010.
99. **van der Horst GTJ, Muijtjens M, Kobayashi K, Takano R, Kanno S, Takao M, de Wit J, Verkerk A, Eker APM, van Leenen D, Buijs R, Bootsma D, Hoeijmakers JHJ, Yasui A.** 1999. Mammalian Cry1 and Cry2 are essential for maintenance of circadian rhythms. Nature **398:**627–630. http://dx.doi.org/10.1038/19323.
100. **Johnson JL, Hamm-Alvarez S, Payne G, Sancar GB, Rajagopalan KV, Sancar A.** 1988. Identification of the second chromophore of *Escherichia coli* and yeast DNA photolyases as 5,10-methenyltetrahydrofolate. Proc Natl Acad Sci U S A **85:**2046–2050. http://dx.doi.org/10.1073/pnas.85.7.2046.
101. **Fujihashi M, Numoto N, Kobayashi Y, Mizushima A, Tsujimura M, Nakamura A, Kawarabayasi Y, Miki K.** 2007. Crystal structure of archaeal photolyase from *Sulfolobus tokodaii* with two FAD molecules: implication of a novel light-harvesting cofactor. J Mol Biol **365:**903–910. http://dx.doi.org/10.1016/j.jmb.2006.10.012.
102. **Ueda T, Kato A, Kuramitsu S, Terasawa H, Shimada I.** 2005. Identification and characterization of a second chromophore of DNA photolyase from Thermus thermophilus HB27. J Biol Chem **280:**36237–36243. http://dx.doi.org/10.1074/jbc.M507972200.
103. **Takao M, Oikawa A, Eker AP, Yasui A.** 1989. Expression of an *Anacystis nidulans* photolyase gene in *Escherichia coli*; functional complementation and modified action spectrum of photoreactivation. Photochem Photobiol **50:**633–637. http://dx.doi.org/10.1111/j.1751-1097.1989.tb04319.x.
104. **Miki K, Tamada T, Nishida H, Inaka K, Yasui A, de Ruiter PE, Eker AP.** 1993. Crystallization and preliminary X-ray diffraction studies of photolyase (photoreactivating enzyme) from the cyanobacterium *Anacystis nidulans*. J Mol Biol **233:**167–169. http://dx.doi.org/10.1006/jmbi.1993.1492.
105. **Kort R, Komori H, Adachi S, Miki K, Eker A.** 2004. DNA apophotolyase from *Anacystis nidulans*: 1.8 Å structure, 8-HDF reconstitution and X-ray-induced FAD reduction. Acta Crystallogr D Biol Crystallogr **60:**1205–1213. http://dx.doi.org/10.1107/S0907444904009321.
106. **Mees A, Klar T, Gnau P, Hennecke U, Eker APM, Carell T, Essen L-O.** 2004. Crystal structure of a photolyase bound to a CPD-like DNA lesion

after *in situ* repair. Science **306:**1789–1793. http://dx.doi.org/10.1126/science.1101598.
107. **Kim ST, Heelis PF, Sancar A.** 1992. Energy transfer (deazaflavin to $FADH_2$) and electron transfer ($FADH2$ to TT) kinetics in Anacystis nidulans photolyase. Biochemistry **31:**11244–11248. http://dx.doi.org/10.1021/bi00160a040.
108. **MacFarlane AW, IV, Stanley RJ.** 2003. *Cis-syn* thymidine dimer repair by DNA photolyase in real time. Biochemistry **42:**8558–8568. http://dx.doi.org/10.1021/bi034015w.
109. **Aubert C, Mathis P, Eker AP, Brettel K.** 1999. Intraprotein electron transfer between tyrosine and tryptophan in DNA photolyase from *Anacystis nidulans*. Proc Natl Acad Sci U S A **96:**5423–5427. http://dx.doi.org/10.1073/pnas.96.10.5423.
110. **Sancar A.** 2008. Structure and function of photolyase and *in vivo* enzymology: 50th anniversary. J Biol Chem **283:**32153–32157. http://dx.doi.org/10.1074/jbc.R800052200.
111. **Ashton WT, Brown RD, Jacobson F, Walsh C.** 1979. Synthesis of 7,8-didemethyl-8-hydroxy-5-deazariboflavin. J Am Chem Soc **101:**4419–4420. http://dx.doi.org/10.1021/ja00509a083.
112. **Pol A, van der Drift C, Vogels GD, Cuppen TJHM, Laarhoven WH.** 1980. Comparison of coenzyme F_{420} from *Methanobacterium bryantii* with 7- and 8-hydroxy-10-methyl-5-deazaisoalloxazine. Biochem Biophys Res Commun **92:**255–260. http://dx.doi.org/10.1016/0006-291X(80)91546-6.
113. **Ashton WT, Brown RD.** 1980. Synthesis of 8-demethyl-8-hydroxy-5-deazariboflavins. J Heterocycl Chem **17:**1709–1712. http://dx.doi.org/10.1002/jhet.5570170813.
114. **Jaenchen R, Schonheit P, Thauer RK.** 1984. Studies on the biosynthesis of coenzyme F_{420} in methanogenic bacteria. Arch Microbiol **137:**362–365. http://dx.doi.org/10.1007/BF00410735.
115. **Reuke B, Korn S, Eisenreich W, Bacher A.** 1992. Biosynthetic precursors of deazaflavins. J Bacteriol **174:**4042–4049.
116. **Graupner M, White RH.** 2001. Biosynthesis of the phosphodiester bond in coenzyme F_{420} in the methanoarchaea. Biochemistry **40:**10859–10872. http://dx.doi.org/10.1021/bi0107703.
117. **Graupner M, Xu H, White RH.** 2002. Characterization of the 2-phospho-L-lactate transferase enzyme involved in coenzyme F_{420} biosynthesis in *Methanococcus jannaschii*. Biochemistry **41:**3754–3761.
118. **Choi K-P, Bair TB, Bae Y-M, Daniels L.** 2001. Use of transposon Tn5367 mutagenesis and a nitroimidazopyran-based selection system to demonstrate a requirement for *fbiA* and *fbiB* in coenzyme F_{420} biosynthesis by *Mycobacterium bovis* BCG. J Bacteriol **183:**7058–7066. http://dx.doi.org/10.1128/JB.183.24.7058-7066.2001.
119. **Forouhar F, Abashidze M, Xu H, Grochowski LL, Seetharaman J, Hussain M, Kuzin A, Chen Y, Zhou W, Xiao R, Acton TB, Montelione GT, Galinier A, White RH, Tong L.** 2008. Molecular insights into the biosynthesis of the F_{420} coenzyme. J Biol Chem **283:**11832–11840. http://dx.doi.org/10.1074/jbc.M710352200.
120. **Li H, Graupner M, Xu H, White RH.** 2003. CofE catalyzes the addition of two glutamates to F_{420}-0 in F_{420} coenzyme biosynthesis in *Methanococcus jannaschii*. Biochemistry **42:**9771–9778. http://dx.doi.org/10.1021/bi034779b.
121. **Rehan AM, Bashiri G, Paterson NG, Baker EN, Squire CJ.** 2011. Cloning, expression, purification, crystallization and preliminary X-ray studies of the C-terminal domain of Rv3262 (FbiB) from *Mycobacterium tuberculosis*. Acta Crystallogr Sect F Struct Biol Cryst Commun **67:**1274–1277. http://dx.doi.org/10.1107/S1744309111028958.
122. **Nakano T, Miyake K, Endo H, Dairi T, Mizukami T, Katsumata R.** 2004. Identification and cloning of the gene involved in the final step of chlortetracycline biosynthesis in *Streptomyces aureofaciens*. Biosci Biotechnol Biochem **68:**1345–1352. http://dx.doi.org/10.1271/bbb.68.1345.
123. **Nocek B, Evdokimova E, Proudfoot M, Kudritska M, Grochowski LL, White RH, Savchenko A, Yakunin A, Edwards FA, Joachimiak A.** 2007. Structure of an amide bond forming F420:γγ-glutamyl ligase from Archaeoglobus fulgidus - a member of a new family of non-ribosomal peptide synthases. J Mol Biol **372:**456–469. http://dx.doi.org/10.1016/j.jmb.2007.06.063.
124. **Gorris LG, van der Drift C.** 1994. Cofactor contents of methanogenic bacteria reviewed. Biofactors **4:**139–145.
125. **Bair TB, Isabelle DW, Daniels L.** 2001. Structures of coenzyme F_{420} in *Mycobacterium* species. Arch Microbiol **176:**37–43. http://dx.doi.org/10.1007/s002030100290.
126. **Graupner M, White RH.** 2003. *Methanococcus jannaschii* coenzyme F_{420} analogs contain a terminal α-linked glutamate. J Bacteriol **185:**4662–4665. http://dx.doi.org/10.1128/JB.185.15.4662-4665.2003.
127. **Kimachi T, Tanaka K, Yoneda F.** 1991. Synthesis of a proposed isomer of F_{420} having α-glutamyl bonding. J Heterocycl Chem **28:**439–443. http://dx.doi.org/10.1002/jhet.5570280244.
128. **Li H, Xu H, Graham DE, White RH.** 2003. Glutathione synthetase homologs encode alpha-L-glutamate ligases for methanogenic coenzyme F_{420} and tetrahydrosarcinapterin biosyntheses. Proc Natl Acad Sci U S A **100:**9785–9790. http://dx.doi.org/10.1073/pnas.1733391100.
129. **Graupner M, Xu H, White RH.** 2000. Identification of an archaeal 2-hydroxy acid dehydrogenase catalyzing reactions involved in coenzyme biosynthesis in methanoarchaea. J Bacteriol **182:**3688–3692. http://dx.doi.org/10.1128/JB.182.13.3688-3692.2000.
130. **Grochowski LL, Xu H, White RH.** 2006. Identification of lactaldehyde dehydrogenase in *Methanocaldococcus jannaschii* and its involvement in production of lactate for F_{420} biosynthesis. J Bacteriol **188:**2836–2844. http://dx.doi.org/10.1128/JB.188.8.2836-2844.2006.
131. **Grochowski LL, Xu H, White RH.** 2008. Identification and characterization of the 2-phospho-L-lactate guanylyltransferase involved in coenzyme F_{420} biosynthesis. Biochemistry **47:**3033–3037. http://dx.doi.org/10.1021/bi702475t.
132. **Guerra-Lopez D, Daniels L, Rawat M.** 2007. *Mycobacterium smegmatis* mc^2 155 *fbiC* and MSMEG_2392 are involved in triphenylmethane dye decolorization and coenzyme F_{420} biosynthesis. Microbiology **153:**2724–2732. http://dx.doi.org/10.1099/mic.0.2006/009241-0.
133. **Möller-Zinkhan D, Börner G, Thauer RK.** 1989. Function of methanofuran, tetrahydromethanopterin, and coenzyme F_{420} in *Archaeoglobus fulgidus*. Arch Microbiol **152:**362–368. http://dx.doi.org/10.1007/BF00425174.
134. **Gorris LG, Voet AC, van der Drift C.** 1991. Structural characteristics of methanogenic cofactors in the non-methanogenic archaebacterium *Archaeoglobus fulgidus*. Biofactors **3:**29–35.
135. **Vornolt J, Kunow J, Stetter KO, Thauer RK.** 1995. Enzymes and coenzymes of the carbon monoxide dehydrogenase pathway for autotrophic CO_2 fixation in *Archaeoglobus lithotrophicus* and the lack of carbon monoxide dehydrogenase in the heterotrophic *A. profundus*. Arch Microbiol **163:**112–118. http://dx.doi.org/10.1007/BF00381784.
136. **de Wit LEA, Eker APM.** 1987. 8-Hydroxy-5-deazaflavin-dependent electron transfer in the extreme halophile *Halobacterium cutirubrum*. FEMS Microbiol Lett **48**(1-2):121–125. http://dx.doi.org/10.1111/j.1574-6968.1987.tb02527.x.
137. **Haroon MF, Hu S, Shi Y, Imelfort M, Keller J, Hugenholtz P, Yuan Z, Tyson GW.** 2013. Anaerobic oxidation of methane coupled to nitrate reduction in a novel archaeal lineage. Nature **500:**567–570. http://dx.doi.org/10.1038/nature12375.
138. **Wu D, Hugenholtz P, Mavromatis K, Pukall RR, Dalin E, Ivanova NN, Kunin V, Goodwin L, Wu M, Tindall BJ, Hooper SD, Pati A, Lykidis A, Spring S, Anderson IJ, D'haeseleer P, Zemla A, Singer M, Lapidus A, Nolan M, Copeland A, Han C, Chen F, Cheng J-F, Lucas S, Kerfeld C, Lang E, Gronow S, Chain P, Bruce D, Rubin EM, Kyrpides NC, Klenk H-P, Eisen JA, D'haeseleer, Zemla PA, Singer M, Lapidus A, Nolan M, Copeland A, Han C, Chen F, Cheng J-F, Lucas S, Kerfeld C, Lang E, Gronow S, Chain P, Bruce D, Rubin EM, Kyrpides NC, Klenk H-P, Eisen JA.** 2009. A phylogeny-driven genomic encyclopaedia of *Bacteria* and *Archaea*. Nature **462:**1056–1060. http://dx.doi.org/10.1038/nature08656.
139. **Rinke C, Schwientek P, Sczyrba A, Ivanova NN, Anderson IJ, Cheng J-F, Darling A, Malfatti S, Swan BK, Gies EA, Dodsworth JA, Hedlund BP, Tsiamis G, Sievert SM, Liu W-T, Eisen JA, Hallam SJ, Kyrpides NC, Stepanauskas R, Rubin EM, Hugenholtz P, Woyke T.** 2013. Insights into the phylogeny and coding potential of microbial dark matter. Nature **499:**431–437. http://dx.doi.org/10.1038/nature12352.
140. **Kozubal MA, Romine M, Jennings RD, Jay ZJ, Tringe SG, Rusch DB, Beam JP, McCue LA, Inskeep WP.** 2013. *Geoarchaeota*: a new candidate phylum in the Archaea from high-temperature acidic iron mats in Yellowstone National Park. ISME J **7:**622–634. http://dx.doi.org/10.1038/ismej.2012.132.
141. **Evans PN, Parks DH, Chadwick GL, Robbins SJ, Orphan VJ, Golding SD, Tyson GW.** 2015. Methane metabolism in the archaeal phylum *Bathyarchaeota* revealed by genome-centric metagenomics. Science **350:**434–438. http://dx.doi.org/10.1126/science.aac7745.
142. **Spang A, Saw JH, Jorgensen SL, Zaremba-Niedzwiedzka K, Martijn J, Lind AE, van Eijk R, Schleper C, Guy L, Ettema TJG.** 2015. Complex

archaea that bridge the gap between prokaryotes and eukaryotes. Nature **521:**173–179. http://dx.doi.org/10.1038/nature14447.

143. **Spang A, Poehlein A, Offre P, Zumbragel S, Haider S, Rychlik N, Nowka B, Schmeisser C, Lebedeva EV, Rattei T, Bohm C, Schmid M, Galushko A, Hatzenpichler R, Weinmaier T, Daniel R, Schleper C, Spieck E, Streit W, Wagner M.** 2012. The genome of the ammonia-oxidizing Candidatus *Nitrososphaera gargensis*: insights into metabolic versatility and environmental adaptations. Environ Microbiol **14:**3122–3145. http://dx.doi.org/10.1111/j.1462-2920.2012.02893.x.
144. **Palatinszky M, Herbold C, Jehmlich N, Pogoda M, Han P, von Bergen M, Lagkouvardos I, Karst SM, Galushko A, Koch H, Berry D, Daims H, Wagner M.** 2015. Cyanate as an energy source for nitrifiers. Nature **524:**105–108. http://dx.doi.org/10.1038/nature14856.
145. **Purwantini E, Gillis TP, Daniels L.** 1997. Presence of F_{420}-dependent glucose-6-phosphate dehydrogenase in *Mycobacterium* and *Nocardia* species, but absence from *Streptomyces* and *Corynebacterium* species and methanogenic Archaea. FEMS Microbiol Lett **146:**129–134. http://dx.doi.org/10.1111/j.1574-6968.1997.tb10182.x.
146. **Kuo MS, Yurek DA, Coats JH, Li GP.** 1989. Isolation and identification of 7,8-didemethyl-8-hydroxy-5-deazariboflavin, an unusual cosynthetic factor in streptomycetes, from *Streptomyces lincolnensis*. J Antibiot (Tokyo) **42:**475–478. http://dx.doi.org/10.7164/antibiotics.42.475.
147. **Janssen PH.** 2006. Identifying the dominant soil bacterial taxa in libraries of 16S rRNA and 16S rRNA genes. Appl Environ Microbiol **72:**1719–1728. http://dx.doi.org/10.1128/AEM.72.3.1719-1728.2006.
148. **Purwantini E, Daniels L.** 1998. Molecular analysis of the gene encoding F_{420}-dependent glucose-6-phosphate dehydrogenase from *Mycobacterium smegmatis*. J Bacteriol **180:**2212–2219.
149. **Mejean A, Paci G, Gautier V, Ploux O.** 2014. Biosynthesis of anatoxin-a and analogues (anatoxins) in cyanobacteria. Toxicon **91:**15–22. http://dx.doi.org/10.1016/j.toxicon.2014.07.016.
150. **Vitt S, Ma K, Warkentin E, Moll J, Pierik AJ, Shima S, Ermler U.** 2014. The F_{420}-reducing [NiFe]-hydrogenase complex from *Methanothermobacter marburgensis*, the first X-ray structure of a group 3 family member. J Mol Biol **426:**2813–2826. http://dx.doi.org/10.1016/j.jmb.2014.05.024.
151. **Thauer RK.** 1998. Biochemistry of methanogenesis: a tribute to Marjory Stephenson. Microbiology **144:**2377–2406. http://dx.doi.org/10.1099/00221287-144-9-2377.
152. **Zeikus JG, Fuchs G, Kenealy W, Thauer RK.** 1977. Oxidoreductases involved in cell carbon synthesis of *Methanobacterium thermoautotrophicum*. J Bacteriol **132:**604–613.
153. **Daniels L, Fuchs G, Thauer RK, Zeikus JG.** 1977. Carbon monoxide oxidation by methanogenic bacteria. J Bacteriol **132:**118–126.
154. **Hedderich R, Whitman W.** 2013. Physiology and biochemistry of the methane-producing Archaea, p 635–662. *In* Rosenberg E, DeLong E, Lory S, Stackebrandt E, Thompson F (ed), The prokaryotes. Springer, Berlin, Germany.
155. **Heiss G, Hofmann KW, Trachtmann N, Walters DM, Rouvière P, Knackmuss HJ.** 2002. npd gene functions of *Rhodococcus* (*opacus*) *erythropolis* HL PM-1 in the initial steps of 2,4,6-trinitrophenol degradation. Microbiology **148:**799–806. http://dx.doi.org/10.1099/00221287-148-3-799.
156. **Enßle M, Zirngibl C, Linder D, Thauer RK.** 1991. Coenzyme F_{420} dependent N^5, N^{10}-methylenetetrahydromethanopterin dehydrogenase in methanol grown *Methanosarcina barkeri*. Arch Microbiol **155:**483–490. http://dx.doi.org/10.1007/BF00244966.
157. **Mukhopadhyay B, Purwantini E, Daniels L.** 1993. Effect of methanogenic substrates on coenzyme F_{420}-dependent N^5,N^{10}-methylene-H_4MPT dehydrogenase, N^5,N^{10}-methenyl-H_4MPT cyclohydrolase and F_{420}-reducing hydrogenase activities in *Methanosarcina barkeri*. Arch Microbiol **159:**141–146. http://dx.doi.org/10.1007/BF00250274.
158. **Escalante-Semerena JC, Rinehart KL, Wolfe RS.** 1984. Tetrahydromethanopterin, a carbon carrier in methanogenesis. J Biol Chem **259:**9447–9455.
159. **Shima S, Warkentin E, Grabarse W, Sordel M, Wicke M, Thauer RK, Ermler U.** 2000. Structure of coenzyme F_{420} dependent methylenetetrahydromethanopterin reductase from two methanogenic archaea. J Mol Biol **300:**935–950. http://dx.doi.org/10.1006/jmbi.2000.3909.
160. **Warkentin E, Mamat B, Sordel-Klippert M, Wicke M, Thauer RK, Iwata M, Iwata S, Ermler U, Shima S.** 2001. Structures of $F_{420}H_2$:$NADP^+$ oxidoreductase with and without its substrates bound. EMBO J **20:**6561–6569. http://dx.doi.org/10.1093/emboj/20.23.6561.
161. **Seedorf H, Hagemeier CH, Shima S, Thauer RK, Warkentin E, Ermler U.** 2007. Structure of coenzyme $F_{420}H_2$ oxidase (FprA), a di-iron flavoprotein from methanogenic *Archaea* catalyzing the reduction of O_2 to H_2O. FEBS J **274:**1588–1599. http://dx.doi.org/10.1111/j.1742-4658.2007.05706.x.
162. **Bäumer S, Ide T, Jacobi C, Johann A, Gottschalk G, Deppenmeier U.** 2000. The $F_{420}H_2$ dehydrogenase from *Methanosarcina mazei* is a redox-driven proton pump closely related to NADH dehydrogenases. J Biol Chem **275:**17968–17973. http://dx.doi.org/10.1074/jbc.M000650200.
163. **Bashiri G, Squire CJ, Moreland NJ, Baker EN.** 2008. Crystal structures of F_{420}-dependent glucose-6-phosphate dehydrogenase FGD1 involved in the activation of the anti-tuberculosis drug candidate PA-824 reveal the basis of coenzyme and substrate binding. J Biol Chem **283:**17531–17541. http://dx.doi.org/10.1074/jbc.M801854200.
164. **Cellitti SE, Shaffer J, Jones DH, Mukherjee T, Gurumurthy M, Bursulaya B, Boshoff HI, Choi I, Nayyar A, Lee YS, Cherian J, Niyomrattanakit P, Dick T, Manjunatha UH, Barry CE, Spraggon G, Geierstanger BH.** 2012. Structure of Ddn, the deazaflavin-dependent nitroreductase from *Mycobacterium tuberculosis* involved in bioreductive activation of PA-824. Structure **20:**101–112. http://dx.doi.org/10.1016/j.str.2011.11.001.
165. **Mashalidis EH, Gittis AG, Tomczak A, Abell C, Barry CE, Garboczi DN.** 2015. Molecular insights into the binding of coenzyme F_{420} to the conserved protein Rv1155 from *Mycobacterium tuberculosis*. Protein Sci **24:**729–740. http://dx.doi.org/10.1002/pro.2645.
166. **Ceh K, Demmer U, Warkentin E, Moll J, Thauer RK, Shima S, Ermler U.** 2009. Structural basis of the hydride transfer mechanism in F_{420}-dependent methylenetetrahydromethanopterin dehydrogenase. Biochemistry **48:**10098–10105. http://dx.doi.org/10.1021/bi901104d.
167. **Mills DJ, Vitt S, Strauss M, Shima S, Vonck J.** 2013. De novo modeling of the F_{420}-reducing [NiFe]-hydrogenase from a methanogenic archaeon by cryo-electron microscopy. eLife **2:**e00218. http://dx.doi.org/10.7554/eLife.00218.
168. **Liu Y, Whitman WB.** 2008. Metabolic, phylogenetic, and ecological diversity of the methanogenic archaea. Ann N Y Acad Sci **1125:**171–189. http://dx.doi.org/10.1196/annals.1419.019.
169. **Brochier C, Forterre P, Gribaldo S.** 2004. Archaeal phylogeny based on proteins of the transcription and translation machineries: tackling the *Methanopyrus kandleri* paradox. Genome Biol **5:**R17. http://dx.doi.org/10.1186/gb-2004-5-3-r17.
170. **Bapteste E, Brochier C, Boucher Y.** 2005. Higher-level classification of the *Archaea*: evolution of methanogenesis and methanogens. Archaea **1:**353–363. http://dx.doi.org/10.1155/2005/859728.
171. **Gribaldo S, Brochier-Armanet C.** 2006. The origin and evolution of *Archaea*: a state of the art. Philos Trans R Soc B Biol Sci **361:**1007–1022. http://dx.doi.org/10.1098/rstb.2006.1841.
172. **Brochier-Armanet C, Forterre P, Gribaldo S.** 2011. Phylogeny and evolution of the *Archaea*: one hundred genomes later. Curr Opin Microbiol **14:**274–281. http://dx.doi.org/10.1016/j.mib.2011.04.015.
173. **Borrel G, O'Toole PW, Harris HMB, Peyret P, Brugère JF, Gribaldo S.** 2013. Phylogenomic data support a seventh order of methylotrophic methanogens and provide insights into the evolution of methanogenesis. Genome Biol Evol **5:**1769–1780. http://dx.doi.org/10.1093/gbe/evt128.
174. **Whiticar MJ, Faber E, Schoell M.** 1986. Biogenic methane formation in marine and freshwater environments: CO_2 reduction vs. acetate fermentation - isotope evidence. Geochim Cosmochim Acta **50:**693–709. http://dx.doi.org/10.1016/0016-7037(86)90346-7.
175. **Krzycki JA, Kenealy WR, DeNiro MJ, Zeikus JG.** 1987. Stable carbon isotope fractionation by *Methanosarcina barkeri* during methanogenesis from acetate, methanol, or carbon dioxide-hydrogen. Appl Environ Microbiol **53:**2597–2599.
176. **Smith MR, Mah RA.** 1978. Growth and methanogenesis by *Methanosarcina* strain 227 on acetate and methanol. Appl Environ Microbiol **36:**870–879.
177. **Zeikus JG, Kerby R, Krzycki JA.** 1985. Single-carbon chemistry of acetogenic and methanogenic bacteria. Sci **227:**1167–1173. http://dx.doi.org/10.1126/science.3919443.
178. **Ferry JG.** 2010. How to make a living by exhaling methane. Annu Rev Microbiol **64:**453–473. http://dx.doi.org/10.1146/annurev.micro.112408.134051.
179. **Widdel F, Rouvière PE, Wolfe RS.** 1988. Classification of secondary alcohol-utilizing methanogens including a new thermophilic isolate. Arch Microbiol **150:**477–481. http://dx.doi.org/10.1007/BF00422290.
180. **Jablonski PE, DiMarco AA, Bobik TA, Cabell MC, Ferry JG.** 1990.

Protein content and enzyme activities in methanol- and acetate-grown *Methanosarcina thermophila*. J Bacteriol **172:**1271–1275.
181. **Abbanat DR, Ferry JG.** 1991. Resolution of component proteins in an enzyme complex from *Methanosarcina thermophila* catalyzing the synthesis or cleavage of acetyl-CoA. Proc Natl Acad Sci U S A **88:**3272–3276. http://dx.doi.org/10.1073/pnas.88.8.3272.
182. **Thauer RK, Kaster A-K, Seedorf H, Buckel W, Hedderich R.** 2008. Methanogenic archaea: ecologically relevant differences in energy conservation. Nat Rev Microbiol **6:**579–591. http://dx.doi.org/10.1038/nrmicro1931.
183. **Greening C, Biswas A, Carere CR, Jackson CJ, Taylor MC, Stott MB, Cook GM, Morales SE.** 2016. Genomic and metagenomic surveys of hydrogenase diversity indicate H2 is a widely utilised energy source for microbial growth and survival. ISME J **10:**761–777. http://dx.doi.org/10.1038/ismej.2015.153.
184. **Schauer NL, Brown DP, Ferry JG.** 1982. Kinetics of formate metabolism in *Methanobacterium formicicum* and *Methanospirillum hungatei*. Appl Environ Microbiol **44:**549–554.
185. **Jones JB, Stadtman TC.** 1981. Selenium-dependent and selenium-independent formate dehydrogenases of *Methanococcus vannielii*. Separation of the two forms and characterization of the purified selenium-independent form. J Biol Chem **256:**656–663.
186. **Zinder SH, Anguish T.** 1992. Carbon monoxide, hydrogen, and formate metabolism during methanogenesis from acetate by thermophilic cultures of *Methanosarcina* and *Methanothrix* strains. Appl Environ Microbiol **58:**3323–3329.
187. **Miller TL, Wolin MJ.** 1985. *Methanosphaera stadtmaniae* gen. nov., sp. nov.: a species that forms methane by reducing methanol with hydrogen. Arch Microbiol **141:**116–122. http://dx.doi.org/10.1007/BF00423270.
188. **Jetten MSM, Stams AJM, Zehnder AJB.** 1992. Methanogenesis from acetate: a comparison of the acetate metabolism in *Methanothrix soehngenii* and *Methanosarcina* spp. FEMS Microbiol Lett **88:**181–198. http://dx.doi.org/10.1111/j.1574-6968.1992.tb04987.x.
189. **Conrad R.** 2009. The global methane cycle: recent advances in understanding the microbial processes involved. Environ Microbiol Rep **1:**285–292. http://dx.doi.org/10.1111/j.1758-2229.2009.00038.x.
190. **Schauer NL, Ferry JG.** 1986. Composition of the coenzyme F_{420}-dependent formate dehydrogenase from *Methanobacterium formicicum*. J Bacteriol **165:**405–411.
191. **Johnson EF, Mukhopadhyay B.** 2008. Coenzyme F_{420}-dependent sulfite reductase-enabled sulfite detoxification and use of sulfite as a sole sulfur source by *Methanococcus maripaludis*. Appl Environ Microbiol **74:**3591–3595. http://dx.doi.org/10.1128/AEM.00098-08.
192. **Seedorf H, Dreisbach A, Hedderich R, Shima S, Thauer RK.** 2004. $F_{420}H_2$ oxidase (FprA) from *Methanobrevibacter arboriphilus*, a coenzyme F_{420}-dependent enzyme involved in O_2 detoxification. Arch Microbiol **182:**126–137.
193. **Welte C, Deppenmeier U.** 2011. Re-evaluation of the function of the F_{420} dehydrogenase in electron transport of *Methanosarcina mazei*. FEBS J **278:**1277–1287. http://dx.doi.org/10.1111/j.1742-4658.2011.08048.x.
194. **Baresi L, Wolfe RS.** 1981. Levels of coenzyme F_{420}, coenzyme M, hydrogenase, and methyl coenzyme M methylreductase in acetate-grown *Methanosarcina*. Appl Environ Microbiol **41:**388–391.
195. **Barber RD, Zhang L, Harnack M, Olson MV, Kaul R, Ingram-Smith C, Smith KS.** 2011. Complete genome sequence of *Methanosaeta concilii*, a specialist in aceticlastic methanogenesis. J Bacteriol **193:**3668–3669. http://dx.doi.org/10.1128/JB.05031-11.
196. **Zhu J, Zheng H, Ai G, Zhang G, Liu D, Liu X, Dong X.** 2012. The genome characteristics and predicted function of methyl-group oxidation pathway in the obligate aceticlastic methanogens, *Methanosaeta* spp. PLoS One **7:**e36756. http://dx.doi.org/10.1371/journal.pone.0036756.
197. **Nelson-Sathi S, Dagan T, Landan G, Janssen A, Steel M, McInerney JO, Deppenmeier U, Martin WF.** 2012. Acquisition of 1,000 eubacterial genes physiologically transformed a methanogen at the origin of *Haloarchaea*. Proc Natl Acad Sci U S A **109:**20537–20542. http://dx.doi.org/10.1073/pnas.1209119109.
198. **Kunow J, Linder D, Stetter KO, Thauer RK.** 1994. $F_{420}H_2$: quinone oxidoreductase from *Archaeoglobus fulgidus*. Eur J Biochem **223:**503–511. http://dx.doi.org/10.1111/j.1432-1033.1994.tb19019.x.
199. **Brüggemann H, Falinski F, Deppenmeier U.** 2001. Structure of the $F_{420}H_2$:quinone oxidoreductase of Archaeoglobus fulgidus: identification and overproduction of the $F_{420}H_2$-oxidizing subunit. Eur J Biochem **5814:**5810–5814.
200. **Hocking WP, Stokke R, Roalkvam I, Steen IH.** 2014. Identification of key components in the energy metabolism of the hyperthermophilic sulfate-reducing archaeon *Archaeoglobus fulgidus* by transcriptome analyses. Front Microbiol **5:**95. http://dx.doi.org/10.3389/fmicb.2014.00095.
201. **Kunow J, Schwörer B, Stetter KO, Thauer RK.** 1993. A F_{420}-dependent NADP reductase in the extremely thermophilic sulfate-reducing *Archaeoglobus fulgidus*. Arch Microbiol **160:**199–205.
202. **Möller-Zinkhan D, Thauer R.** 1990. Anaerobic lactate oxidation to 3 CO_2 by *Archaeoglobus fulgidus* via the carbon monoxide dehydrogenase pathway: demonstration of the acetyl-CoA carbon-carbon cleavage reaction in cell extracts. Arch Microbiol **153:**215–218. http://dx.doi.org/10.1007/BF00249070.
203. **Klenk H-P, Clayton RA, Tomb J-F, White O, Nelson KE, Ketchum KA, Dodson RJ, Gwinn M, Hickey EK, Peterson JD, Richardson DL, Kerlavage AR, Graham DE, Kyrpides NC, Fleischmann RD, Quackenbush J, Lee NH, Sutton GG, Gill S, Kirkness EF, Dougherty BA, McKenney K, Adams MD, Loftus B, Peterson S, Reich CI, McNeil LK, Badger JH, Glodek A, Zhou L, Overbeek R, Gocayne JD, Weidman JF, McDonald L, Utterback T, Cotton MD, Spriggs T, Artiach P, Kaine BP, Sykes SM, Sadow PW, D'Andrea KP, Bowman C, Fujii C, Garland SA, Mason TM, Olsen GJ, Fraser CM, Smith HO, Woese CR, Venter JC.** 1997. The complete genome sequence of the hyperthermophilic, sulphate-reducing archaeon *Archaeoglobus fulgidus*. Nature **390:**364–370. http://dx.doi.org/10.1038/37052.
204. **Boetius A, Ravenschlag K, Schubert CJ, Rickert D, Widdel F, Gieseke A, Amann R, Jorgensen BB, Witte U, Pfannkuche O.** 2000. A marine microbial consortium apparently mediating anaerobic oxidation of methane. Nature **407:**623–626. http://dx.doi.org/10.1038/35036572.
205. **Raghoebarsing AA, Pol A, van de Pas-Schoonen KT, Smolders AJP, Ettwig KF, Rijpstra WIC, Schouten S, Damste JSS, Op den Camp HJM, Jetten MSM, Strous M.** 2006. A microbial consortium couples anaerobic methane oxidation to denitrification. Nature **440:**918–921. http://dx.doi.org/10.1038/nature04617.
206. **Orphan VJ, House CH, Hinrichs K-U, McKeegan KD, DeLong EF.** 2001. Methane-consuming archaea revealed by directly coupled isotopic and phylogenetic analysis. Science **293:**484–487. http://dx.doi.org/10.1126/science.1061338.
207. **Wegener G, Krukenberg V, Riedel D, Tegetmeyer HE, Boetius A.** 2015. Intercellular wiring enables electron transfer between methanotrophic archaea and bacteria. Nature **526:**587–590. http://dx.doi.org/10.1038/nature15733.
208. **Knittel K, Boetius A.** 2009. Anaerobic oxidation of methane: progress with an unknown process. Annu Rev Microbiol **63:**311–334. http://dx.doi.org/10.1146/annurev.micro.61.080706.093130.
209. **Reeburgh WS.** 2007. Oceanic methane biogeochemistry. Chem Rev **107:**486–513. http://dx.doi.org/10.1021/cr050362v.
210. **Orphan VJ, House CH, Hinrichs K-U, McKeegan KD, DeLong EF.** 2002. Multiple archaeal groups mediate methane oxidation in anoxic cold seep sediments. Proc Natl Acad Sci U S A **99:**7663–7668. http://dx.doi.org/10.1073/pnas.072210299.
211. **Niemann H, Losekann T, de Beer D, Elvert M, Nadalig T, Knittel K, Amann R, Sauter EJ, Schluter M, Klages M, Foucher JP, Boetius A.** 2006. Novel microbial communities of the Haakon Mosby mud volcano and their role as a methane sink. Nature **443:**854–858. http://dx.doi.org/10.1038/nature05227.
212. **Kruger M, Meyerdierks A, Glockner FO, Amann R, Widdel F, Kube M, Reinhardt R, Kahnt J, Bocher R, Thauer RK, Shima S.** 2003. A conspicuous nickel protein in microbial mats that oxidize methane anaerobically. Nature **426:**878–881. http://dx.doi.org/10.1038/nature02207.
213. **Scheller S, Goenrich M, Boecher R, Thauer RK, Jaun B.** 2010. The key nickel enzyme of methanogenesis catalyses the anaerobic oxidation of methane. Nature **465:**606–608. http://dx.doi.org/10.1038/nature09015.
214. **Kojima H, Moll J, Kahnt J, Fukui M, Shima S.** 2014. A reversed genetic approach reveals the coenzyme specificity and other catalytic properties of three enzymes putatively involved in anaerobic oxidation of methane with sulfate. Environ Microbiol **16:**3431–3442. http://dx.doi.org/10.1111/1462-2920.12475.
215. **Wang F-P, Zhang Y, Chen Y, He Y, Qi J, Hinrichs K-U, Zhang X-X, Xiao X, Boon N.** 2014. Methanotrophic archaea possessing diverging methane-oxidizing and electron-transporting pathways. ISME J **8:**1069–1078. http://dx.doi.org/10.1038/ismej.2013.212.
216. **Meyerdierks A, Kube M, Kostadinov I, Teeling H, Glöckner FO,**

Reinhardt R, Amann R. 2010. Metagenome and mRNA expression analyses of anaerobic methanotrophic archaea of the ANME-1 group. Environ Microbiol **12:**422–439. http://dx.doi.org/10.1111/j.1462-2920.2009.02083.x.

217. **Michaelis W, Seifert R, Nauhaus K, Treude T, Thiel V, Blumenberg M, Knittel K, Gieseke A, Peterknecht K, Pape T, Boetius A, Amann R, Jørgensen BB, Widdel F, Peckmann J, Pimenov NV, Gulin MB.** 2002. Microbial reefs in the black sea fueled by anaerobic oxidation of methane. Science **297:**1013–1015. http://dx.doi.org/10.1126/science.1072502.
218. **Knittel K, Lösekann T, Boetius A, Kort R, Amann R.** 2005. Diversity and distribution of methanotrophic archaea at cold seeps. Appl Environ Microbiol **71:**467–479. http://dx.doi.org/10.1128/AEM.71.1.467-479.2005.
219. **Muth E, Mörschel E, Klein A.** 1987. Purification and characterization of an 8-hydroxy-5-deazaflavin-reducing hydrogenase from the archaebacterium *Methanococcus voltae*. Eur J Biochem **169:**571–577. http://dx.doi.org/10.1111/j.1432-1033.1987.tb13647.x.
220. **Fiebig K, Friedrich B.** 1989. Purification of the F_{420}-reducing hydrogenase from *Methanosarcina barkeri* (strain Fusaro). Eur J Biochem **184:**79–88. http://dx.doi.org/10.1111/j.1432-1033.1989.tb14992.x.
221. **Halboth S, Klein A.** 1992. Methanococcus voltae harbors four gene clusters potentially encoding two [NiFe] and two [NiFeSe] hydrogenases, each of the cofactor F_{420}-reducing or F_{420}-non-reducing types. Mol Gen Genet **233:**217–224. http://dx.doi.org/10.1007/BF00587582.
222. **Vaupel M, Thauer RK.** 1998. Two F_{420}-reducing hydrogenases in *Methanosarcina barkeri*. Arch Microbiol **169:**201–205. http://dx.doi.org/10.1007/s002030050561.
223. **Brodersen J, Gottschalk G, Deppenmeier U.** 1999. Membrane-bound $F_{420}H_2$-dependent heterodisulfide reduction in *Methanococcus voltae*. Arch Microbiol **171:**115–121. http://dx.doi.org/10.1007/s002030050686.
224. **Kulkarni G, Kridelbaugh DM, Guss AM, Metcalf WW.** 2009. Hydrogen is a preferred intermediate in the energy-conserving electron transport chain of *Methanosarcina barkeri*. Proc Natl Acad Sci U S A **106:**15915–15920. http://dx.doi.org/10.1073/pnas.0905914106.
225. **Hendrickson EL, Leigh J.** 2008. Roles of coenzyme F_{420}-reducing hydrogenases and hydrogen- and F_{420}-dependent methylenetetrahydromethanopterin dehydrogenases in reduction of F_{420} and production of hydrogen during methanogenesis. J Bacteriol **190:**4818–4821. http://dx.doi.org/10.1128/JB.00255-08.
226. **Vignais PM, Billoud B.** 2007. Occurrence, classification, and biological function of hydrogenases: an overview. Chem Rev **107:**4206–4272. http://dx.doi.org/10.1021/cr050196r.
227. **Allegretti M, Mills DJ, McMullan G, Kühlbrandt W, Vonck J.** 2014. Atomic model of the F_{420}-reducing [NiFe] hydrogenase by electron cryomicroscopy using a direct electron detector. eLife **3:**e01963. http://dx.doi.org/10.7554/eLife.01963.
228. **Lünsdorf H, Niedrig M, Fiebig K.** 1991. Immunocytochemical localization of the coenzyme F_{420}-reducing hydrogenase in *Methanosarcina barkeri* Fusaro. J Bacteriol **173:**978–984.
229. **Baron SF, Brown DP, Ferry JG.** 1987. Locations of the hydrogenases of *Methanobacterium formicicum* after subcellular fractionation of cell extract. J Bacteriol **169:**3823–3825.
230. **Baron SF, Ferry JG.** 1989. Purification and properties of the membrane-associated coenzyme F_{420}-reducing hydrogenase from *Methanobacterium formicicum*. J Bacteriol **171:**3846–3853.
231. **Kojima N, Fox JA, Hausinger RP, Daniels L, Orme-Johnson WH, Walsh C.** 1983. Paramagnetic centers in the nickel-containing, deazaflavin-reducing hydrogenase from *Methanobacterium thermoautotrophicum*. Proc Natl Acad Sci U S A **80:**378–382. http://dx.doi.org/10.1073/pnas.80.2.378.
232. **Lindahl PA, Kojima N, Hausinger RP, Fox JA, Teo BK, Walsh CT, Orme-Johnson WH.** 1984. Nickel and iron EXAFS of F_{420}-reducing hydrogenase from *Methanobacterium thermoautotrophicum*. J Am Chem Soc **106:**3062–3064. http://dx.doi.org/10.1021/ja00322a068.
233. **Fox JA, Livingston DJ, Orme-Johnson WH, Walsh CT.** 1987. 8-Hydroxy-5-deazaflavin-reducing hydrogenase from *Methanobacterium thermoautotrophicum*: 1. Purification and characterization. Biochemistry **26:**4219–4227.
234. **Yamazaki S, Tsai L, Stadtman TC, Teshima T, Nakaji A, Shiba T.** 1985. Stereochemical studies of a selenium-containing hydrogenase from *Methanococcus vannielii*: determination of the absolute configuration of C-5 chirally labeled dihydro-8-hydroxy-5-deazaflavin cofactor. Proc Natl Acad Sci U S A **82:**1364–1366. http://dx.doi.org/10.1073/pnas.82.5.1364.
235. **Livingston DJ, Fox JA, Orme-Johnson WH, Walsh CT.** 1987. 8-Hydroxy-5-deazaflavin-reducing hydrogenase from *Methanobacterium thermoautotrophicum*: 2. Kinetic and hydrogen-transfer studies. Derivation of a steady-state rate equation for deazaflavin-reducing hydrogenase. Biochemistry **26:**4228–4237.
236. **Sorgenfrei O, Müller S, Pfeiffer M, Sniezko I, Klein A.** 1997. The [NiFe] hydrogenases of *Methanococcus voltae*: genes, enzymes and regulation. Arch Microbiol **167:**189–195. http://dx.doi.org/10.1007/s002030050434.
237. **Sorgenfrei O, Duin EC, Klein A, Albracht SP.** 1997. Changes in the electronic structure around Ni in oxidized and reduced selenium-containing hydrogenases from *Methanococcus voltae*. Eur J Biochem **247:**681–687. http://dx.doi.org/10.1111/j.1432-1033.1997.00681.x.
238. **Berghöfer Y, Agha-Amiri K, Klein A.** 1994. Selenium is involved in the negative regulation of the expression of selenium-free [NiFe] hydrogenases in *Methanococcus voltae*. Mol Gen Genet **242:**369–373.
239. **Noll I, Müller S, Klein A.** 1999. Transcriptional regulation of genes encoding the selenium-free [NiFe]-hydrogenases in the archaeon *Methanococcus voltae* involves positive and negative control elements. Genetics **152:**1335–1341.
240. **Jeon JH, Lim JK, Kim M-S, Yang T-J, Lee S-H, Bae SS, Kim YJ, Lee SH, Lee J-H, Kang SG, Lee HS.** 2015. Characterization of the *frhAGB*-encoding hydrogenase from a non-methanogenic hyperthermophilic archaeon. Extremophiles **19:**109–118. http://dx.doi.org/10.1007/s00792-014-0689-y.
241. **Belay N, Sparling R, Daniels L.** 1986. Relationship of formate to growth and methanogenesis by *Methanococcus thermolithotrophicus*. Appl Environ Microbiol **52:**1080–1085.
242. **Wood GE, Haydock AK, John A, Leigh JA.** 2003. Function and regulation of the formate dehydrogenase genes of the methanogenic archaeon *Methanococcus maripaludis*. J Bacteriol **185:**2548–2554. http://dx.doi.org/10.1128/JB.185.8.2548-2554.2003.
243. **Schauer NL, Ferry JG.** 1980. Metabolism of formate in *Methanobacterium formicicum*. J Bacteriol **142:**800–807.
244. **Thiele JH, Zeikus JG.** 1988. Control of interspecies electron flow during anaerobic digestion: significance of formate transfer versus hydrogen transfer during syntrophic methanogenesis in flocs. Appl Environ Microbiol **54:**20–29.
245. **Shuber AP, Orr EC, Recny MA, Schendel PF, May HD, Schauer NL, Ferry JG.** 1986. Cloning, expression, and nucleotide sequence of the formate dehydrogenase genes from *Methanobacterium formicicum*. J Biol Chem **261:**12942–12947.
246. **Baron SF, Williams DS, May HD, Patel PS, Aldrich HC, Ferry JG.** 1989. Immunogold localization of coenzyme F_{420}-reducing formate dehydrogenase and coenzyme F_{420}-reducing hydrogenase in *Methanobacterium formicicum*. Arch Microbiol **151:**307–313. http://dx.doi.org/10.1007/BF00406556.
247. **Boyington JC, Gladyshev VN, Khangulov SV, Stadtman TC, Sun PD.** 1997. Crystal structure of formate dehydrogenase H: catalysis involving Mo, molybdopterin, selenocysteine, and an Fe4S4 cluster. Science **275:**1305–1308. http://dx.doi.org/10.1126/science.275.5304.1305.
248. **Barber MJ, Siegel LM, Schauer NL, May HD, Ferry JG.** 1983. Formate dehydrogenase from *Methanobacterium formicicum*. Electron paramagnetic resonance spectroscopy of the molybdenum and iron-sulfur centers. J Biol Chem **258:**10839–10845.
249. **May HD, Patel PS, Ferry JG.** 1988. Effect of molybdenum and tungsten on synthesis and composition of formate dehydrogenase in *Methanobacterium formicicum*. J Bacteriol **170:**3384–3389.
250. **May HD, Schauer NL, Ferry JG.** 1986. Molybdopterin cofactor from *Methanobacterium formicicum* formate dehydrogenase. J Bacteriol **166:**500–504.
251. **Johnson JL, Bastian NR, Schauer NL, Ferry JG, Rajagopalan KV.** 1991. Identification of molybdopterin guanine dinucleotide in formate dehydrogenase from *Methanobacterium formicicum*. FEMS Microbiol Lett **61:**213–216.
252. **Barber MJ, May HD, Ferry JG.** 1986. Inactivation of formate dehydrogenase from *Methanobacterium formicicum* by cyanide. Biochemistry **25:**8150–8155. http://dx.doi.org/10.1021/bi00373a004.
253. **Schauer NL, Ferry JG.** 1983. FAD requirement for the reduction of coenzyme F_{420} by formate dehydrogenase from *Methanobacterium formicicum*. J Bacteriol **155:**467–472.

254. **Schauer NL, Ferry JG, Honek JF, Orme-Johnson WH, Walsh C.** 1986. Mechanistic studies of the coenzyme F_{420} reducing formate dehydrogenase from *Methanobacterium formicicum*. Biochemistry **25:**7163–7168. http://dx.doi.org/10.1021/bi00370a059.
255. **Seedorf H, Kahnt J, Pierik AJ, Thauer RK.** 2005. *Si*-face stereospecificity at C5 of coenzyme F420 for F420H2 oxidase from methanogenic *Archaea* as determined by mass spectrometry. FEBS J **272:**5337–5342. http://dx.doi.org/10.1111/j.1742-4658.2005.04931.x.
256. **Lupa B, Hendrickson EL, Leigh JA, Whitman WB.** 2008. Formate-dependent H_2 production by the mesophilic methanogen *Methanococcus maripaludis*. Appl Environ Microbiol **74:**6584–6590. http://dx.doi.org/10.1128/AEM.01455-08.
257. **Baron SF, Ferry JG.** 1989. Reconstitution and properties of a coenzyme F_{420}-mediated formate hydrogenlyase system in *Methanobacterium formicicum*. J Bacteriol **171:**3854–3859.
258. **Thauer RK.** 2012. The Wolfe cycle comes full circle. Proc Natl Acad Sci U S A **109:**15084–15085. http://dx.doi.org/10.1073/pnas.1213193109.
259. **Costa KC, Wong PM, Wang T, Lie TJ, Dodsworth JA, Swanson I, Burn JA, Hackett M, Leigh JA.** 2010. Protein complexing in a methanogen suggests electron bifurcation and electron delivery from formate to heterodisulfide reductase. Proc Natl Acad Sci U S A **107:**11050–11055. http://dx.doi.org/10.1073/pnas.1003653107.
260. **Costa KC, Lie TJ, Xia Q, Leigh JA.** 2013. VhuD facilitates electron flow from H2 or formate to heterodisulfide reductase in *Methanococcus maripaludis*. J Bacteriol **195:**5160–5165. http://dx.doi.org/10.1128/JB.00895-13.
261. **Costa KC, Lie TJ, Jacobs MA, Leigh JA.** 2013. H_2-independent growth of the hydrogenotrophic methanogen *Methanococcus maripaludis*. mBio **4:**e00062-13. http://dx.doi.org/10.1128/mBio.00062-13.
262. **Lohner ST, Deutzmann JS, Logan BE, Leigh J, Spormann AM.** 2014. Hydrogenase-independent uptake and metabolism of electrons by the archaeon *Methanococcus maripaludis*. ISME J **8:**1673–1681. http://dx.doi.org/10.1038/ismej.2014.82.
263. **Sattler C, Wolf S, Fersch J, Goetz S, Rother M.** 2013. Random mutagenesis identifies factors involved in formate-dependent growth of the methanogenic archaeon *Methanococcus maripaludis*. Mol Genet Genomics **288:**413–424. http://dx.doi.org/10.1007/s00438-013-0756-6.
264. **Jones JB, Dilworth GL, Stadtman TC.** 1979. Occurrence of selenocysteine in the selenium-dependent formate dehydrogenase of *Methanococcus vannielii*. Arch Biochem Biophys **195:**255–260. http://dx.doi.org/10.1016/0003-9861(79)90351-5.
265. **Jones JB, Stadtman TC.** 1977. *Methanococcus vannielii*: culture and effects of selenium and tungsten on growth. J Bacteriol **130:**1404–1406.
266. **Hendrickson EL, Kaul R, Zhou Y, Bovee D, Chapman P, Chung J, Conway de Macario E, Dodsworth JA, Gillett W, Graham DE, Hackett M, Haydock AK, Kang A, Land ML, Levy R, Lie TJ, Major TA, Moore BC, Porat I, Palmeiri A, Rouse G, Saenphimmachak C, Söll D, Van Dien S, Wang T, Whitman WB, Xia Q, Zhang Y, Larimer FW, Olson MV, Leigh JA.** 2004. Complete genome sequence of the genetically tractable hydrogenotrophic methanogen *Methanococcus maripaludis*. J Bacteriol **186:**6956–6969. http://dx.doi.org/10.1128/JB.186.20.6956-6969.2004.
267. **Rother M, Mathes I, Lottspeich F, Böck A.** 2003. Inactivation of the *selB* gene in *Methanococcus maripaludis*: effect on synthesis of selenoproteins and their sulfur-containing homologs. J Bacteriol **185:**107–114. http://dx.doi.org/10.1128/JB.185.1.107-114.2003.
268. **Stock T, Selzer M, Connery S, Seyhan D, Resch A, Rother M.** 2011. Disruption and complementation of the selenocysteine biosynthesis pathway reveals a hierarchy of selenoprotein gene expression in the archaeon *Methanococcus maripaludis*. Mol Microbiol **82:**734–747. http://dx.doi.org/10.1111/j.1365-2958.2011.07850.x.
269. **Maeder DL, Anderson I, Brettin TS, Bruce DC, Gilna P, Han CS, Lapidus A, Metcalf WW, Saunders E, Tapia R, Sowers KR.** 2006. The *Methanosarcina barkeri* genome: comparative analysis with *Methanosarcina acetivorans* and *Methanosarcina mazei* reveals extensive rearrangement within methanosarcinal genomes. J Bacteriol **188:**7922–7931. http://dx.doi.org/10.1128/JB.00810-06.
270. **Frimmer U, Widdel F.** 1989. Oxidation of ethanol by methanogenic bacteria. Arch Microbiol **152:**479–483. http://dx.doi.org/10.1007/BF00446933.
271. **Widdel F, Wolfe RS.** 1989. Expression of secondary alcohol dehydrogenase in methanogenic bacteria and purification of the F_{420}-specific enzyme from *Methanogenium thermophilum* strain TCI. Arch Microbiol **152:**322–328. http://dx.doi.org/10.1007/BF00425168.
272. **Bleicher K, Winter J.** 1991. Purification and properties of F420- and $NADP^+$-dependent alcohol dehydrogenases of Methanogenium liminatans and Methanobacterium palustre, specific for secondary alcohols. Eur J Biochem **200:**43–51. http://dx.doi.org/10.1111/j.1432-1033.1991.tb21046.x.
273. **Klein AR, Berk H, Purwantini E, Daniels L, Thauer RK.** 1996. Si-face stereospecificity at C5 of coenzyme F_{420} for F_{420}-dependent glucose-6-phosphate dehydrogenase from *Mycobacterium smegmatis* and F_{420}-dependent alcohol dehydrogenase from *Methanoculleus thermophilicus*. Eur J Biochem **239:**93–97. http://dx.doi.org/10.1111/j.1432-1033.1996.0093u.x.
274. **Escalante-Semerena JC, Leigh JA, Rinehart KL, Wolfe RS.** 1984. Formaldehyde activation factor, tetrahydromethanopterin, a coenzyme of methanogenesis. Proc Natl Acad Sci U S A **81:**1976–1980. http://dx.doi.org/10.1073/pnas.81.7.1976.
275. **te Brommelstroet BW, Hensgens CM, Keltjens JT, van der Drift C, Vogels GD.** 1991. Purification and characterization of coenzyme F420-dependent 5,10-methylenetetrahydromethanopterin dehydrogenase from *Methanobacterium thermoautotrophicum* strain delta H. Biochim Biophys Acta **1073:**77–84. http://dx.doi.org/10.1016/0304-4165(91)90185-J.
276. **Klein AR, Koch J, Stetter KO, Thauer RK.** 1993. Two N^5, N^{10}-methylenetetrahydromethanopterin dehydrogenases in the extreme thermophile Methanopyrus kandleri: characterization of the coenzyme F_{420}-dependent enzyme. Arch Microbiol **160:**186–192.
277. **Mukhopadhyay B, Purwantini E, Pihl TD, Reeve JN, Daniels L.** 1995. Cloning, sequencing, and transcriptional analysis of the coenzyme F420-dependent methylene-5,6,7,8-tetrahydromethanopterin dehydrogenase gene from Methanobacterium thermoautotrophicum strain Marburg and functional expression in Escherichia coli. J Biol Chem **270:**2827–2832. http://dx.doi.org/10.1074/jbc.270.6.2827.
278. **Klein AR, Thauer RK.** 1997. Overexpression of the coenzyme-F_{420}-dependent N^5,N^{10}-methylenetetrahydromethanopterin dehydrogenase gene from the hyperthermophilic *Methanopyrus kandleri*. Eur J Biochem **245:**386–391. http://dx.doi.org/10.1111/j.1432-1033.1997.t01-1-00386.x.
279. **Ma K, Thauer RK.** 1990. Purification and properties of N^5, N^{10}-methylenetetrahydromethanopterin reductase from Methanobacterium thermoautotrophicum (strain Marburg). Eur J Biochem **191:**187–193. http://dx.doi.org/10.1111/j.1432-1033.1990.tb19109.x.
280. **te Brömmelstroet BW, Hensgens CM, Keltjens JT, van der Drift C, Vogels GD.** 1990. Purification and properties of 5,10-methylenetetrahydromethanopterin reductase, a coenzyme F_{420}-dependent enzyme, from *Methanobacterium thermoautotrophicum* strain delta H. J Biol Chem **265:**1852–1857.
281. **Ma K, Linder D, Stetter KO, Thauer RK.** 1991. Purification and properties of N^5,N^{10}-methylenetetrahydromethanopterin reductase (coenzyme F_{420}-dependent) from the extreme thermophile *Methanopyrus kandleri*. Arch Microbiol **155:**593–600. http://dx.doi.org/10.1007/BF00245355.
282. **Ma K, Thauer RK.** 1990. *N^5*, *N^{10}*-Methylenetetrahydromethanopterin reductase from *Methanosarcina barkeri*. FEMS Microbiol Lett **70:**119–123. http://dx.doi.org/10.1111/j.1574-6968.1990.tb13963.x.
283. **Vaupel M, Thauer RK.** 1995. Coenzyme F_{420}-dependent *N^5*,*N^{10}*-methylenetetrahydromethanopterin reductase (Mer) from *Methanobacterium thermoautotrophicum* strain Marburg. Cloning, sequencing, transcriptional analysis, and functional expression in *Escherichia coli* of the *mer* gene. Eur J Biochem **231:**773–778. http://dx.doi.org/10.1111/j.1432-1033.1995.0773d.x.
284. **te Brömmelstroet BWJ, Geerts WJ, Keltjens JT, van der Drift C, Vogels GD.** 1991. Purification and properties of 5,10-methylenetetrahydromethanopterin dehydrogenase and 5,10-methylenetetrahydromethanopterin reductase, two coenzyme F_{420}-dependent enzymes, from *Methanosarcina barkeri*. Biochim Biophys Acta **1079:**293–302. http://dx.doi.org/10.1016/0167-4838(91)90072-8.
285. **Warkentin E, Hagemeier CH, Shima S, Thauer RK, Ermler U.** 2005. The structure of F420-dependent methylenetetrahydromethanopterin dehydrogenase: a crystallographic "superstructure" of the selenomethionine-labelled protein crystal structure. Acta Crystallogr Sect D Biol Crystallogr **61:**198–202. http://dx.doi.org/10.1107/S0907444904030732.
286. **Hagemeier CH, Shima S, Warkentin E, Thauer RK, Ermler U.** 2003. Coenzyme F_{420}-dependent methylenetetrahydromethanopterin dehydrogenase from *Methanopyrus kandleri*: the selenomethionine-labelled and non-labelled enzyme crystallized in two different forms. Acta Crys-

tallogr D Biol Crystallogr **59:**1653–1655. http://dx.doi.org/10.1107/S0907444903014896.

287. **Klein AR, Thauer RK.** 1995. Re-face specificity at C14a of methylenetetrahydromethanopterin and Si-face specificity at C5 of coenzyme F_{420} for coenzyme F_{420}-dependent methylenetetrahydromethanopterin dehydrogenase from methanogenic *Archaea*. Eur J Biochem **227:**169–174. http://dx.doi.org/10.1111/j.1432-1033.1995.tb20373.x.
288. **Bartoschek S, Buurman G, Thauer RK, Geierstanger BH, Weyrauch JP, Griesinger C, Nilges M, Hutter MC, Helms V.** 2001. Re-face stereospecificity of methylenetetrahydromethanopterin and methylenetetrahydrofolate dehydrogenases is predetermined by intrinsic properties of the substrate. Chembiochem **2**(7-8):530–541. http://dx.doi.org/10.1002/1439-7633(20010803)2:7/8<530::AID-CBIC530>3.0.CO;2-0.
289. **Kunow J, Schworer B, Setzke E, Thauer RK.** 1993. Si-face stereospecificity at C5 of coenzyme F_{420} for F_{420}-dependent N^5,N^{10}-methylenetetrahydromethanopterin dehydrogenase, F_{420}-dependent N^5,N^{10}-methylenetetrahydromethanopterin. Eur J Biochem **214:**641–646. http://dx.doi.org/10.1111/j.1432-1033.1993.tb17964.x.
290. **von Bunau R, Zirngibl C, Thauer RK, Klein A.** 1991. Hydrogen-forming and coenzyme-F_{420}-reducing methylene tetrahydromethanopterin dehydrogenase are genetically distinct enzymes in *Methanobacterium thermoautotrophicum* (Marburg). Eur J Biochem **202:**1205–1208. http://dx.doi.org/10.1111/j.1432-1033.1991.tb16491.x.
291. **Shima S, Pilak O, Vogt S, Schick M, Stagni MS, Meyer-Klaucke W, Warkentin E, Thauer RK, Ermler U.** 2008. The crystal structure of [Fe]-hydrogenase reveals the geometry of the active site. Science **321:**572–575. http://dx.doi.org/10.1126/science.1158978.
292. **Zirngibl C, Hedderich R, Thauer RK.** 1990. N^5,N^{10}-Methylenetetrahydromethanopterin dehydrogenase from *Methanobacterium thermoautotrophicum* has hydrogenase activity. FEBS Lett **261:**112–116. http://dx.doi.org/10.1016/0014-5793(90)80649-4.
293. **Hendrickson EL, Haydock AK, Moore BC, Whitman WB, Leigh JA.** 2007. Functionally distinct genes regulated by hydrogen limitation and growth rate in methanogenic Archaea. Proc Natl Acad Sci U S A **104:**8930–8934. http://dx.doi.org/10.1073/pnas.0701157104.
294. **Pennings JL, Vermeij P, de Poorter LM, Keltjens JT, Vogels GD.** 2000. Adaptation of methane formation and enzyme contents during growth of *Methanobacterium thermoautotrophicum* (strain deltaH) in a fed-batch fermentor. Antonie Van Leeuwenhoek **77:**281–291. http://dx.doi.org/10.1023/A:1002443012525.
295. **Nolling J, Pihl TD, Vriesema A, Reeve JN.** 1995. Organization and growth phase-dependent transcription of methane genes in two regions of the *Methanobacterium thermoautotrophicum* genome. J Bacteriol **177:**2460–2468.
296. **Pennings JLA, Keltjens JT, Vogels GD.** 1998. Isolation and characterization of *Methanobacterium thermoautotrophicum* ΔH mutants unable to grow under hydrogen-deprived conditions. J Bacteriol **180:**2676–2681.
297. **Afting C, Hochheimer A, Thauer RK.** 1998. Function of H_2-forming methylenetetrahydromethanopterin dehydrogenase from *Methanobacterium thermoautotrophicum* in coenzyme F_{420} reduction with H_2. Arch Microbiol **169:**206–210. http://dx.doi.org/10.1007/s002030050562.
298. **Afting C, Kremmer E, Brucker C, Hochheimer A, Thauer RK.** 2000. Regulation of the synthesis of H_2-forming methylenetetrahydromethanopterin dehydrogenase (Hmd) and of HmdII and HmdIII in Methanothermobacter marburgensis. Arch Microbiol **174:**225–232. http://dx.doi.org/10.1007/s002030000197.
299. **Schmitz RA, Linder D, Stetter KO, Thauer RK.** 1991. N^5,N^{10}-Methylenetetrahydromethanopterin reductase (coenzyme F_{420}-dependent) and formylmethanofuran dehydrogenase from the hyperthermophile *Archaeoglobus fulgidus*. Arch Microbiol **156:**427–434. http://dx.doi.org/10.1007/BF00248722.
300. **Schworer B, Breitung J, Klein AR, Stetter KO, Thauer RK.** 1993. Formylmethanofuran: tetrahydromethanopterin formyltransferase and N^5,N^{10}-methylenetetrahydromethanopterin dehydrogenase from the sulfate-reducing Archaeoglobus fulgidus: similarities with the enzymes from methanogenic Archaea. Arch Microbiol **159:**225–232. http://dx.doi.org/10.1007/BF00248476.
301. **Vorholt JA, Chistoserdova L, Lidstrom ME, Thauer RK.** 1998. The NADP-dependent methylene tetrahydromethanopterin dehydrogenase in *Methylobacterium extorquens* AM1. J Bacteriol **180:**5351–5356.
302. **Vorholt JA, Kalyuzhnaya MG, Hagemeier CH, Lidstrom ME, Chistoserdova L.** 2005. MtdC, a novel class of methylene tetrahydromethanopterin dehydrogenases. J Bacteriol **187:**6069–6074. http://dx.doi.org/10.1128/JB.187.17.6069-6074.2005.
303. **Deppenmeier U, Blaut M, Mahlmann A, Gottschalk G.** 1990. Reduced coenzyme F_{420}: heterodisulfide oxidoreductase, a proton-translocating redox system in methanogenic bacteria. Proc Natl Acad Sci U S A **87:**9449–9453. http://dx.doi.org/10.1073/pnas.87.23.9449.
304. **Deppenmeier U, Lienard T, Gottschalk G.** 1999. Novel reactions involved in energy conservation by methanogenic archaea. FEBS Lett **457:**291–297. http://dx.doi.org/10.1016/S0014-5793(99)01026-1.
305. **Bäumer S, Murakami E, Brodersen J, Gottschalk G, Ragsdale SW, Deppenmeier U.** 1998. The $F_{420}H_2$:heterodisulfide oxidoreductase system from *Methanosarcina* species: 2-hydroxyphenazine mediates electron transfer from $F_{420}H_2$ dehydrogenase to heterodisulfide reductase. FEBS Lett **428:**295–298. http://dx.doi.org/10.1016/S0014-5793(98)00555-9.
306. **Ide T, Bäumer S, Deppenmeier U.** 1999. Energy conservation by the H2:heterodisulfide oxidoreductase from *Methanosarcina mazei* Gö1: identification of two proton-translocating segments. J Bacteriol **181:**4076–4080.
307. **Heiden S, Hedderich R, Setzke E, Thauer RK.** 1994. Purification of a two-subunit cytochrome *b*-containing heterodisulfide reductase from methanol-grown *Methanosarcina barkeri*. Eur J Biochem **221:**855–861. http://dx.doi.org/10.1111/j.1432-1033.1994.tb18800.x.
308. **Beifuss U, Tietze M, Bäumer S, Deppenmeier U.** 2000. Methanophenazine: structure, total synthesis, and function of a new cofactor from methanogenic archaea. Angew Chem Int Ed **39:**2470–2472. http://dx.doi.org/10.1002/1521-3773(20000717)39:14<2470::AID-ANIE2470>3.0.CO;2-R.
309. **Abken HJ, Tietze M, Brodersen J, Bäumer S, Beifuss U, Deppenmeier U.** 1998. Isolation and characterization of methanophenazine and function of phenazines in membrane-bound electron transport of *Methanosarcina mazei* Go1. J Bacteriol **180:**2027–2032.
310. **Brodersen J, Bäumer S, Abken H-J, Gottschalk G, Deppenmeier U.** 1999. Inhibition of membrane-bound electron transport of the methanogenic archaeon *Methanosarcina mazei* Gö1 by diphenyleneiodonium. Eur J Biochem **259:**218–224. http://dx.doi.org/10.1046/j.1432-1327.1999.00017.x.
311. **Kühn W, Fiebig K, Walther R, Gottschalk G.** 1979. Presence of a cytochrome b_{559} in *Methanosarcina barkeri*. FEBS Lett **105:**271–274. http://dx.doi.org/10.1016/0014-5793(79)80627-4.
312. **Kühn W, Gottschalk G.** 1983. Characterization of the cytochromes occurring in *Methanosarcina* species. Eur J Biochem **135:**89–94. http://dx.doi.org/10.1111/j.1432-1033.1983.tb07621.x.
313. **Abken H-J, Deppenmeier U.** 1997. Purification and properties of an $F_{420}H_2$ dehydrogenase from *Methanosarcina mazei* Go1. FEMS Microbiol Lett **154:**231–237. http://dx.doi.org/10.1016/S0378-1097(97)00330-3.
314. **Haase P, Deppenmeier U, Blaut M, Gottschalk G.** 1992. Purification and characterization of $F_{420}H_2$-dehydrogenase from *Methanolobus tindarius*. Eur J Biochem **531:**527–531.
315. **Westenberg DJ, Braune A, Ruppert C, Müller V, Herzberg C, Gottschalk G, Blaut M.** 1999. The $F_{420}H_2$-dehydrogenase from *Methanolobus tindarius*: cloning of the *ffd* operon and expression of the genes in *Escherichia coli*. FEMS Microbiol Lett **170:**389–398. http://dx.doi.org/10.1111/j.1574-6968.1999.tb13399.x.
316. **Efremov RG, Sazanov LA.** 2011. Respiratory complex I: "steam engine" of the cell? Curr Opin Struct Biol **21:**532–540. http://dx.doi.org/10.1016/j.sbi.2011.07.002.
317. **Efremov RG, Sazanov LA.** 2012. The coupling mechanism of respiratory complex I - a structural and evolutionary perspective. Biochim Biophys Acta **1817:**1785–1795. http://dx.doi.org/10.1016/j.bbabio.2012.02.015.
318. **Deppenmeier U.** 2004. The membrane-bound electron transport system of *Methanosarcina* species. J Bioenerg Biomembr **36:**55–64. http://dx.doi.org/10.1023/B:JOBB.0000019598.64642.97.
319. **Sazanov LA.** 2015. A giant molecular proton pump: structure and mechanism of respiratory complex I. Nat Rev Mol Cell Biol **16:**375–388. http://dx.doi.org/10.1038/nrm3997.
320. **Baradaran R, Berrisford JM, Minhas GS, Sazanov LA.** 2013. Crystal structure of the entire respiratory complex I. Nature **494:**443–448. http://dx.doi.org/10.1038/nature11871.
321. **Galagan JE, Nusbaum C, Roy A, Endrizzi MG, Macdonald P, FitzHugh W, Calvo S, Engels R, Smirnov S, Atnoor D, Brown A, Allen N, Naylor J, Stange-Thomann N, DeArellano K, Johnson R, Linton L, McEwan P, McKernan K, Talamas J, Tirrell A, Ye W, Zimmer A,**

Barber RD, Cann I, Graham DE, Grahame DA, Guss AM, Hedderich R, Ingram-Smith C, Kuettner HC, Krzycki JA, Leigh JA, Li W, Liu J, Mukhopadhyay B, Reeve JN, Smith K, Springer TA, Umayam LA, White O, White RH, Conway de Macario E, Ferry JG, Jarrell KF, Jing H, Macario AJL, Paulsen I, Pritchett M, Sowers KR, Swanson RV, Zinder SH, Lander E, Metcalf WW, Birren B. 2002. The genome of *M. acetivorans* reveals extensive metabolic and physiological diversity. Genome Res **12:**532–542. http://dx.doi.org/10.1101/gr.223902.

322. **Guss AM, Kulkarni G, Metcalf WW.** 2009. Differences in hydrogenase gene expression between *Methanosarcina acetivorans* and *Methanosarcina barkeri*. J Bacteriol **191:**2826–2833. http://dx.doi.org/10.1128/JB.00563-08.
323. **Guss AM, Mukhopadhyay B, Zhang JK, Metcalf WW.** 2005. Genetic analysis of *mch* mutants in two *Methanosarcina* species demonstrates multiple roles for the methanopterin-dependent C-1 oxidation/reduction pathway and differences in H_2 metabolism between closely related species. Mol Microbiol **55:**1671–1680. http://dx.doi.org/10.1111/j.1365-2958.2005.04514.x.
324. **Lessner DJ, Li L, Li Q, Rejtar T, Andreev VP, Reichlen M, Hill K, Moran JJ, Karger BL, Ferry JG.** 2006. An unconventional pathway for reduction of CO2 to methane in CO-grown Methanosarcina acetivorans revealed by proteomics. Proc Natl Acad Sci U S A **103:**17921–17926. http://dx.doi.org/10.1073/pnas.0608833103.
325. **Welte C, Kallnik V, Grapp M, Bender G, Ragsdale S, Deppenmeier U.** 2010. Function of Ech hydrogenase in ferredoxin-dependent, membrane-bound electron transport in *Methanosarcina mazei*. J Bacteriol **192:**674–678. http://dx.doi.org/10.1128/JB.01307-09.
326. **Deppenmeier U, Johann A, Hartsch T, Merkl R, Schmitz RA, Martinez-Arias R, Henne A, Wiezer A, Bäumer S, Jacobi C, Brüggemann H, Lienard T, Christmann A, Bömeke M, Steckel S, Bhattacharyya A, Lykidis A, Overbeek R, Klenk H-P, Gunsalus RP, Fritz H-J, Gottschalk G.** 2002. The genome of *Methanosarcina mazei*: evidence for lateral gene transfer between bacteria and archaea. J Mol Microbiol Biotechnol **4:**453–461.
327. **Welte C, Deppenmeier U.** 2011. Membrane-bound electron transport in *Methanosaeta thermophila*. J Bacteriol **193:**2868–2870. http://dx.doi.org/10.1128/JB.00162-11.
328. **Arshad A, Speth DR, De Graaf RM, den Camp HJM, Jetten MSM, Welte CU.** 2015. A metagenomics-based metabolic model of nitrate-dependent anaerobic oxidation of methane by *Methanoperedens*-like archaea. Front Microbiol **6:**1423. http://dx.doi.org/10.3389/fmicb.2015.01423.
329. **Silaghi-Dumitrescu R, Ng KY, Viswanathan R, Kurtz DM, Jr.** 2005. A flavo-diiron protein from *Desulfovibrio vulgaris* with oxidase and nitric oxide reductase activities. Evidence for an *in vivo* nitric oxide scavenging function. Biochemistry **44:**3572–3579.
330. **Tholen A, Pester M, Brune A.** 2007. Simultaneous methanogenesis and oxygen reduction by *Methanobrevibacter cuticularis* at low oxygen fluxes. FEMS Microbiol Ecol **62:**303–312. http://dx.doi.org/10.1111/j.1574-6941.2007.00390.x.
331. **Angel R, Claus P, Conrad R.** 2012. Methanogenic archaea are globally ubiquitous in aerated soils and become active under wet anoxic conditions. ISME J **6:**847–862. http://dx.doi.org/10.1038/ismej.2011.141.
332. **Kaster AK, Goenrich M, Seedorf H, Liesegang H, Wollherr A, Gottschalk G, Thauer RK.** 2011. More than 200 genes required for methane formation from H_2 and CO_2 and energy conservation are present in Methanothermobacter marburgensis and Methanothermobacter thermautotrophicus. Archaea **1:**973848.
333. **Balderston WL, Payne WJ.** 1976. Inhibition of methanogenesis in salt marsh sediments and whole-cell suspensions of methanogenic bacteria by nitrogen oxides. Appl Environ Microbiol **32:**264–269.
334. **Rothe O, Thomm M.** 2000. A simplified method for the cultivation of extreme anaerobic *Archaea* based on the use of sodium sulfite as reducing agent. Extremophiles **4:**247–252. http://dx.doi.org/10.1007/PL00010716.
335. **Daniels L, Belay N, Rajagopal BS.** 1986. Assimilatory reduction of sulfate and sulfite by methanogenic bacteria. Appl Environ Microbiol **51:**703–709.
336. **Susanti D, Mukhopadhyay B.** 2012. An intertwined evolutionary history of methanogenic archaea and sulfate reduction. PLoS One **7:**e45313. http://dx.doi.org/10.1371/journal.pone.0045313.
337. **Johnson EF, Mukhopadhyay B.** 2008. A novel coenzyme F_{420} dependent sulfite reductase and a small sulfite reductase in methanogenic archaea, p 202–216. *In* Dahl C, Friedrich CG (ed), Microbial sulfur metabolism. Springer, Berlin, Germany.
338. **Susanti D, Wong JH, Vensel WH, Loganathan U, DeSantis R, Schmitz RA, Balsera M, Buchanan BB, Mukhopadhyay B.** 2014. Thioredoxin targets fundamental processes in a methane-producing archaeon, *Methanocaldococcus jannaschii*. Proc Natl Acad Sci U S A **111:**2608–2613. http://dx.doi.org/10.1073/pnas.1324240111.
339. **Moura JJG, Moura I, Santos H, Xavier AV, Scandellari M, LeGall J.** 1982. Isolation of P_{590} from *Methanosarcina barkeri*: evidence for the presence of sulfite reductase activity. Biochem Biophys Res Commun **108:**1002–1009. http://dx.doi.org/10.1016/0006-291X(82)92099-X.
340. **Eguchi S, Nakata H, Nishio N, Nagai S.** 1984. $NADP^+$ reduction by a methanogen using HCOOH or H_2 as electron donor. Appl Microbiol Biotechnol **20:**213–217.
341. **Jones JB, Stadtman TC.** 1980. Reconstitution of a formate-NADP+ oxidoreductase from formate dehydrogenase and a 5-deazaflavin-linked NADP+ reductase isolated from *Methanococcus vannielii*. J Biol Chem **255:**1049–1053.
342. **Yamazaki S, Tsai L.** 1980. Purification and properties of 8-hydroxy-5-deazaflavin-dependent $NADP^+$ reductase from Methanococcus vannielii. J Biol Chem **255:**6462–6465.
343. **Dudley Eirich L, Dugger RS.** 1984. Purification and properties of an F_{420}-dependent NADP reductase from *Methanobacterium thermoautotrophicum*. Biochim Biophys Acta **802:**454–458. http://dx.doi.org/10.1016/0304-4165(84)90364-7.
344. **Berk H, Thauer RK.** 1998. $F_{420}H_2$:NADP oxidoreductase from *Methanobacterium thermoautotrophicum*: identification of the encoding gene via functional overexpression in *Escherichia coli*. FEBS Lett **438:**124–126. http://dx.doi.org/10.1016/S0014-5793(98)01288-5.
345. **Elias DA, Juck DF, Berry KA, Sparling R.** 2000. Purification of the $NADP^+$:F_{420} oxidoreductase of *Methanosphaera stadtmanae*. Can J Microbiol **46:**998–1003. http://dx.doi.org/10.1139/w00-090.
346. **Yamazaki S, Tsai L, Stadtman TC, Jacobson FS, Walsh C.** 1980. Stereochemical studies of 8-hydroxy-5-deazaflavin-dependent $NADP^+$ reductase from Methanococcus vannielii. J Biol Chem **255:**9025–9027.
347. **Schönheit P, Keweloh H, Thauer RK.** 1981. Factor F_{420} degradation in *Methanobacterium thermoautotrophicum* during exposure to oxygen. FEMS Microbiol Lett **12:**347–349. http://dx.doi.org/10.1111/j.1574-6968.1981.tb07671.x.
348. **Hausinger RP, Orme-Johnson WH, Walsh C.** 1985. Factor 390 chromophores: phosphodiester between AMP or GMP and methanogen factor 420. Biochemistry **24:**1629–1633. http://dx.doi.org/10.1021/bi00328a010.
349. **Kiener A, Orme-Johnson W, Walsh C.** 1988. Reversible conversion of coenzyme F420 to the 8-OH-AMP and 8-OH-GMP esters, F390-A and F390-G, on oxygen exposure and reestablishment of anaerobiosis in *Methanobacterium thermoautotrophicum*. Arch Microbiol **150:**249–253. http://dx.doi.org/10.1007/BF00407788.
350. **Keltjens JT, Vogels GD.** 1989. The ATP-dependent synthesis of factor 390 by cell-free extracts of *Methanobacterium thermoautotrophicum* (strain ΔH). FEMS Microbiol Lett **60:**5–10. http://dx.doi.org/10.1111/j.1574-6968.1989.tb03409.x.
351. **Gloss LM, Hausinger RP.** 1988. Methanogen factor 390 formation: species distribution, reversibility and effects of non-oxidative cellular stresses. Biofactors **1:**237–240.
352. **van de Wijngaard WMH, Vermey P, Van der Drift C.** 1991. Formation of factor 390 by cell extracts of *Methanosarcina barkeri*. J Bacteriol **173:**2710–2711.
353. **Gloss LM, Hausinger RP.** 1987. Reduction potential characterization of methanogen factor 390. FEMS Microbiol Lett **48:**143–145. http://dx.doi.org/10.1111/j.1574-6968.1987.tb02531.x.
354. **Vermeij P, Detmers FJM, Broers FJM, Keltjens JT, Van Der Drift C.** 1994. Purification and characterization of coenzyme F_{390} synthetase from *Methanobacterium thermoautotrophicum* (strain ΔH). Eur J Biochem **226:**185–191. http://dx.doi.org/10.1111/j.1432-1033.1994.tb20040.x.
355. **Vermeij P, van der Steen RJ, Keltjens JT, Vogels GD, Leisinger T.** 1996. Coenzyme F_{390} synthetase from *Methanobacterium thermoautotrophicum* Marburg belongs to the superfamily of adenylate-forming enzymes. J Bacteriol **178:**505–510.
356. **Kengen SW, von den Hoff HW, Keltjens JT, van der Drift C, Vogels GD.** 1991. F_{390} synthetase and F_{390} hydrolase from *Methanobacterium thermoautotrophicum* (strain delta H). Biofactors **3:**61–65.
357. **Vermeij P, Vinke E, Keltjens JT, Van Der Drift C.** 1995. Purification

and properties of coenzyme F_{390} hydrolase from *Methanobacterium thermoautotrophicum* (strain Marburg). Eur J Biochem **234:**592–597. http://dx.doi.org/10.1111/j.1432-1033.1995.592_b.x.
358. **Vermeij P, Pennings JL, Maassen SM, Keltjens JT, Vogels GD.** 1997. Cellular levels of factor 390 and methanogenic enzymes during growth of *Methanobacterium thermoautotrophicum* deltaH. J Bacteriol **179:**6640–6648.
359. **Morgan RM, Pihl TD, Nolling J, Reeve JN.** 1997. Hydrogen regulation of growth, growth yields, and methane gene transcription in *Methanobacterium thermoautotrophicum* deltaH. J Bacteriol **179:**889–898.
360. **Saviola B, Bishai W.** 2006. The genus *Mycobacterium* - medical, p 919–933. *In* Dworkin M, Falkow S, Rosenberg E, Schleifer K-H, Stackebrandt E (ed), The prokaryotes. Springer, New York, NY.
361. **Hartmans S, de Bont JM, Stackebrandt E.** 2006. The genus *Mycobacterium* - nonmedical, p 889–918. *In* Dworkin M, Falkow S, Rosenberg E, Schleifer K-H, Stackebrandt E (ed), The prokaryotes. Springer, New York, NY.
362. **Cole ST, Eiglmeier K, Parkhill J, James KD, Thomson NR, Wheeler PR, Honore N, Garnier T, Churcher C, Harris D, Mungall K, Basham D, Brown D, Chillingworth T, Connor R, Davies RM, Devlin K, Duthoy S, Feltwell T, Fraser A, Hamlin N, Holroyd S, Hornsby T, Jagels K, Lacroix C, Maclean J, Moule S, Murphy L, Oliver K, Quail MA, Rajandream M-A, Rutherford KM, Rutter S, Seeger K, Simon S, Simmonds M, Skelton J, Squares R, Squares S, Stevens K, Taylor K, Whitehead S, Woodward JR, Barrell BG.** 2001. Massive gene decay in the leprosy bacillus. Nature **409:**1007–1011. http://dx.doi.org/10.1038/35059006.
363. **Hasan MR, Rahman M, Jaques S, Purwantini E, Daniels L.** 2010. Glucose 6-phosphate accumulation in mycobacteria: implications for a novel F_{420}-dependent anti-oxidant defense system. J Biol Chem **285:**19135–19144. http://dx.doi.org/10.1074/jbc.M109.074310.
364. **Bashiri G, Perkowski EF, Turner AP, Feltcher ME, Braunstein M, Baker EN.** 2012. Tat-dependent translocation of an F_{420}-binding protein of *Mycobacterium tuberculosis*. PLoS One **7:**e45003. http://dx.doi.org/10.1371/journal.pone.0045003.
365. **Purwantini E, Mukhopadhyay B.** 2013. Rv0132c of *Mycobacterium tuberculosis* encodes a coenzyme F420-dependent hydroxymycolic acid dehydrogenase. PLoS One **8:**e81985. http://dx.doi.org/10.1371/journal.pone.0081985.
366. **Yuan Y, Zhu Y, Crane DD, Barry CE, III.** 1998. The effect of oxygenated mycolic acid composition on cell wall function and macrophage growth in *Mycobacterium tuberculosis*. Mol Microbiol **29:**1449–1458. http://dx.doi.org/10.1046/j.1365-2958.1998.01026.x.
367. **Dubnau E, Chan J, Raynaud C, Mohan VP, Lanéelle M-A, Yu K, Quémard A, Smith I, Daffé M.** 2000. Oxygenated mycolic acids are necessary for virulence of *Mycobacterium tuberculosis* in mice. Mol Microbiol **36:**630–637.
368. **Sambandan D, Dao DN, Weinrick BC, Vilchèze C, Gurcha SS, Ojha A, Kremer L, Besra GS, Hatfull GF, Jacobs WR, Jr.** 2013. Keto-mycolic acid-dependent pellicle formation confers tolerance to drug-sensitive *Mycobacterium tuberculosis*. mBio **4:**e00222-13. http://dx.doi.org/10.1128/mBio.00222-13.
369. **Kumar A, Deshane JS, Crossman DK, Bolisetty S, Yan B-S, Kramnik I, Agarwal A, Steyn AJC.** 2008. Heme oxygenase-1-derived carbon monoxide induces the *Mycobacterium tuberculosis* dormancy regulon. J Biol Chem **283:**18032–18039. http://dx.doi.org/10.1074/jbc.M802274200.
370. **Nambu S, Matsui T, Goulding CW, Takahashi S, Ikeda-Saito M.** 2013. A new way to degrade heme: the *Mycobacterium tuberculosis* enzyme MhuD catalyzes heme degradation without generating CO. J Biol Chem **288:**10101–10109. http://dx.doi.org/10.1074/jbc.M112.448399.
371. **Contreras H, Chim N, Credali A, Goulding CW.** 2014. Heme uptake in bacterial pathogens. Curr Opin Chem Biol **19:**34–41. http://dx.doi.org/10.1016/j.cbpa.2013.12.014.
372. **Stocker R, Yamamoto Y, McDonagh AF, Glazer AN, Ames BN.** 1987. Bilirubin is an antioxidant of possible physiological importance. Science **235:**1043–1046. http://dx.doi.org/10.1126/science.3029864.
373. **Barañano DE, Rao M, Ferris CD, Snyder SH.** 2002. Biliverdin reductase: a major physiologic cytoprotectant. Proc Natl Acad Sci U S A **99:**16093–16098. http://dx.doi.org/10.1073/pnas.252626999.
374. **Cook GM, Greening C, Hards K, Berney M.** 2014. Energetics of pathogenic bacteria and opportunities for drug development. Adv Microb Physiol **65:**1–62. http://dx.doi.org/10.1016/bs.ampbs.2014.08.001.
375. **Berney M, Greening C, Conrad R, Jacobs WR, Cook GM.** 2014. An obligately aerobic soil bacterium activates fermentative hydrogen production to survive reductive stress during hypoxia. Proc Natl Acad Sci U S A **111:**11479–11484. http://dx.doi.org/10.1073/pnas.1407034111.
376. **Darwin KH, Ehrt S, Gutierrez-Ramos J-C, Weich N, Nathan CF.** 2003. The proteasome of *Mycobacterium tuberculosis* is required for resistance to nitric oxide. Science **302:**1963–1966. http://dx.doi.org/10.1126/science.1091176.
377. **MacMicking J, Xie Q, Nathan C.** 1997. Nitric oxide and macrophage function. Annu Rev Immunol **15:**323–350. http://dx.doi.org/10.1146/annurev.immunol.15.1.323.
378. **Yu K, Mitchell C, Xing Y, Magliozzo RS, Bloom BR, Chan J.** 1999. Toxicity of nitrogen oxides and related oxidants on mycobacteria: *M. tuberculosis* is resistant to peroxynitrite anion. Tuber Lung Dis **79:**191–198. http://dx.doi.org/10.1054/tuld.1998.0203.
379. **Darwin KH, Nathan CF.** 2005. Role for nucleotide excision repair in virulence of *Mycobacterium tuberculosis*. Infect Immun **73:**4581–4587. http://dx.doi.org/10.1128/IAI.73.8.4581-4587.2005.
380. **Chopra I, Roberts M.** 2001. Tetracycline antibiotics: mode of action, applications, molecular biology, and epidemiology of bacterial resistance. Microbiol Mol Biol Rev **65:**232–260. http://dx.doi.org/10.1128/MMBR.65.2.232-260.2001.
381. **McCormick JRD, Hirsch U, Sjolander NO, Doerschuk AP.** 1960. Cosynthesis of tetracyclines by pairs of *Streptomyces aureofaciens* mutants. J Am Chem Soc **82:**5006–5007. http://dx.doi.org/10.1021/ja01503a066.
382. **Rhodes PM, Winskill N, Friend EJ, Warren M.** 1981. Biochemical and genetic characterization of *Streptomyces rimosus* mutants impaired in oxytetracycline biosynthesis. J Gen Microbiol **124:**329–338.
383. **McCormick JRD, Sjolander NO, Miller PA, Hirsch U, Arnold NH, Doerschuk AP.** 1958. The biological reduction of 7-chloro-5A(11A)-dehydrotetracycline to 7-chlorotetracycline by *Streptomyces aureofaciens*. J Am Chem Soc **80:**6460–6461. http://dx.doi.org/10.1021/ja01556a080.
384. **McCormick JRD, Morton GO.** 1982. Identity of cosynthetic factor 1 of *Streptomyces aureofaciens* and fragment F_O from coenzyme F_{420} of *Methanobacterium* species. J Am Chem Soc **104:**4014–4015. http://dx.doi.org/10.1021/ja00378a044.
385. **Zhang W, Watanabe K, Cai X, Jung ME, Tang Y, Zhan J.** 2008. Identifying the minimal enzymes required for anhydrotetracycline biosynthesis. J Am Chem Soc **130:**6068–6069. http://dx.doi.org/10.1021/ja800951e.
386. **Wang P, Kim W, Pickens LB, Gao X, Tang Y.** 2012. Heterologous expression and manipulation of three tetracycline biosynthetic pathways. Angew Chem Int Ed **51:**11136–11140. http://dx.doi.org/10.1002/anie.201205426.
387. **Novotná J, Neužil J, Hoš'álek Z.** 1989. Spectrophotometric identification of 8-hydroxy-5-deazaflavin: NADPH oxidoreductase activity in streptomycetes producing tetracyclines. FEMS Microbiol Lett **59**(1-2): 241–245. http://dx.doi.org/10.1111/j.1574-6968.1989.tb03118.x.
388. **Coats JH, Li GP, Kuo MS, Yurek DA.** 1989. Discovery, production, and biological assay of an unusual flavenoid cofactor involved in lincomycin biosynthesis. J Antibiot (Tokyo) **42:**472–474. http://dx.doi.org/10.7164/antibiotics.42.472.
389. **Kuo MS, Yurek DA, Coats JH, Chung ST, Li GP.** 1992. Isolation and identification of 3-propylidene-delta 1-pyrroline-5-carboxylic acid, a biosynthetic precursor of lincomycin. J Antibiot (Tokyo) **45:**1773–1777. http://dx.doi.org/10.7164/antibiotics.45.1773.
390. **Birkenmeyer RD, Kagan F.** 1970. Lincomycin. XI. Synthesis and structure of clindamycin. A potent antibacterial agent. J Med Chem **13:**616–619.
391. **Peschke U, Schmidt H, Zhang H-Z, Piepersberg W.** 1995. Molecular characterization of the lincomycin-production gene cluster of *Streptomyces lincolnensis* 78-11. Mol Microbiol **16:**1137–1156. http://dx.doi.org/10.1111/j.1365-2958.1995.tb02338.x.
392. **Hurley LH.** 1980. Elucidation and formulation of novel biosynthetic pathways leading to the pyrrolo[1,4]benzodiazepine antibiotics anthramycin, tomaymycin, and sibiromycin. Acc Chem Res **13:**263–269. http://dx.doi.org/10.1021/ar50152a003.
393. **Li W, Khullar A, Chou S, Sacramo A, Gerratana B.** 2009. Biosynthesis of sibiromycin, a potent antitumor antibiotic. Appl Environ Microbiol **75:**2869–2878. http://dx.doi.org/10.1128/AEM.02326-08.
394. **Ikeno S, Aoki D, Hamada M, Hori M, Tsuchiya KS.** 2006. DNA sequencing and transcriptional analysis of the kasugamycin biosynthetic gene cluster from *Streptomyces kasugaensis* M338-M1. J Antibiot (Tokyo) **59:**18–28. http://dx.doi.org/10.1038/ja.2006.4.

395. **Hu Y, Phelan V, Ntai I, Farnet CM, Zazopoulos E, Bachmann BO.** 2007. Benzodiazepine biosynthesis in *Streptomyces refuineus*. Chem Biol **14:**691–701. http://dx.doi.org/10.1016/j.chembiol.2007.05.009.
396. **Ebert S, Fischer P, Knackmuss HJ.** 2001. Converging catabolism of 2,4,6-trinitrophenol (picric acid) and 2,4-dinitrophenol by *Nocardioides simplex* FJ2-1A. Biodegradation **12:**367–376. http://dx.doi.org/10.1023/A:1014447700775.
397. **Fida TT, Palamuru S, Pandey G, Spain JC.** 2014. Aerobic biodegradation of 2,4-dinitroanisole by *Nocardioides* sp. strain JS1661. Appl Environ Microbiol **80:**7725–7731. http://dx.doi.org/10.1128/AEM.02752-14.
398. **Lenke H, Pieper DH, Bruhn C, Knackmuss HJ.** 1992. Degradation of 2,4-dinitrophenol by two *Rhodococcus erythropolis* strains, HL 24-1 and HL 24-2. Appl Environ Microbiol **58:**2928–2932.
399. **Ju K-S, Parales RE.** 2010. Nitroaromatic compounds, from synthesis to biodegradation. Microbiol Mol Biol Rev **74:**250–272. http://dx.doi.org/10.1128/MMBR.00006-10.
400. **Wackett LP.** 2009. Questioning our perceptions about evolution of biodegradative enzymes. Curr Opin Microbiol **12:**244–251. http://dx.doi.org/10.1016/j.mib.2009.05.001.
401. **Haritash AK, Kaushik CP.** 2009. Biodegradation aspects of polycyclic aromatic hydrocarbons (PAHs): a review. J Hazard Mater **169:**1–15. http://dx.doi.org/10.1016/j.jhazmat.2009.03.137.
402. **McLeod MP, Warren RL, Hsiao WWL, Araki N, Myhre M, Fernandes C, Miyazawa D, Wong W, Lillquist AL, Wang D, Dosanjh M, Hara H, Petrescu A, Morin RD, Yang G, Stott JM, Schein JE, Shin H, Smailus D, Siddiqui AS, Marra MA, Jones SJM, Holt R, Brinkman FSL, Miyauchi K, Fukuda M, Davies JE, Mohn WW, Eltis LD.** 2006. The complete genome of *Rhodococcus* sp. RHA1 provides insights into a catabolic powerhouse. Proc Natl Acad Sci U S A **103:**15582–15587.
403. **Martínková L, Uhnáková B, Pátek M, Nešvera J, Køen V.** 2009. Biodegradation potential of the genus *Rhodococcus*. Environ Int **35:**162–177. http://dx.doi.org/10.1016/j.envint.2008.07.018.
404. **Purwantini E, Daniels L.** 1996. Purification of a novel coenzyme F_{420}-dependent glucose-6-phosphate dehydrogenase from *Mycobacterium smegmatis*. J Bacteriol **178:**2861–2866.
405. **Wheeler PR.** 1983. Catabolic pathways for glucose, glycerol and 6-phosphogluconate in *Mycobacterium leprae* grown in armadillo tissues. Microbiology **129:**1481–1495. http://dx.doi.org/10.1099/00221287-129-5-1481.
406. **Minnikin DE, Minnikin SM, Parlett JH, Goodfellow M, Magnusson M.** 1984. Mycolic acid patterns of some species of *Mycobacterium*. Arch Microbiol **139:**225–231.
407. **DeMaio J, Zhang Y, Ko C, Young DB, Bishai WR.** 1996. A stationary-phase stress-response sigma factor from *Mycobacterium tuberculosis*. Proc Natl Acad Sci U S A **93:**2790–2794. http://dx.doi.org/10.1073/pnas.93.7.2790.
408. **Geiman DE, Kaushal D, Ko C, Tyagi S, Manabe YC, Schroeder BG, Fleischmann RD, Morrison NE, Converse PJ, Chen P, Bishai WR.** 2004. Attenuation of late-stage disease in mice infected by the *Mycobacterium tuberculosis* mutant lacking the SigF alternate sigma factor and identification of SigF-dependent genes by microarray analysis. Infect Immun **72:**1733–1745. http://dx.doi.org/10.1128/IAI.72.3.1733-1745.2004.
409. **Lapalikar GV, Taylor MC, Warden AC, Onagi H, Hennessy JE, Mulder RJ, Scott C, Brown SE, Russell RJ, Easton CJ, Oakeshott JG.** 2012. Cofactor promiscuity among F_{420}-dependent reductases enables them to catalyse both oxidation and reduction of the same substrate. Catal Sci Technol **2:**1560–1567. http://dx.doi.org/10.1039/c2cy20129a.
410. **Jackson CJ, Taylor MC, Tattersall DB, French NG, Carr PD, Ollis DL, Russell RJ, Oakeshott JG.** 2008. Cloning, expression, purification, crystallization and preliminary X-ray studies of a pyridoxine 5′-phosphate oxidase from *Mycobacterium smegmatis*. Acta Crystallogr Sect F Struct Biol Cryst Commun **64:**435–437. http://dx.doi.org/10.1107/S1744309108011512.
411. **Pédelacq JD, Rho BS, Kim CY, Waldo GS, Lekin TP, Segelke BW, Rupp B, Hung LW, Kim S-I, Terwilliger TC.** 2006. Crystal structure of a putative pyridoxine 5′-phosphate oxidase (Rv2607) from *Mycobacterium tuberculosis*. Proteins Struct Funct Genet **62:**563–569.
412. **di Salvo ML, Safo MK, Musayev FN, Bossa F, Schirch V.** 2003. Structure and mechanism of *Escherichia coli* pyridoxine 5′-phosphate oxidase. Biochim Biophys Acta **1647:**76–82. http://dx.doi.org/10.1016/S1570-9639(03)00060-8.
413. **Musayev FN, Di Salvo ML, Ko T-P, Schirch V, Safo MK.** 2003. Structure and properties of recombinant human pyridoxine 5′-phosphate oxidase. Protein Sci **12:**1455–1463. http://dx.doi.org/10.1110/ps.0356203.
414. **Guo Y, Guo G, Mao X, Zhang W, Xiao J, Tong W, Liu T, Xiao B, Liu X, Feng Y.** 2008. Functional identification of HugZ, a heme oxygenase from *Helicobacter pylori*. BMC Microbiol **8:**226. http://dx.doi.org/10.1186/1471-2180-8-226.
415. **Hu Y, Jiang F, Guo Y, Shen X, Zhang Y, Zhang R, Guo G, Mao X, Zou Q, Wang D-C.** 2011. Crystal structure of HugZ, a novel heme oxygenase from *Helicobacter pylori*. J Biol Chem **286:**1537–1544. http://dx.doi.org/10.1074/jbc.M110.172007.
416. **Zhang R, Zhang J, Guo G, Mao X, Tong W, Zhang Y, Wang D-C, Hu Y, Zou Q.** 2011. Crystal structure of *Campylobacter jejuni* ChuZ: a split-barrel family heme oxygenase with a novel heme-binding mode. Biochem Biophys Res Commun **415:**82–87. http://dx.doi.org/10.1016/j.bbrc.2011.10.016.
417. **Hilario E, Li Y, Niks D, Fan L.** 2012. The structure of a *Xanthomonas* general stress protein involved in citrus canker reveals its flavin-binding property. Acta Crystallogr Sect D Biol Crystallogr **68:**846–853. http://dx.doi.org/10.1107/S0907444912014126.
418. **Canaan S, Sulzenbacher G, Roig-Zamboni V, Scappuccini-Calvo L, Frassinetti F, Maurin D, Cambillau C, Bourne Y.** 2005. Crystal structure of the conserved hypothetical protein Rv1155 from *Mycobacterium tuberculosis*. FEBS Lett **579:**215–221. http://dx.doi.org/10.1016/j.febslet.2004.11.069.
419. **Biswal BK, Au K, Cherney MM, Garen C, James MNG.** 2006. The molecular structure of Rv2074, a probable pyridoxine 5′-phosphate oxidase from *Mycobacterium tuberculosis*, at 1.6 Å resolution. Acta Crystallogr Sect F Struct Biol Cryst Commun **62:**735–742. http://dx.doi.org/10.1107/S1744309106025012.
420. **Safo MK, Musayev FN, di Salvo ML, Schirch V.** 2001. X-ray structure of *Escherichia coli* pyridoxine 5′-phosphate oxidase complexed with pyridoxal 5′-phosphate at 2.0 Å resolution. J Mol Biol **310:**817–826. http://dx.doi.org/10.1006/jmbi.2001.4734.
421. **de Souza GA, Leversen NA, Malen H, Wiker HG.** 2011. Bacterial proteins with cleaved or uncleaved signal peptides of the general secretory pathway. J Proteomics **75:**502–510. http://dx.doi.org/10.1016/j.jprot.2011.08.016.
422. **He Z, De Buck J.** 2010. Cell wall proteome analysis of *Mycobacterium smegmatis* strain mc^2155. BMC Microbiol **10:**121. http://dx.doi.org/10.1186/1471-2180-10-121.
423. **Abdalla MY, Ahmad IM, Switzer B, Britigan BE.** 2015. Induction of heme oxygenase-1 contributes to survival of *Mycobacterium abscessus* in human macrophages-like THP-1 cells. Redox Biol **4:**328–339. http://dx.doi.org/10.1016/j.redox.2015.01.012.
424. **Yamaguchi T, Komoda Y, Nakajima H.** 1994. Biliverdin-IX alpha reductase and biliverdin-IX beta reductase from human liver. Purification and characterization. J Biol Chem **269:**24343–24348.
425. **Schluchter WM, Glazer AN.** 1997. Characterization of cyanobacterial biliverdin reductase: conversion of biliverdin to bilirubin is important for normal phycobiliprotein biosynthesis. J Biol Chem **272:**13562–13569. http://dx.doi.org/10.1074/jbc.272.21.13562.
426. **Fisher AJ, Thompson TB, Thoden JB, Baldwin TO, Rayment I.** 1996. The 1.5-Å resolution crystal structure of bacterial luciferase in low salt conditions. J Biol Chem **271:**21956–21968. http://dx.doi.org/10.1074/jbc.271.36.21956.
427. **Chaiyen P, Suadee C, Wilairat P.** 2001. A novel two-protein component flavoprotein hydroxylase. Eur J Biochem **268:**5550–5561. http://dx.doi.org/10.1046/j.1432-1033.2001.02490.x.
428. **Kertesz MA, Schmidt-Larbig K, Wuest T.** 1999. A novel reduced flavin mononucleotide-dependent methanesulfonate sulfonatase encoded by the sulfur-regulated *msu* operon of *Pseudomonas aeruginosa*. J Bacteriol **181:**1464–1473.
429. **Flatt PM, Mahmud T.** 2007. Biosynthesis of aminocyclitol-aminoglycoside antibiotics and related compounds. Nat Prod Rep **24:**358–392. http://dx.doi.org/10.1039/B603816F.
430. **Lenke H, Knackmuss HJ.** 1992. Initial hydrogenation during catabolism of picric acid by *Rhodococcus erythropolis* HL 24-2. Appl Environ Microbiol **58:**2933–2937.
431. **Lenke H, Knackmuss H.** 1996. Initial hydrogenation and extensive reduction of substituted 2,4-dinitrophenols. Appl Environ Microbiol **62:**784–790.
432. **Hofmann KW, Knackmuss H, Heiss G.** 2004. Nitrite elimination and hydrolytic ring cleavage in 2,4,6-trinitrophenol (picric acid) degrada-

tion. Appl Environ Microbiol **70:**2854–2860. http://dx.doi.org/10.1128/AEM.70.5.2854-2860.2004.
433. **Walters DM, Russ R, Knackmuss HJ, Rouviere PE.** 2001. High-density sampling of a bacterial operon using mRNA differential display. Gene **273:**305–315. http://dx.doi.org/10.1016/S0378-1119(01)00597-2.
434. **Nga DP, Altenbuchner J, Heiss GS.** 2004. NpdR, a repressor involved in 2,4,6-trinitrophenol degradation in *Rhodococcus opacus* HL PM-1. J Bacteriol **186:**98–103. http://dx.doi.org/10.1128/JB.186.1.98-103.2004.
435. **Heiss G, Trachtmann N, Abe Y, Takeo M, Knackmuss H-J.** 2003. Homologous *npdGI* genes in 2,4-dinitrophenol- and 4-nitrophenol-degrading *Rhodococcus* spp. Appl Environ Microbiol **69:**2748–2754. http://dx.doi.org/10.1128/AEM.69.5.2748-2754.2003.
436. **Ghosh A, Khurana M, Chauhan A, Takeo M, Chakraborti AK, Jain RK.** 2010. Degradation of 4-nitrophenol, 2-chloro-4-nitrophenol, and 2,4-nitrophenol by *Rhodococcus imtechensis* strain RKJ300. Environ Sci Technol **44:**1069–1077. http://dx.doi.org/10.1021/es9034123.
437. **Shen J, Zhang J, Zuo Y, Wang L, Sun X, Li J, Han W, He R.** 2009. Biodegradation of 2,4,6-trinitrophenol by *Rhodococcus* sp. isolated from a picric acid-contaminated soil. J Hazard Mater **163:**1199–1206. http://dx.doi.org/10.1016/j.jhazmat.2008.07.086.
438. **Takeo M, Abe Y, Negoro S, Heiss G.** 2003. Simultaneous degradation of 4-nitrophenol and picric acid by two different mechanisms of *Rhodococcus* sp. PN1. J Chem Eng Japan **36:**1178–1184. http://dx.doi.org/10.1252/jcej.36.1178.
439. **Behrend C, Heesche-Wagner K.** 1999. Formation of hydride-Meisenheimer complexes of picric acid (2,4,6-trinitrophenol) and 2,4-dinitrophenol during mineralization of picric acid by *Nocardioides* sp. strain CB 22-2. Appl Environ Microbiol **65:**1372–1377.
440. **Vorbeck C, Lenke H, Fischer P, Knackmuss HJ.** 1994. Identification of a hydride-Meisenheimer complex as a metabolite of 2,4,6-trinitrotoluene by a *Mycobacterium* strain. J Bacteriol **176:**932–934.
441. **Vorbeck C, Lenke H, Fischer P, Spain JC, Knackmuss HJ.** 1998. Initial reductive reactions in aerobic microbial metabolism of 2,4,6-trinitrotoluene. Appl Environ Microbiol **64:**246–252.
442. **World Health Organization.** 2014. Global tuberculosis report 2014. World Health Organization, Geneva, Switzerland.
443. **Lienhardt C, Glaziou P, Uplekar M, Lonnroth K, Getahun H, Raviglione M.** 2012. Global tuberculosis control: lessons learnt and future prospects. Nat Rev Microbiol **10:**407–416.
444. **Zumla A, Nahid P, Cole ST.** 2013. Advances in the development of new tuberculosis drugs and treatment regimens. Nat Rev Drug Discov **12:**388–404. http://dx.doi.org/10.1038/nrd4001.
445. **Murray CW, Rees DC.** 2009. The rise of fragment-based drug discovery. Nat Chem **1:**187–192. http://dx.doi.org/10.1038/nchem.217.
446. **Matsumoto M, Hashizume H, Tomishige T, Kawasaki M, Tsubouchi H, Sasaki H, Shimokawa Y, Komatsu M.** 2006. OPC-67683, a nitro-dihydro-imidazooxazole derivative with promising action against tuberculosis *in vitro* and in mice. PLoS Med **3:**e466. http://dx.doi.org/10.1371/journal.pmed.0030466.
447. **Denny WA.** 2015. TBA-354: a new drug for the treatment of persistent tuberculosis. Chem New Zeal **1:**18–22.
448. **Tasneen R, Williams K, Amoabeng O, Minkowski A, Mdluli KE, Upton AM, Nuermberger EL.** 2015. Contribution of the nitroimidazoles PA-824 and TBA-354 to the activity of novel regimens in murine models of tuberculosis. Antimicrob Agents Chemother **59:**129–135. http://dx.doi.org/10.1128/AAC.03822-14.
449. **Saliu OY, Crismale C, Schwander SK, Wallis RS.** 2007. Bactericidal activity of OPC-67683 against drug-tolerant *Mycobacterium tuberculosis*. J Antimicrob Chemother **60:**994–998. http://dx.doi.org/10.1093/jac/dkm291.
450. **Tyagi S, Nuermberger E, Yoshimatsu T, Williams K, Rosenthal I, Lounis N, Bishai W, Grosset J.** 2005. Bactericidal activity of the nitroimidazopyran PA-824 in a murine model of tuberculosis. Antimicrob Agents Chemother **49:**2289–2293. http://dx.doi.org/10.1128/AAC.49.6.2289-2293.2005.
451. **Lenaerts AJ, Gruppo V, Marietta KS, Johnson CM, Driscoll DK, Tompkins NM, Rose JD, Reynolds RC, Orme IM.** 2005. Preclinical testing of the nitroimidazopyran PA-824 for activity against *Mycobacterium tuberculosis* in a series of in vitro and in vivo models. Antimicrob Agents Chemother **49:**2294–2301. http://dx.doi.org/10.1128/AAC.49.6.2294-2301.2005.
452. **Gler MT, Skripconoka V, Sanchez-Garavito E, Xiao H, Cabrera-Rivero JL, Vargas-Vasquez DE, Gao M, Awad M, Park S-K, Shim TS, Suh GY, Danilovits M, Ogata H, Kurve A, Chang J, Suzuki K, Tupasi T, Koh W-J, Seaworth B, Geiter LJ, Wells CD.** 2012. Delamanid for multidrug-resistant pulmonary tuberculosis. N Engl J Med **366:**2151–2160. http://dx.doi.org/10.1056/NEJMoa1112433.
453. **Skripconoka V, Danilovits M, Pehme L, Tomson T, Skenders G, Kummik T, Cirule A, Leimane V, Kurve A, Levina K, Geiter LJ, Manissero D, Wells CD.** 2013. Delamanid improves outcomes and reduces mortality in multidrug-resistant tuberculosis. Eur Respir J **41:**1393–1400. http://dx.doi.org/10.1183/09031936.00125812.
454. **Gupta R, Gao M, Cirule A, Xiao H, Geiter LJ, Wells CD.** 2015. Delamanid for extensively drug-resistant tuberculosis. N Engl J Med **373:**291–292. http://dx.doi.org/10.1056/NEJMc1415332.
455. **Diacon AH, Dawson R, von Groote-Bidlingmaier F, Symons G, Venter A, Donald PR, van Niekerk C, Everitt D, Winter H, Becker P, Mendel CM, Spigelman MK.** 2012. 14-day bactericidal activity of PA-824, bedaquiline, pyrazinamide, and moxifloxacin combinations: a randomised trial. Lancet **380:**986–993. http://dx.doi.org/10.1016/S0140-6736(12)61080-0.
456. **Dawson R, Diacon AH, Everitt D, van Niekerk C, Donald PR, Burger DA, Schall R, Spigelman M, Conradie A, Eisenach K, Venter A, Ive P, Page-Shipp L, Variava E, Reither K, Ntinginya NE, Pym A, von Groote-Bidlingmaier F, Mendel CM.** 2015. Efficiency and safety of the combination of moxifloxacin, pretomanid (PA-824), and pyrazinamide during the first 8 weeks of antituberculosis treatment: a phase 2b, open-label, partly randomised trial in patients with drug-susceptible or drug-resistant pul. Lancet **385:**1738–1747. http://dx.doi.org/10.1016/S0140-6736(14)62002-X.
457. **Mohamed AE, Ahmed FH, Arulmozhiraja S, Lin CY, Taylor MC, Krausz ER, Jackson CJ, Coote ML.** 15 February 2016. Protonation state of $F_{420}H_2$ in the prodrug-activating deazaflavin dependent nitroreductase (Ddn) from *Mycobacterium tuberculosis*. Mol Biosyst Epub ahead of print.
458. **Gurumurthy M, Mukherjee T, Dowd CS, Singh R, Niyomrattanakit P, Tay JA, Nayyar A, Lee YS, Cherian J, Boshoff HI, Dick T, Barry CE, III, Manjunatha UH.** 2012. Substrate specificity of the deazaflavin-dependent nitroreductase from *Mycobacterium tuberculosis* responsible for the bioreductive activation of bicyclic nitroimidazoles. FEBS J **279:**113–125. http://dx.doi.org/10.1111/j.1742-4658.2011.08404.x.
459. **Manjunatha U, Boshoff HI, Barry CE.** 2009. The mechanism of action of PA-824: novel insights from transcriptional profiling. Commun Integr Biol **2:**215–218. http://dx.doi.org/10.4161/cib.2.3.7926.
460. **Manjunatha UH, Lahiri R, Randhawa B, Dowd CS, Krahenbuhl JL, Barry CE.** 2006. *Mycobacterium leprae* is naturally resistant to PA-824. Antimicrob Agents Chemother **50:**3350–3354. http://dx.doi.org/10.1128/AAC.00488-06.
461. **Haver HL, Chua A, Ghode P, Lakshminarayana SB, Singhal A, Mathema B, Wintjens R, Bifani P.** 2015. Mutations in genes for the F_{420} biosynthetic pathway and a nitroreductase enzyme are the primary resistance determinants in spontaneous in vitro-selected PA-824-resistant mutants of *Mycobacterium tuberculosis*. Antimicrob Agents Chemother **59:**5316–5323. http://dx.doi.org/10.1128/AAC.00308-15.
462. **Bloemberg GV, Keller PM, Stucki D, Trauner A, Borrell S, Latshang T, Coscolla M, Rothe T, Hömke R, Ritter C, Feldmann J, Schulthess B, Gagneux S, Böttger EC.** 2015. Acquired resistance to bedaquiline and delamanid in therapy for tuberculosis. N Engl J Med **373:**1986–1988. http://dx.doi.org/10.1056/NEJMc1505196.
463. **Ashtekar DR, Costa-Perira R, Nagrajan K, Vishvanathan N, Bhatt AD, Rittel W.** 1993. *In vitro* and *in vivo* activities of the nitroimidazole CGI 17341 against *Mycobacterium tuberculosis*. Antimicrob Agents Chemother **37:**183–186. http://dx.doi.org/10.1128/AAC.37.2.183.
464. **Kirschke S, Bousquet P, Ciais P, Saunois M, Canadell JG, Dlugokencky EJ, Bergamaschi P, Bergmann D, Blake DR, Bruhwiler L, Cameron-Smith P, Castaldi S, Chevallier F, Feng L, Fraser A, Heimann M, Hodson EL, Houweling S, Josse B, Fraser PJ, Krummel PB, Lamarque J-F, Langenfelds RL, Le Quere C, Naik V, O'Doherty S, Palmer PI, Pison I, Plummer D, Poulter B, Prinn RG, Rigby M, Ringeval B, Santini M, Schmidt M, Shindell DT, Simpson IJ, Spahni R, Steele LP, Strode SA, Sudo K, Szopa S, van der Werf GR, Voulgarakis A, van Weele M, Weiss RF, Williams JE, Zeng G.** 2013. Three decades of global methane sources and sinks. Nat Geosci **6:**813–823. http://dx.doi.org/10.1038/ngeo1955.
465. **Buddle BM, Denis M, Attwood GT, Altermann E, Janssen PH, Ronimus RS, Pinares-Patiño CS, Muetzel S, Neil Wedlock D.** 2011. Strat-

egies to reduce methane emissions from farmed ruminants grazing on pasture. Vet J **188:**11–17. http://dx.doi.org/10.1016/j.tvjl.2010.02.019.
466. **Cottle DJ, Nolan JV, Wiedemann SG.** 2011. Ruminant enteric methane mitigation: a review. Anim Prod Sci **51:**491–514. http://dx.doi.org/10.1071/AN10163.
467. **Kumar S, Choudhury P, Carro M, Griffith G, Dagar S, Puniya M, Calabro S, Ravella S, Dhewa T, Upadhyay R, Sirohi S, Kundu S, Wanapat M, Puniya A.** 2014. New aspects and strategies for methane mitigation from ruminants. Appl Microbiol Biotechnol **98:**31–44. http://dx.doi.org/10.1007/s00253-013-5365-0.
468. **Hristov AN, Oh J, Giallongo F, Frederick TW, Harper MT, Weeks HL, Branco AF, Moate PJ, Deighton MH, Williams SRO, Kindermann M, Duval S.** 2015. An inhibitor persistently decreased enteric methane emission from dairy cows with no negative effect on milk production. Proc Natl Acad Sci U S A **112:**10663–10668. http://dx.doi.org/10.1073/pnas.1504124112.
469. **Martínez-Fernández G, Abecia L, Arco A, Cantalapiedra-Hijar G, Martín-García AI, Molina-Alcaide E, Kindermann M, Duval S, Yáñez-Ruiz DR.** 2014. Effects of ethyl-3-nitrooxy propionate and 3-nitrooxypropanol on ruminal fermentation, microbial abundance, and methane emissions in sheep. J Dairy Sci **97:**3790–3799. http://dx.doi.org/10.3168/jds.2013-7398.
470. **Taylor MC, Scott C, Grogan G.** 2013. F_{420}-dependent enzymes - potential for applications in biotechnology. Trends Biotechnol **31:**63–64. http://dx.doi.org/10.1016/j.tibtech.2012.09.003.
471. **Wagacha JM, Muthomi JW.** 2008. Mycotoxin problem in Africa: current status, implications to food safety and health and possible management strategies. Int J Food Microbiol **124:**1–12. http://dx.doi.org/10.1016/j.ijfoodmicro.2008.01.008.
472. **Ciegler A, Lillehoj EB, Peterson RE, Hall HH.** 1966. Microbial detoxification of aflatoxin. Appl Microbiol **14:**934–939.
473. **Teniola OD, Addo PA, Brost IM, Farber P, Jany K-D, Alberts JF, van Zyl WH, Steyn PS, Holzapfel WH.** 2005. Degradation of aflatoxin B1 by cell-free extracts of *Rhodococcus erythropolis* and *Mycobacterium fluoranthenivorans* sp. nov. DSM44556(T). Int J Food Microbiol **105:**111–117. http://dx.doi.org/10.1016/j.ijfoodmicro.2005.05.004.
474. **Alberts JF, Engelbrecht Y, Steyn PS, Holzapfel WH, van Zyl WH.** 2006. Biological degradation of aflatoxin B_1 by *Rhodococcus erythropolis* cultures. Int J Food Microbiol **109:**121–126. http://dx.doi.org/10.1016/j.ijfoodmicro.2006.01.019.
475. **Jones JJ, Falkinham JO.** 2003. Decolorization of malachite green and crystal violet by waterborne pathogenic mycobacteria. Antimicrob Agents Chemother **47:**2323–2326. http://dx.doi.org/10.1128/AAC.47.7.2323-2326.2003.
476. **Srivastava S, Sinha R, Roy D.** 2004. Toxicological effects of malachite green. Aquat Toxicol **66:**319–329. http://dx.doi.org/10.1016/j.aquatox.2003.09.008.
477. **Spain JC, Hughes JB, Knackmuss H-J.** 2000. Biodegradation of nitroaromatic compounds and explosives. CRC Press, Boca Raton, FL.
478. **Snellinx Z, Nepovim A, Taghavi S, Vangronsveld J, Vanek T, van der Lelie D.** 2002. Biological remediation of explosives and related nitroaromatic compounds. Environ Sci Pollut Res Int **9:**48–61. http://dx.doi.org/10.1007/BF02987316.
479. **Schmid A, Dordick JS, Hauer B, Kiener A, Wubbolts M, Witholt B.** 2001. Industrial biocatalysis today and tomorrow. Nature **409:**258–268. http://dx.doi.org/10.1038/35051736.
480. **Bornscheuer UT, Huisman GW, Kazlauskas RJ, Lutz S, Moore JC, Robins K.** 2012. Engineering the third wave of biocatalysis. Nature **485:**185–194. http://dx.doi.org/10.1038/nature11117.
481. **Stuermer R, Hauer B, Hall M, Faber K.** 2007. Asymmetric bioreduction of activated C=C bonds using enoate reductases from the old yellow enzyme family. Curr Opin Chem Biol **11:**203–213. http://dx.doi.org/10.1016/j.cbpa.2007.02.025.
482. **Amato ED, Stewart JD.** 2015. Applications of protein engineering to members of the old yellow enzyme family. Biotechnol Adv **33:**624–631. http://dx.doi.org/10.1016/j.biotechadv.2015.04.011.
483. **Schrittwieser JH, Velikogne S, Kroutil W.** 2015. Biocatalytic imine reduction and reductive amination of ketones. Adv Synth Catal **357:**1655–1685. http://dx.doi.org/10.1002/adsc.201500213.
484. **Ghislieri D, Turner N.** 2014. Biocatalytic approaches to the synthesis of enantiomerically pure chiral amines. Top Catal **57:**284–300. http://dx.doi.org/10.1007/s11244-013-0184-1.
485. **Kimachi T, Kawase M, Matsuki S, Tanaka K, Yoneda F.** 1990. First total synthesis of coenzyme factor 420. J Chem Soc Perkin Trans 1 **1990:**253–256.
486. **Bashiri G, Rehan AM, Greenwood DR, Dickson JMJ, Baker EN.** 2010. Metabolic engineering of cofactor F420 production in *Mycobacterium smegmatis*. PLoS One **5:**e15803. http://dx.doi.org/10.1371/journal.pone.0015803.
487. **Buckel W, Thauer RK.** 2013. Energy conservation via electron bifurcating ferredoxin reduction and proton/Na^+ translocating ferredoxin oxidation. Biochim Biophys Acta **1827:**94–113. http://dx.doi.org/10.1016/j.bbabio.2012.07.002.
488. **Née G, Zaffagnini M, Trost P, Issakidis-Bourguet E.** 2009. Redox regulation of chloroplastic glucose-6-phosphate dehydrogenase: a new role for f-type thioredoxin. FEBS Lett **583:**2827–2832. http://dx.doi.org/10.1016/j.febslet.2009.07.035.
489. **Tietze M, Beuchle A, Lamla I, Orth N, Dehler M, Greiner G, Beifuss U.** 2003. Redox potentials of methanophenazine and CoB-S-S-CoM, factors involved in electron transport in methanogenic archaea. Chembiochem **4:**333–335. http://dx.doi.org/10.1002/cbic.200390053.
490. **Wagner GC, Kassner RJ, Kamen MD.** 1974. Redox potentials of certain vitamins K: implications for a role in sulfite reduction by obligately anaerobic bacteria. Proc Natl Acad Sci U S A **71:**253–256. http://dx.doi.org/10.1073/pnas.71.2.253.